FINAL REPORT

HYPERBARIC RESPIRATORY HEAT LOSS STUDY

Contract No. N00014-71-C-0099
Requisition No. NR101-840, Code 441

to

OFFICE OF NAVAL RESEARCH
DEPARTMENT OF THE NAVY
WASHINGTON, D.C.

October 31, 1971

WESTINGHOUSE ELECTRIC CORPORATION
UNDERSEAS DIVISION
OCEAN RESEARCH AND ENGINEERING CENTER
ANNAPOLIS, MARYLAND 21404

BA 874

FINAL REPORT

HYPERBARIC RESPIRATORY HEAT LOSS STUDY

Contract No. N00014-71-C-0099
Requisition No. NR101-840, Code 441

to

OFFICE OF NAVAL RESEARCH
DEPARTMENT OF THE NAVY
WASHINGTON, D.C.

October 31, 1971

WESTINGHOUSE ELECTRIC CORPORATION
UNDERSEAS DIVISION
OCEAN RESEARCH AND ENGINEERING CENTER
ANNAPOLIS, MARYLAND 21404

Unclassified

Security Classification

DOCUMENT CONTROL DATA - R & D

Security classification of title, body of abstract and indexing annotation must be entered when the overall report is classified)

1. ORIGINATING ACTIVITY (Corporate author) Westinghouse Electric Corp. Ocean Research and Engineering Center P.O. Box 1488, Annapolis, Md. 21404	2a. REPORT SECURITY CLASSIFICATION Unclassified 2b. GROUP N/A

3. REPORT TITLE

Hyperbaric Respiratory Heat Loss Study

4. DESCRIPTIVE NOTES (Type of report and, inclusive dates)

Final Research Report 4 Jan. 1971 to 31 Oct. 1071

5. AUTHOR(S) (First name, middle initial, last name)

Maxwell W. Goodman
N. Eugene Smith
John W. Colston
Edward L. Rich III

6. REPORT DATE 31 Oct. 1971	7a. TOTAL NO. OF PAGES 148	7b. NO. OF REFS 39

8a. CONTRACT OR GRANT NO. N00014-71-C-0099 b. PROJECT NO c. d.	9a. ORIGINATOR'S REPORT NUMBER(S) None required 9b. OTHER REPORT NO(S) (Any other numbers that may be assigned this report) None

10. DISTRIBUTION STATEMENT

Distribution of this report is unlimited

11. SUPPLEMENTARY NOTES None	12. SPONSORING MILITARY ACTIVITY Office of Naval Research

13. ABSTRACT

A multidepth saturation dive was performed as the vehicle for a study of respiratory heat loss during deep-depth, cold, helium-oxygen breathing. Respiratory heat loss was computed for each of the 137 combinations of depth and inhaled gas temperature for which ventilation and exhalation temperature were measured. Skin site temperatures and other respiratory parameters were also monitored, and the diver-subjects were under visual surveillance.

Exhalation gas temperature was always less than core temperature, regardless of the inhalation gas temperature (about 55, 45 and 35°F). The maximum rate of respiratory heat loss was observed with hard work (high ventilation rate) in 35°F water at 850 feet; about 400 watts (345 kilogram calories per hour). Respiratory symptoms of copious upper airway secretions, chest and back chilling and discomfort, and uncontrollable shaking and shivering reached peak severity during the 850 foot-35°F swims.

Conclusions having significance to operational diving without supplemental heating of the inhaled gas were formulated from the computations of respiratory heat loss, observations of falling core temperatures, and the subjective responses. These are as follows: (1) Dives to 850 feet for exposure durations in excess of 90 minutes in water of 45°F or colder are hazardous; (2) Dives to 650 feet or deeper for exposure durations in excess of 90 minutes in water of 35°F are liable to be characterized by significant task performance degradation.

DD FORM 1 NOV 68 1473 (PAGE 1)

S/N 0101-807-6811

Unclassified

Security Classification

A-31408

TABLE OF CONTENTS

14 KEY WORDS	LINK A		LINK B		LINK C	
	ROLE	WT	ROLE	WT	ROLE	WT
respiratory heat loss						
hyperbaric						
thermal balance						
diving						
saturation diving						
cold water immersion						
respiration						

LIST OF TABLES

LIST OF FIGURES

LIST OF FIGURES (Continued)

APPENDIXES

ABSTRACT

A multidepth saturation dive was performed as the vehicle for a study of respiratory heat loss during deep-depth, cold, helium-oxygen breathing. Respiratory heat loss was computed for each of the 137 combinations of depth and inhaled gas temperature for which ventilation and exhalation temperature were measured. Skin site temperatures and other respiratory parameters were also monitored, and the diver-subjects were under visual surveillance.

Exhalation gas temperature was always less than core temperature, regardless of the inhalation gas temperature (about 55, 45 and 35°F). The maximum rate of respiratory heat loss was observed with hard work (high ventilation rate) in 35°F water at 850 feet; about 400 watts (345 kilogram calories per hour). Respiratory symptoms of copious upper airway secretions, chest and back chilling and discomfort, and uncontrollable shaking and shivering reached peak severity during the 850 foot-35°F swims.

Conclusions having significance to operational diving without supplemental heating of the inhaled gas were formulated from the computations of respiratory heat loss, observations of falling core temperatures, and the subjective responses. These are as follows: (1) Dives to 850 feet for exposure durations in excess of 90 minutes in water of 45°F or colder are hazardous; (2) Dives to 650 feet or deeper for exposure durations in excess of 90 minutes in water of 35°F are liable to be characterized by significant task performance degradation.

SECTION 1

INTRODUCTION

The objective of these studies was to obtain, through immersion experiments with measurement of respiratory heat loss, information which is applicable in the estimation of depth and temperature operating limits for deep diving missions. The emphasis was upon immersion conditions encountered at a simulated depth of 850 feet. Actual mean temperature of inhaled gases approximated and was slightly warmer than that of ambient water temperature. At each experimental depth (450 ft., 650 ft., 850 ft. and 1,000 ft.) and at each controlled wet-pot water temperature (55°F, 45°F, 35°F) the divers were equipped with constant-flow hot water heated wet suits. These data are the first to be generated under conditions which thus mimic those of the operational scenario.

At sea level pressure the heat loss through respiration is relatively constant and is affected directly by the ventilatory air flow rate. Carlson, et. al. (9) estimated that this loss was equal to about 24% of the total body heat generated. Bribbia (4) determined that the heat loss of vaporization in men exercising in Arctic conditions was 9% of the total heat expended and that the water vapor loss was proportional to the ventilation rate. Day (14) computed respiratory heat loss (when the respiratory minute volume was 10 liters per minute and relative humidity was 50%) as follows:

AIR TEMP. (°F)	SENSIBLE HEAT LOSS (BTU/HR.)	LATENT HEAT OF VAPORIZATION (BTU/HR.)	TOTAL R.H.L. (BTU/HR.)
97	0	31	31
68	11	49	60
32	25	59	84

Numerous measurements of respiratory heat exchange have been made under comfortable, cool or hot conditions: Burch (5) (6), Cole (10) (11), Cramer (13), McCutcheon and Taylor (20) (21), Seeley (26) and Walker (31). For tabular resumes of the methods employed by most of the above investigators, as well as others, see the comprehensive review by Carlson (8). The following table of respiratory heat loss data is reproduced from his work:

HEAT LOSS IN RESPIRED AIR

Ambient Temperature		Belding et al. (1945)	Corlette (1942)	Day (1949)	Berg (1933)	Burch (1945)	Goodale (1896)	McCutchan & Taylor (1951)	Seeley (1940)
°C			kilogram calories per hour						
	*								
20	1.		2.0	2.87	0.76	1.9	2.5		
	2.		9.5	12.27	8.72	7.9	8.94		
	3.		11.5	15.14	9.48	9.8	11.44	11.9	12.0
0	1.		5.1	6.16			5.0		
	2.		11.5	14.78			9.43		
	3.	18.5	16.6	20.94			14.43		13.9
-20	1.		8.2	9.25					
	2.		12.12	15.40					
	3.	24.3	20.32	24.65					
-40	1.		11.2	12.52					
	2.		12.23	15.43					
	3.	28.3	23.43	27.95					

* Horizontal rows numbered 1., 2. and 3. are, respectively: the heat loss in warming inspired air (dry) and inspired water vapor; the heat loss in adding water vapor to the inspired air; the total heat loss, that is, the sum of the first two quantities.

Notes: a) Ambient relative humidity is taken as 50 per cent wherever possible. Exception — Berg dried the inspired air for his subjects.

b) The first three vertical columns represent values based on calculation. Day assumed expired air to be 37°C., saturated under all conditions. Corlette and Belding et al. took expired air to be 33°C, saturated.

c) It is assumed that the subject is at rest, comfortably clothed, and ventilating at the rate of 600 *l*/hr. Goodale did not record ventilation quantitatively.

Reproduced from Carlson (8)

Webb reported, in 1955 (34), that the relationship between ambient air and expired air temperatures approximates a linear function, as follows: "Starting at ambient temperature of 25°C, where the expired air temperature is 34°C, for every reduction of 5°C in ambient temperature there is a corresponding decrease of 1°C in the expired air temperature." Although this relationship was enunciated for conditions encountered at sea-level barometric pressure, the concept applied generally indicates that respiratory heat loss will be erroneously overestimated if the factor Δ(T exhaled - T inhaled) is computed by assuming equality of exhaled gas temperature to body temperature. The following table, adapted from Webb's report, compares respiratory heat loss according to his measurements ("B" values) with estimated values derived by assuming that exhaled air was at body temperature ("A" values). Heat loss data is in units of kilogram-calories.

AIR TEMP. (°C)	SENSIBLE HEAT LOSS		LATENT HEAT OF VAPORIZATION		TOTAL R.H.L.		TOTAL (A) HIGHER THAN TOTAL (B) BY
	(A)	(B)	(A)	(B)	(A)	(B)	
20	2.87	2.42	12.27	9.40	15.14	11.81	28%
0	6.16	5.39	14.78	8.35	20.94	13.75	52%
-20	9.25	8.37	15.40	6.96	24.65	15.33	61%
-40	12.58	11.35	15.43	5.92	28.01	17.26	62%

Armstrong, et. al. (2) also reported on respiratory aspects of breathing very cold Arctic air at atmospheric pressure and under subatmospheric conditions as encountered during high altitude flight without the protection of a cockpit canopy. Exposures to ambient temperatures at 40°F to -80°F for 2 to 6 hours did not cause direct laryngeal injury. In this regard Rawlins and Tauber (25) have cautioned that, "Much work has been done on the effects of breathing cold air down to -55°C, but we know of no studies of the effect of prolonged breathing of cold helium mixtures at great depths. At high rates of ventilation with relatively dense gas mixtures of high heat capacity there is a very large heat loss effecting a limited area of the body, the upper respiratory tract. The possibility of laryngeal damage, edema or functional impairment, should be contemplated."

Spealman, et. al. (28) also observed subjects breathing cold (to -83°F) air at atmospheric pressure. These investigators, in contradistinction to Webb, found that the expired air temperature was approximately 36°C in all cases. They reported the following respiratory heat losses per 1,000 liters of respired air (assuming 90% water vapor saturation):

AIR TEMP. (°C)	(°F)	SENSIBLE HEAT LOSS (KCAL.)	LATENT HEAT OF VAPORIZATION (KCAL.)	TOTAL R.H.L. (KCAL.)
56	133	+6.4	+44.7	+51.1
36	97	0.0	0.0	0.0
16	61	6.4	16.9	23.3
-4	25	12.8	22.6	35.4
-24	-11	19.2	24.1	43.3
-44	-47	25.6	24.3	49.9
-64	-83	32.0	24.4	56.4

Note the net gain in respiratory heat for the initial condition (air temperature 133°F). By assuming that inhaled air is completely dry, however, there is a net respiratory heat loss in each instance:

AIR TEMP (°C)	(°F)	TOTAL R.H.L. (KCAL.)
56	133	18.0
36	97	24.4
16	61	30.8
-4	25	37.2
-24	-11	43.6
-44	-47	50.0
-64	-83	56.4

Data on hyperbaric respiratory heat loss was reported in 1966 by Webb and Annis (37). Their study included a panel of diver-subjects during immersion experiments with an open-circuit demand breathing apparatus at simulated depths of 100 feet (4 atm. abs.) and 230 feet (8 atm. abs.). Mean data from their report is as follows:

CONDITION	NO. OF EXPERIMENTS	INHALED TEMP. (°C)	(°F)	ΔT (°C)	R.H.L. (KCAL/MIN)	TOTAL HEAT LOSS (KCAL/MIN)	R.H.L. % of TOTAL
Air, 1 atm.	35	20.9	69.6	13.4	0.56	5.5	9.5
Air, 4 atm.	4	17.0	62.6	16.3	0.90	4.8	17.7
SF6, 1 atm.*	37	20.2	68.4	13.7	0.71	5.0	13.5
80%He, 1 atm.	40	22.7	72.9	11.1	0.48	5.4	9.0
80%He, 4 atm.	8	15.3	59.5	15.4	0.48	3.1	16.3
96%He, 8 atm.	8	16.5	61.7	16.0	0.90	3.8	25.1

* 80% sulfur hexafluoride - 20% oxygen

Albano (1), in his presentation of thermoanalysis in diving, states that, "In the respiratory tree, thermolysis takes place as a result of heating and humidification of the ventilated gas. Because of the effect of heating, air exhaled has a temperature of 37°C, regardless of the temperature of gas inhaled." Table VI of his monograph presents computed projections of respiratory heat loss at 15°C (59°F) and these reflect the influence of his assumption regarding exhalation temperature. For example, with air breathing at 25 liters per minute:

DEPTH (ATM. ABS.)	RESPIRATORY HEAT LOSS (KCAL/MIN)	(KCAL/HR)
1	0.78	46.6
2	0.93	55.6
4	1.23	73.7
8	1.83	109.8

In his excellent review of body heat loss in undersea gaseous environments Webb (35) states that, "The loss of heat in warming cool dry inspired air at 1 Ata is determined by the heat needed to warm the air and to evaporate moisture from the lining of the upper airway. As gas density and specific heat increase, the warming of the gas becomes the dominant element especially since undersea hyperbaric environments are humid. The only unknown is the temperature of the air as it leaves the oronasal portal in expiration. It is not correct to assume that gas leaves at body temperature (37°C), since heat absorbed by the inspired air is returned to the respiratory tract as the warm moist air exits over the previously cooled tissues." In other words, to assume that gas is exhaled at body temperature is to ignore the counter-current heat exchange mechanism of the respiratory passages (19).

U.S. Navy studies (Naval Medical Research Institute - Navy Experimental Diving Unit) on respiratory heat loss from breathing cold gas at high pressures are in publication at this time. Preliminary findings have, however, been communicated. The investigators (Hoke, Jackson, Alexander and Flynn) reported significant problems during bicycle ergometer runs at 800 feet with inhaled gas at 32-35°F: excessive body heat loss, discomfort, shivering and acute respiratory difficulties. They measured respiratory heat loss as high as 780 watts during heavy work (respiratory minute volume = 64 lpm) at 1,000 feet when inhaled temperature was 45°F (7°C). Their conclusions noted that, "These experiments on respiratory heat

loss from breathing cold gases at high pressures show conclusively that at depths beyond 600 feet and water temperatures (i.e. inspired gas temperatures) of 40°F (4.2°C) or less, the results will be progressive negative thermal balance. The rate of heat loss will increase as respiratory minute volume increases at higher work rates. The data show that when respiratory heat loss exceeds about 350 watts the diver will be in danger sooner or later, depending on individual characteristics, because of excessive heat loss. In addition, a certain fraction of divers may exhibit sensitivity to the direct effects of cold gases and produce copious amounts of mucous which can cause acute respiratory difficulty. . . It is difficult to estimate how long any particular diver could withstand an RHL of greater than 350 watts. Therefore, our conclusion is that for safety, thermal comfort, and maximum efficiency, the diver's breathing gas should be heated for dives in excess of 500 feet . . ."

SECTION 2

METHODS AND PROCEDURES

Hyperbaric Facility

All experiments were conducted with the subjects within the wet pot chamber of the Westinghouse hyperbaric facility (Figure 1). Monitoring and surveillance were by direct visual through-port observation and by closed circuit television. Dimensional characteristics of this three-compartment facility are as follows:

CHAMBER	DIMENSIONS (FT)	VOLUME (FT^3)
Entrance Lock	dia 6	102
Main Chamber	dia 8 length 10.3	396
Wet Pot	dia 8.3 length 9.4	346

Saturation Diving

These experiments were performed during the course of a thirteen-day long multi-level saturation dive, May 7- May 19, 1971. Initial compression, and time at 450 feet, was about 1 1/2 days, and just under two days were provided for runs at 650 feet. The remaining time, with excursion diving to 1,000 feet, was at 850 feet depth. The chamber atmosphere composition was 0.3 atm. abs. oxygen, 1.2 atm. abs. nitrogen, balance helium. The usual temperature in the main chamber was 88-90°F. Decompression was in accordance with the following:

DECOMPRESSION SUMMARY

DEPTH (FEET)	TIME (HR. MIN.)	ELAPSED (HR. MIN.)	CLOCK TIME
850-835	1.30	1.30	1600-1730
835-820	2.00	3.30	1730-1930
820	0.30	4.00	1930-2000
820-796	4.00	8.00	2000-2400
796	6.00	14.00	2400-0600

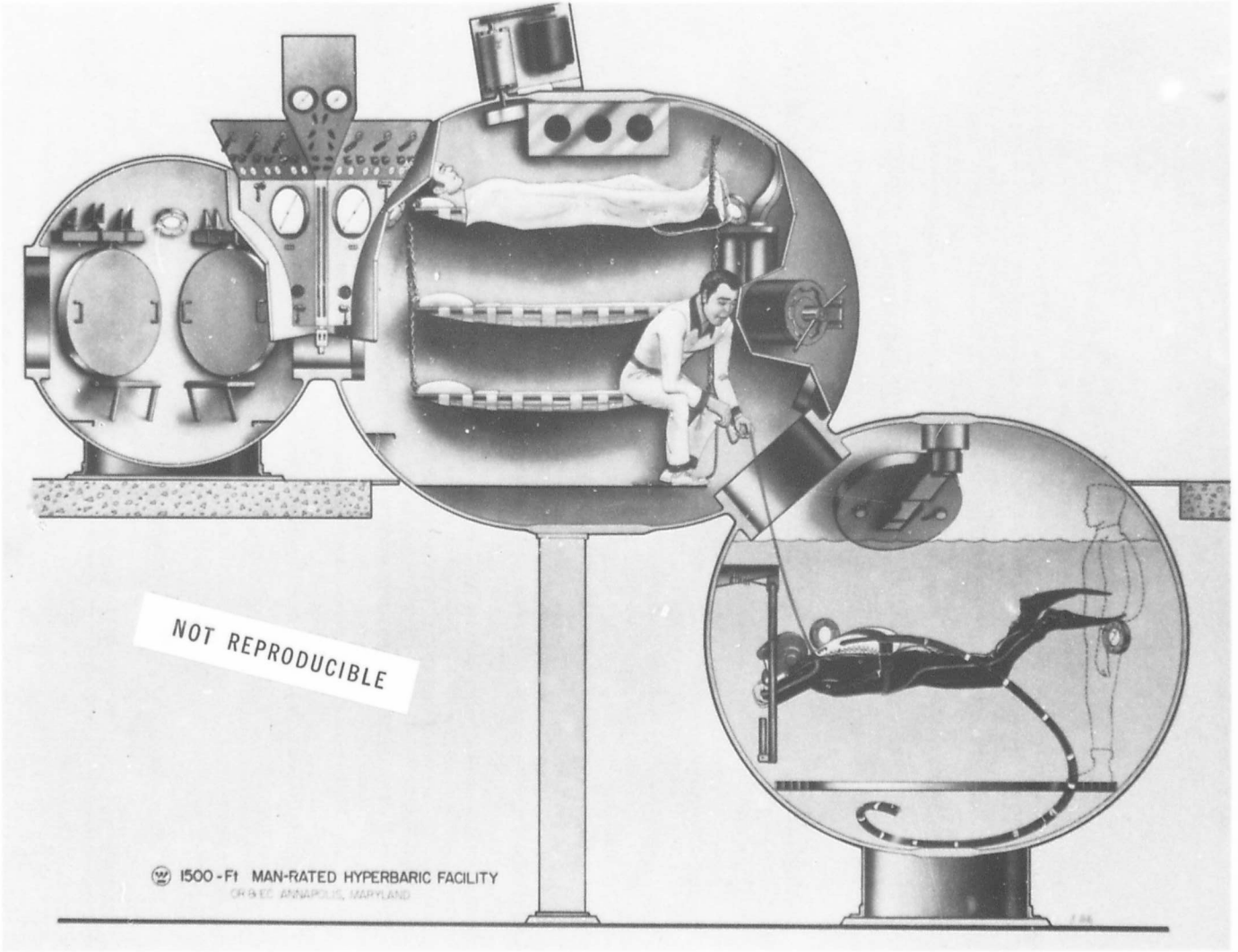

Figure 1. Westinghouse Hyperbaric Facility.

DECOMPRESSION SUMMARY (CONTINUED)

DEPTH (FEET)	TIME (HR. MIN.)	ELAPSED (HR. MIN.)	CLOCK TIME
796-748	8.00	22.00	0600-1400
748	2.00	24.00	1400-1600
748-700	8.00	32.00	1600-2400
700	6.00	38.00	2400-0600
700-652	8.00	46.00	0600-1400
652	2.00	48.00	1400-1600
652-604	8.00	56.00	1600-2400
604	6.00	62.00	2400-0600
604-556	8.00	70.00	0600-1400
556	2.00	72.00	1400-1600
556-508	8.00	80.00	1600-2400
508	6.00	86.00	2400-0600
508-460	8.00	94.00	0600-1400
460	2.00	96.00	1400-1600
460-412	8.00	104.00	1600-2400
412	6.00	110.00	2400-0600
412-400	2.00	112.00	0600-0800
400-370	6.00	118.00	0800-1400
370	2.00	120.00	1400-1600
370-330	8.00	128.00	1600-2400
330	6.00	134.00	2400-0600
330-290	8.00	142.00	0600-1400
290	2.00	144.00	1400-1600
290-250	8.00	152.00	1600-2400
250	6.00	158.00	2400-0600
250-210	8.00	166.00	0600-1400
210	2.00	168.00	1400-1600
210-170	8.00	176.00	1600-2400
170	6.00	182.00	2400-0600
170-130	8.00	190.00	0600-1400
130	2.00	192.00	1400-1600
130-100	6.00	198.00	1600-2200
100-92	2.00	200.00	2200-2400
92	6.00	206.00	2400-0600
92-60	8.00	214.00	0600-1400
60	2.00	216.00	1400-1600
60-50	2.30	218.30	1600-1830
50-33 1/2	5.30	224.00	1830-2400
33 1/2	6.00	230.00	2400-0600
33 1/2-9 1/2	8.00	238.00	0600-1400
9 1/2	2.00	240.00	1400-1600
9 1/2-0	3.10	243.10	1600-1910

Subjects

The panel of diver-subjects was composed of two former U.S. Navy Sealab aquanauts, one of whom was a medical deep-sea diving technician, and a Westinghouse life support group engineer with a background in commercial diving.

SUBJECT	AGE	HEIGHT (IN.)	WEIGHT (LB.)
KC	39	69	170
FA	29	70	153
SZ	27	71	208

Procedure

Since the wet-pot water temperature served to control the temperature of inhaled gas, all swims on a given day at a particular depth were at the same temperature. Each diver-subject made at least one immersion run per full working day. Studies at 450 feet were performed first, followed by compression to, respectively, 650 feet and 850 feet. Runs at 1,000 feet were conducted as excursion dive maneuvers from a saturation level at 850 feet.

When fully dressed, checked out and ready for entry into the cold water in the wet pot the subject descended the ladder and then rigged it to function as an ergometer (described, following). A swim (work) - rest alternation pattern was employed, as follows: dress and enter water, 30 min.; rest and checkout equipment, 10 min.; resting ventilation measurements, 15 min.; light work, 20 min.; rest, 10 min.; moderate work, 20 min.; rest, 10 min.; heavy work, 20 minutes. All measured and derived parameters were referenced to the final portions of each of the four (rest and three work periods) activity levels. These parameters were: inhaled gas temperature, exhaled gas temperature, respiratory minute volume, tidal volume, respiratory frequency, inhalation and exhalation flow rate, exhalation pressure drop, mixed expired oxygen and carbon dioxide fraction, core temperature, skin site temperatures, water and equipment component temperatures.

Water temperatures of exposure were approximately 35°F for runs at 450, 650 and 850 feet, 45 °F for runs at 450, 650, 850 and 1,000 feet, and 55°F for runs at 850 feet only. Each combination of inhaled temperature-depth-activity level (ventilatory volume) was considered as a potential data point for respiratory heat loss. 137 such data points were obtained during the effort.

Breathing Gas Loop

The breathing gas supply was drawn from the main chamber atmosphere at a point about 6 feet from the carbon dioxide canister outflow and one foot above deck level. A positive displacement vane pump (Gast Manufacturing Corporation model 0740-P112A) was employed. The pump was driven by an explosion-proof, Dayton Manufacturing Company electric motor (model 6K040) rated at 0.75 horsepower. Both motor and pump were mounted in a sound-absorbing enclosure and the motor was continually flushed with dry helium. The gas stream was filtered at the pump intake and output (Gast Manufacturing Corporation model B343B and Wilkerson microalescer model 1206-4 filters, respectively). The filtered gas was pumped from the main chamber to the wet pot through approximately 6 feet of 1.5 inch polyethylene hose.

Underwater in the wet pot the gas passed through a submerged cooling coil consisting of 25 feet of 0.5 inch internal diameter copper tubing, a water trap (Bastian-Blessing Company model 8824) at the lowest point of the supply loop, three feet of 0.5 inch internal diameter copper tubing and a 1.5 inch polyvinyl chloride tee-fitting to which a flexible hose and breathing bag was attached.

The breathing bag (see Figure 2) which was inserted in the gas supply line to provide sufficient demand volume for peak inspirations was an Ohio Chemical and Surgical Equipment Company 5 liter rubber anesthesia bag (number 211-2800-100). The center of the breathing bag was at the approximate level of the diver's chest, about two feet below the water surface. It was secured there with a wire frame and rigid support. A flexible hose (Warren E. Collins, number P-521, 1.5 inch internal diameter reinforced polyethylene) connected it to the breathing loop and the gas supply.

The gas supply entered into the breathing gas circuit via a 1.5 inch polyvinyl chloride tee-fitting where it was divided into streams flowing through an exhaust flapper check valve and through a mushroom-type check valve to the mouthpiece breathing valve. The exhaust flapper valve was a Sadd valve (Warren E. Collins no. P-303-1) and the mouthpiece check valves were of the "V" type (Warren E. Collins no. P-315). A rubber mouthpiece (Warren E. Collins no. P-530) was also fitted to the mouthpiece breathing valve body which had been machined from a one inch internal diameter polyvinyl chloride tee-fitting. The inhalation-exhalation thermistor protruded downwards through the vertical aspect of the tee-fitting with

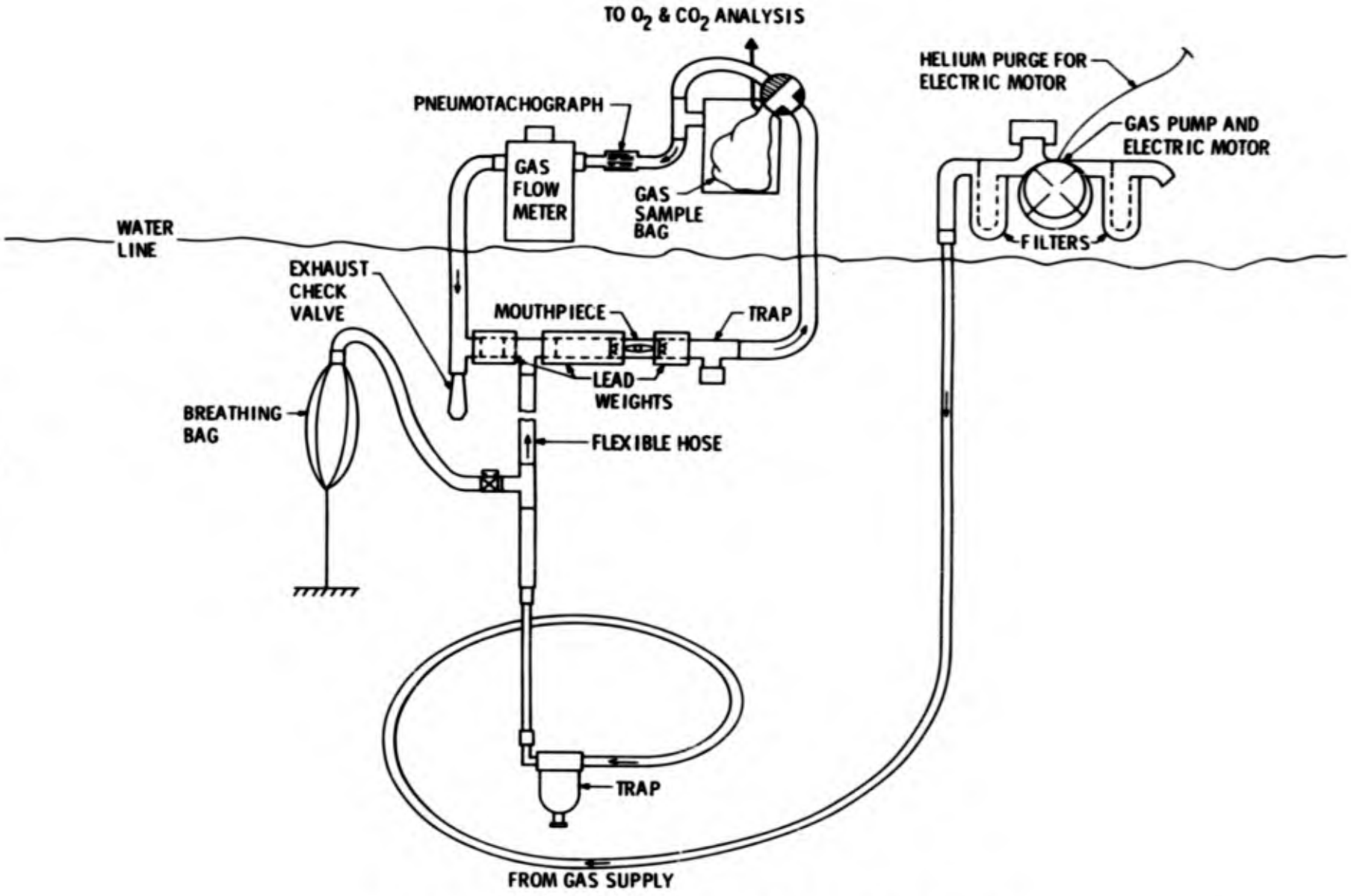

Figure 2. Gas Chilling, Delivery and Breathing System.

the thermistor bead itself exposed at a distance of 0.45 centimeters into the air stream. The maximum protrusion of the protective guard wires was 0.96 centimeters. The thermistor was located 2.2 centimeters from the inhalation and exhalation mushroom check valves and was at a distance of 5.2 centimeters from the cavity margin of the rubber mouthpiece. A saliva trap was placed about 10 centimeters downstream from the exhalation check valve. The mouthpiece breathing valve assembly was weighted with lead to maintain neutral buoyancy.

Suitable lengths of 1.5 inch internal diameter flexible hose conducted the exhalation gas stream vertically up into the main chamber and through the mixed expired gas sampling device, the pneumotachograph head and the dry gasometer (see below). Finally, the flow passed through the above-mentioned exhaust flapper check valve. This latter valve was on the same rigid mount as the divers' mouthpiece and was so placed that its location was at the divers chest level. Thus, the valve outlet was actually located about 2 feet below the water surface level and the entire breathing loop was thereby maintained at a slight positive pressure (about 1 pound per square inch gauge). A United States Gauge Company model 19693 pressure gauge at the pump outlet measured this pressure. (Also see Appendix 3).

Volume, Flow and Pressure Measurements in the Breathing Loop

The dry gasometer was a Parkinson-Cowan type CD-4 which had been modified (Figure 3) so that the inlet and outlet gas flow connections were oriented horizontally instead of vertically. The gasometer was fitted with a potentiometer and an electrical output corresponding to revolutions of the ten liter scale were obtained and recorded on a channel of a Electronic Instrumentation Associates model 1910 recorder. The gasometer was compared to standards at the Standardizing Laboratory at the Westinghouse Defense and Space Center, Baltimore, Maryland, using shop air in the range of 5 to 50 standard liters per minute. The uncertainty of measurement was reported as less than 0.5 standard liters per minute and of voltage as less than 1 millivolt.

The flow measuring system included a Fleisch pneumotachograph size 3, a Honeywell Accudata 113 bridge/DC amplifier and a channel on the Electronic Associates model 1910 recorder. The pneumotachograph was heated during operation. Gas temperature was monitored upstream and downstream of the pneumotachograph head using Yellow Springs Instrument Company type 421 thermistor probes. A Statham Instruments Inc. PM 97 TC-350 0.05 PSID pressure transducer was used to sense pressure drop across the pneumotachograph tubules. (Also see Appendix 4).

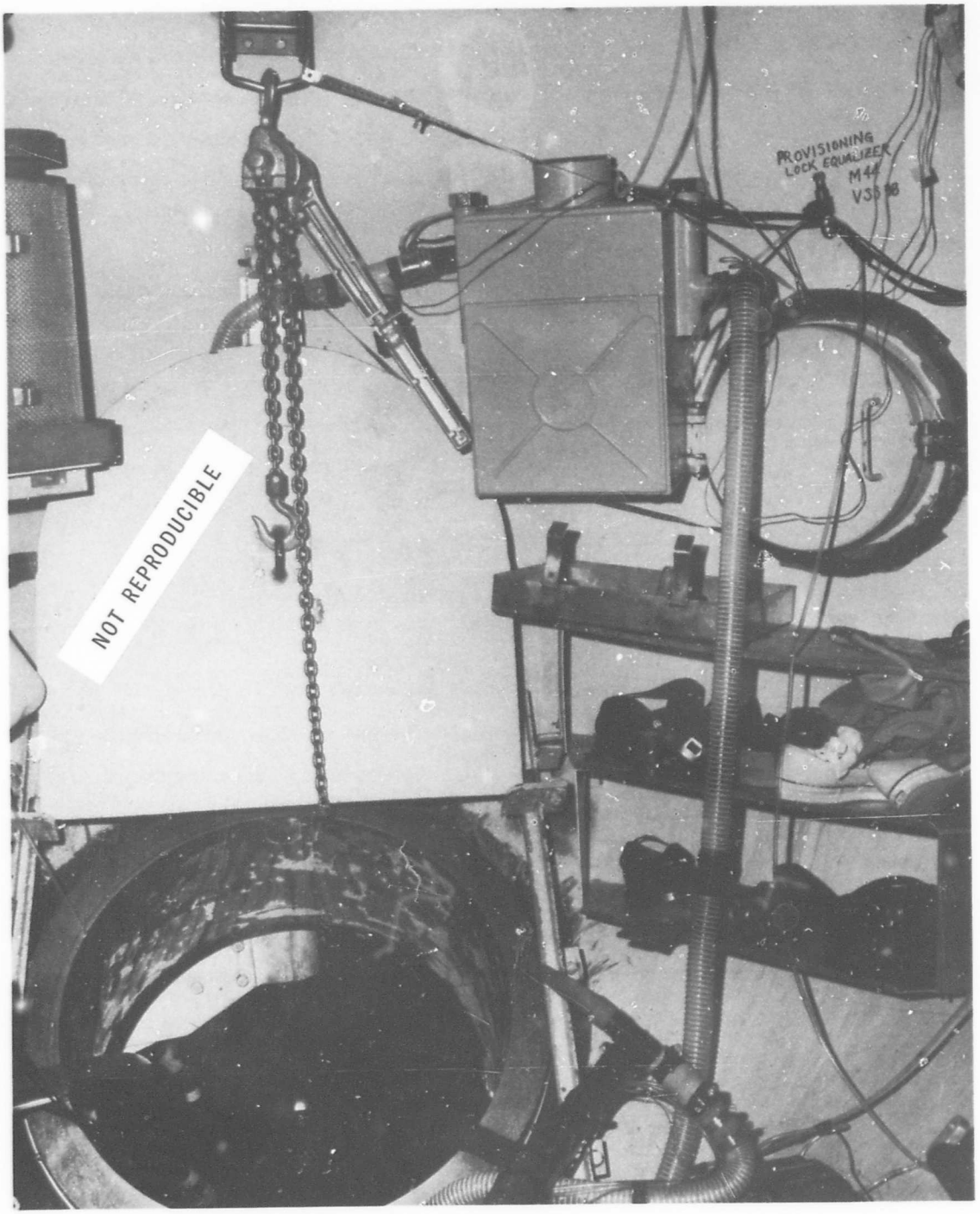

Figure 3. Interior of Main Chamber, Showing Modified Parkinson-Cowan Type CD-4 Gasometer.

One side of a Statham Instruments Inc. PM 60 TC-350 0.15 PSID differential pressure transducer was connected via a flush tap to the central cavity of the mouthpiece breathing valve. The other side, referenced to the same location on the external surface of the valve body, was kept free of water by means of a trickle flow of helium from the same source which supplied the pump and motor enclosure. This signal was processed with a Honeywell Accudata 113 bridge/DC amplifier and recorded with the Electronic Associates model 1910 recorder.

Oxygen - Carbon Dioxide Analysis

Mixed expired gas was collected during the final minutes of each of the 139 immersion tests. The gas sampling system (Figure 4) consisted of a 30 liter neoprene latex meteorological balloon (Warren E. Collins no. P-342-30) mounted inside a five gallon polyethylene container. The gas sample bag inlet valve (Warren E. Collins no. P-321) was normally open, allowing the gas stream to bypass the bag. During sampling the gas entering the bag displaced gas enclosed within the surrounding rigid container into the breathing gas loop, replacing the sampled volume. The outlet tee-fitting from the polyethylene container was a 1.5 inch polyvinylchloride fitting. The polyethylene container was also modified with a transparent lucite window for observing the degree of inflation of the enclosed balloon. Gas for analysis was withdrawn via tygon tubing affixed to the sampling port of the inlet stop-cock valve, through internal and external hull valves and fittings. A custom-manifold of needle valves, filters and rotometer flowmeters was used to divide the controlled flow through a Beckman Instruments Co. model E-2 oxygen analyzer and IR-315 carbon dioxide analyzer. Samples of this mixed expired effluent were also collected for Scholander microgasometric analysis.

Inhalation and Exhalation Temperature Measurement

A micro-bead thermistor (Victory Engineering Corporation type E31A401C) was used to measure the temperature of respired gas. The thermistor bead is about 0.005 inches in diameter and is mounted on 0.00075 inch diameter wires. Its time constant in still air is 0.12 seconds. The time constant in helium at 30 atmospheres absolute pressure with a flow of 100 feet per minute is 0.0102 seconds. Other characteristics of this thermistor are as follows: resistance approximately 1000 ohms at 25°C with a temperature coefficient of -3.2% per degree C at 25°C; dissipation constant approximately 0.045 MW/°C in still air. The

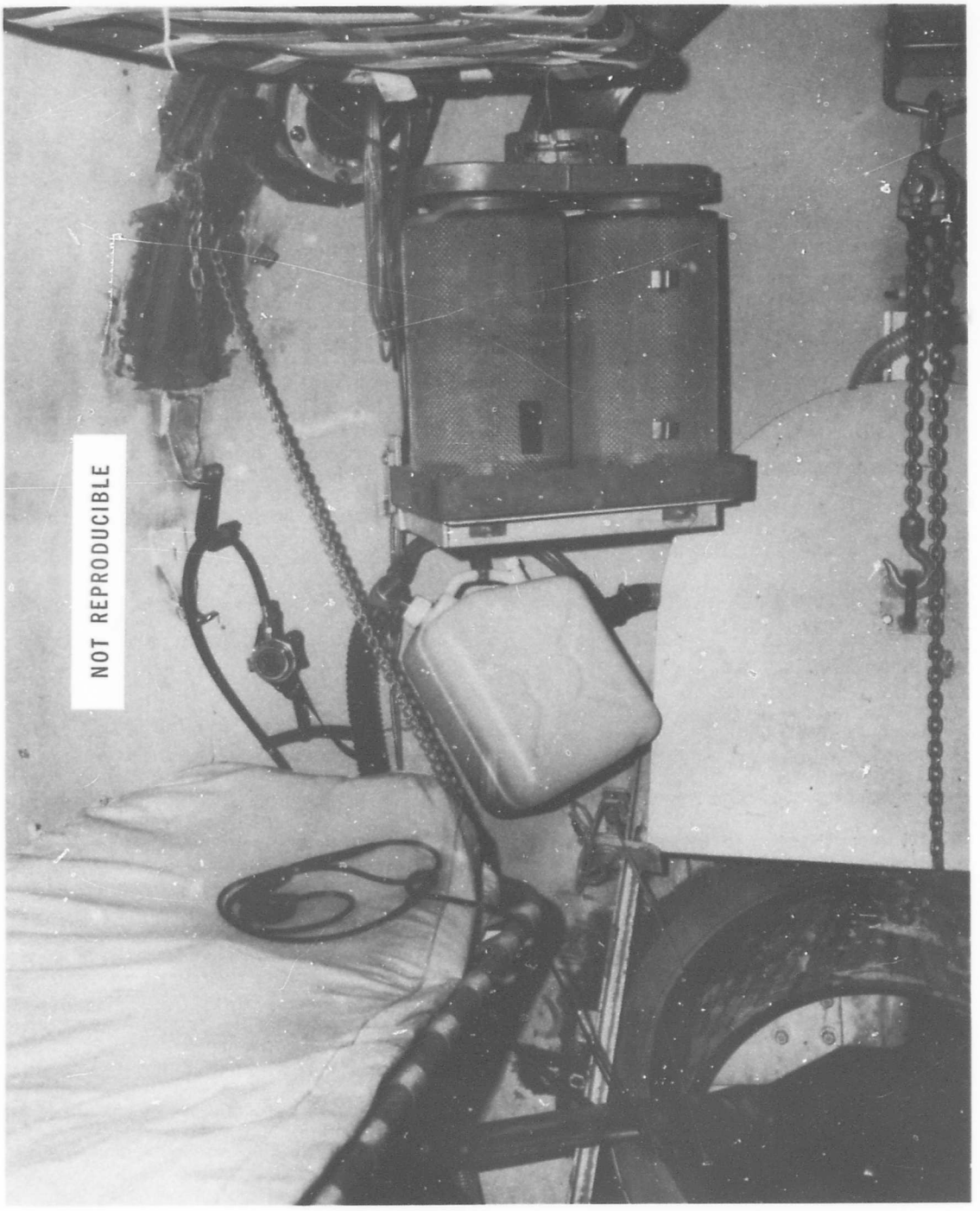

Figure 4. Interior Of Main Chamber, Showing Rigid Container for Mixed Expired Gas Collection Bag.

thermistor is mounted on a Victory Engineering Corporation TO-18 type header, and the thermistor-header was further protected by means of a pair of guard loops of number 24 gauge wire which crossed and surrounded the thermistor at a distance of not less than 16 diameters.

The signal conditioning bridge was designed to produce an output of 0-20 millivolts direct current for a temperature span of 0-40°C. Linearity was ±0.4°C over this range and was attained by means of the equal slope criterion and the linearity equation supplied by the manufacturer. The maximum self heating error, despite the low dissipation constant of the thermistor, was 0.1°C. A stabilized mercury cell (Mallory RM-12R) was used to obtain a constant voltage source for the bridge. Variations were less than ±0.1%.

The recorder was a Texas Instruments Company, Servo/Riter II model FS01N6B, and provided a 6-inch span for 0-20MV DC. The chart was readable to 0.1°C. For a span step response of 0.4 seconds the recorder accuracy was ±0.25% and linearity was ±0.1%. Recorder input impedance was matched to the load of the bridge.

Calibration of the complete system provided a correction curve which was applied to the raw data. Based on combined time response accuracies, a total step response of not less than 99.6% in 0.5 seconds was attained.

Thermistor mounting and location in the mouthpiece is described, preceding (see above), concurrently with other components of the breathing gas loop.

Appendix 2 provides further engineering documentation regarding the selection and use of the inhalation-exhalation thermistor.

Other Temperature Measurements

Skin site temperatures were obtained using Yellow Springs Instrument Company type 409 thermistors fastened to the divers with Band-Aid clear tape, as follows (Figure 5):

Thermistor No.		Location
1.	-	Head - on the neck below the hairline and behind the right ear
2.	-	Arm - on the lateral surface of the right biceps
3.	-	Chest - just above the right nipple

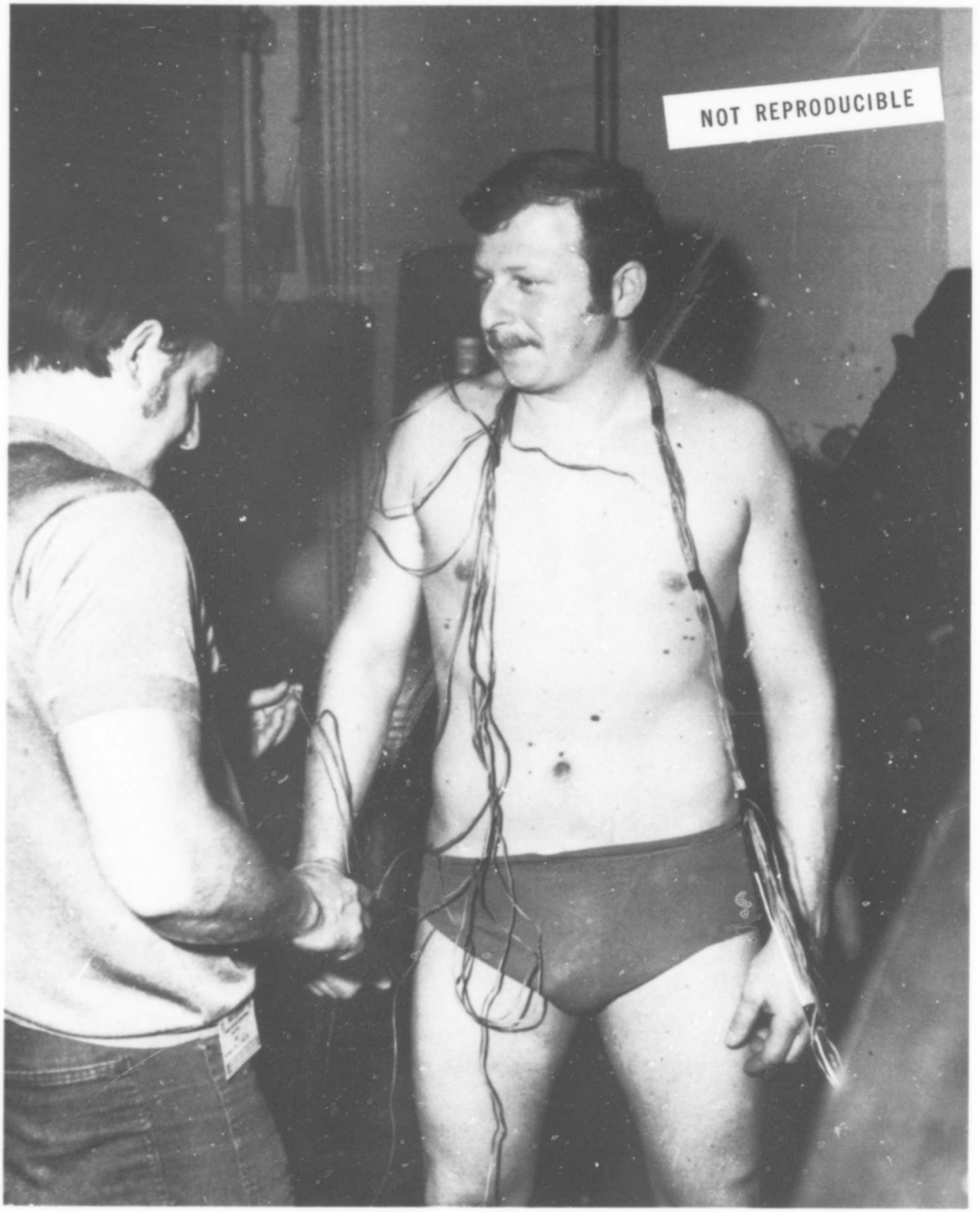

Figure 5. Subject Being Outfitted With Thermistor Harness.

Thermistor No.		Location
4.	-	Back - on the surface of the right scapula
5.	-	Thigh - on the lateral surface of the right thigh
6.	-	Calf - on the lateral surface of the right calf
7.	-	Finger - on the medial surface of the right second phalange midway between the tip and the first joint
8.	-	Toe - on the medial surface of the right large toe midway between the tip and the first joint
10.	-	Forearm - on the lateral surface of the right forearm

Mean weighted skin temperature was computed according to the method of Teichner (29):

Tmws = 1.5 (T chest + T back + T thigh +T calf/8 + T head/10 + T arm/14)

Additional temperature recording was done with thermistors placed in the following locations:

Thermistor No.		Location
9.	-	Rectum - inserted approximately 9 centimeters beyond the anal verge
11.	-	in the wet pot water approximately at diver level and 4 inches from the hull
12.	-	in the hot water umbilical flow 1 inch from suit connection
13.	-	inside the suits, various locations
14.	-	on the gas pump housing
15.	-	on the electric motor housing
16.	-	in the gas stream immediately prior to the pneumotachograph
17.	-	in the gas stream immediately after the pneumotachograph and prior to the gasometer
18.	-	in the gas stream immediately after the gasometer

The precise location for the wet pot thermistor was found through prior investigation not to be critical when the chiller pump was operating and circulating the water. Thermistor 12 was placed in the umbilical rather than switching it among the various suits. The function of thermistor 13 was to establish an exit temperature for the hot water leaving the suit. Thermistors 14 and 15 were used as safety monitors in the event the pump or motor began to fail and overheat.

Yellow Springs Instrument Company series 400 probes were employed for these measurements. The bridge was designed using linearization criteria and computer data processing in the same manner as the inhalation-exhalation thermistor bridge. Because of the higher dissipation constants of these probes an output of 0-40 millivolts DC was provided for a range of 0-40°C. Probes used to measure skin temperatures, gas temperatures (other than respired gas) and water temperature (YSI type 409) have a time constant of 1.7 seconds in stirred water. The rectal probe, YSI type 401, has a time constant of 7 seconds in stirred water.

A Hewlett-Packard model 2900D scanner selected the thermistor to be monitored and connected it to a digital voltmeter (Hewlett-Packard model 3460D). This provided a visual output and a signal to a Hewlett-Packard model 5050B digital printer which printed the temperature in 4 digits on a paper tape.

Calibration for Temperature Measurement

An Anschutz fractional degree, precision grade, Centigrade thermometer, range -12 to 61°C, certified by the National Bureau of Standards, and accurate to 0.2°C was used for calibration checks before and after the dive. Overall steady state accuracy of the thermistor-recorder systems after adjustment for calibration was within 0.3°C.

Ergometer

A spring-and-weight trapeeze ergometer was deployed underwater in the wet pot and provided the means of achieving serially increasing ventilatory volumes in response to the swimming work efforts thus applied. Since ventilatory volume, rather than simulated speed at thrust output was the parameter of interest, the assembled ergometer was not calibrated in units of work or work equivalents.

The variable, which was displayed to the swimming diver (Figure 6) and to topside (Figure 7) was displacement. A pointer, fastened to the ladder-trapeeze at the diver position, was situated several inches from the prone diver's face and indicated position in inches from the wall. A light cable directed vertically across a porthole, counter-weighted and with a pointer displayed the trapeeze position to topside supervisors. The movement of the ladder-trapeeze, as the diver pressed against the horizontal swim bar, was from a vertical, free-hanging position to a small angle where the base of the ladder contacted the chamber hull. The zero position was thus established at this hard-into-the-hull position, and displacement was marked in inches from the hull at the swim bar, 29 inches from the pivot.

The weight and spring loadings were applied at a greater distance, 41 inches from the pivot, thus causing an amplification of (41/29 = 1.41) force to the diver. For this application 5 lbs. of lead divers' weight-belt weights were used in a reverse pull arrangement (see Figure 8). A spring (K=1 lb./inch) was mounted at the end of the trapeeze to provide an increase in load such that it was the maximum at maximum displacement from the vertical. The operating range was thus measured from the hull, beginning with an arbitrary zero in that position and the load decreased as the distance from the hull increased. The divers were thus swimming against a force that was a combination of the amplified weight loading and the horizontal component of the spring. It was felt that the divers could better regulate their swimming thrust output by working against an increase in load over a short displacement. In operation, the divers swim at a rate to displace the ladder to markings on the indicator.

Suit Description

The suits worn during all tests were free flooding hot water suits style Diving Unlimited Mk XAD. The suit is of one piece construction which includes torso, hood, arms, and legs sections. Boots and gloves are worn as separate items. The suit is a nominal 1/4 inch neoprene foam with nylon on each side.

Hot water enters the suit at a manifold block on the right hip, from which it is directed into six outlet tubes. One tube leads to each of the arms and legs, one to the front of the body, and one to the back and head (Figure 9). Each tube has exhaust ports which vary in

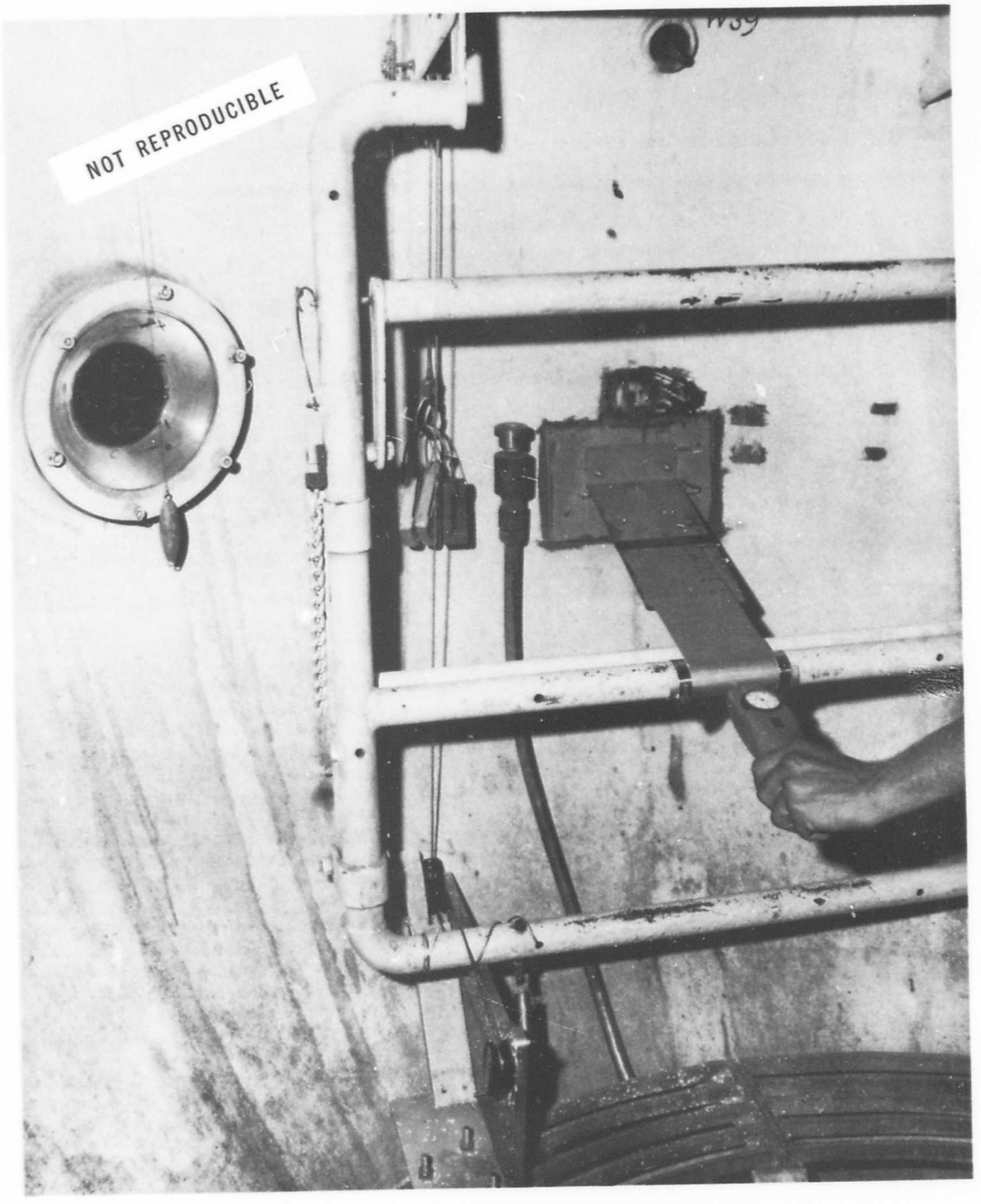

Figure 6. Interior Of Wet Pot, Showing Ergometer And Diver Display Device.

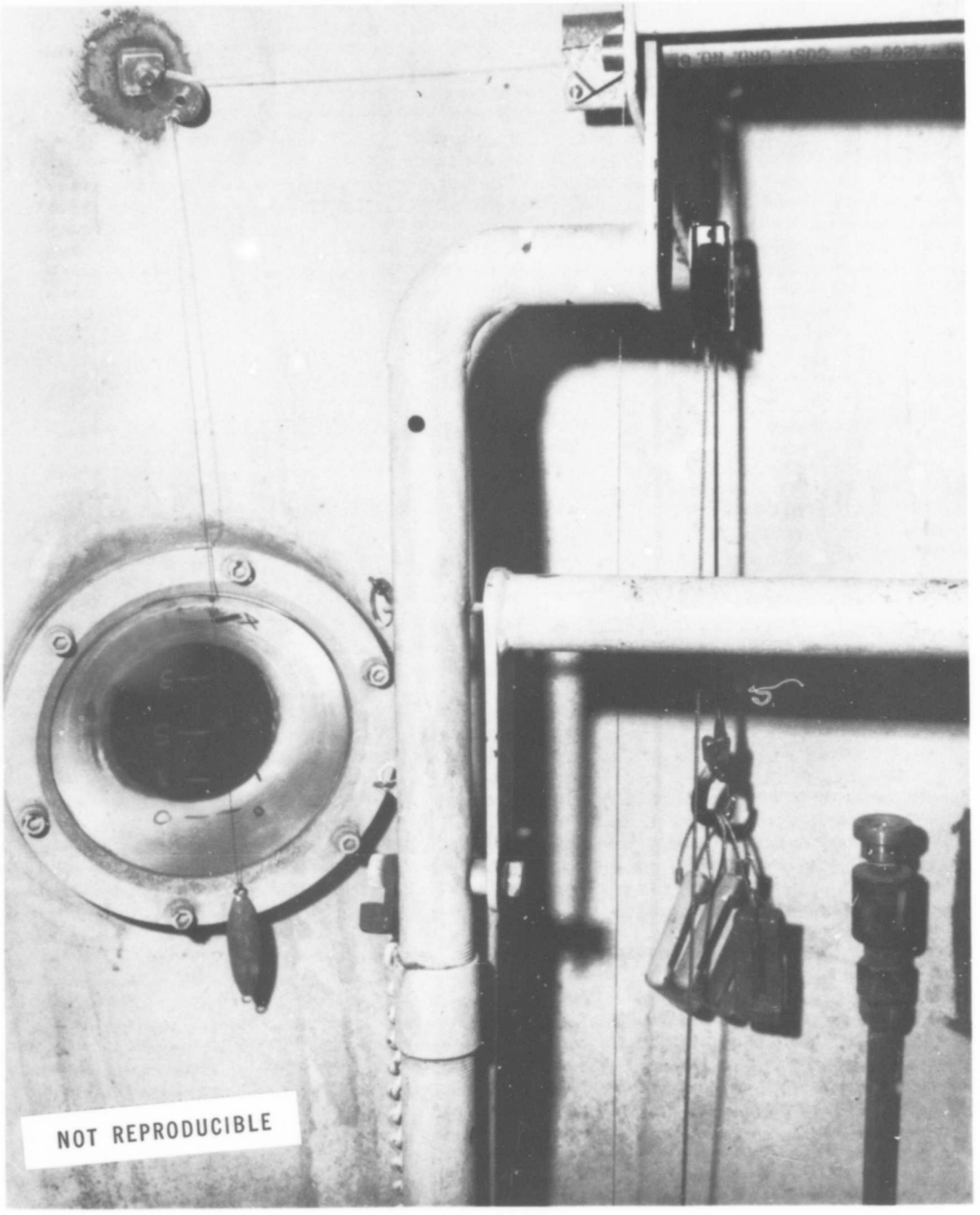

Figure 7. Interior Of Wet Pot, Showing Ergometer and Topside Display Method.

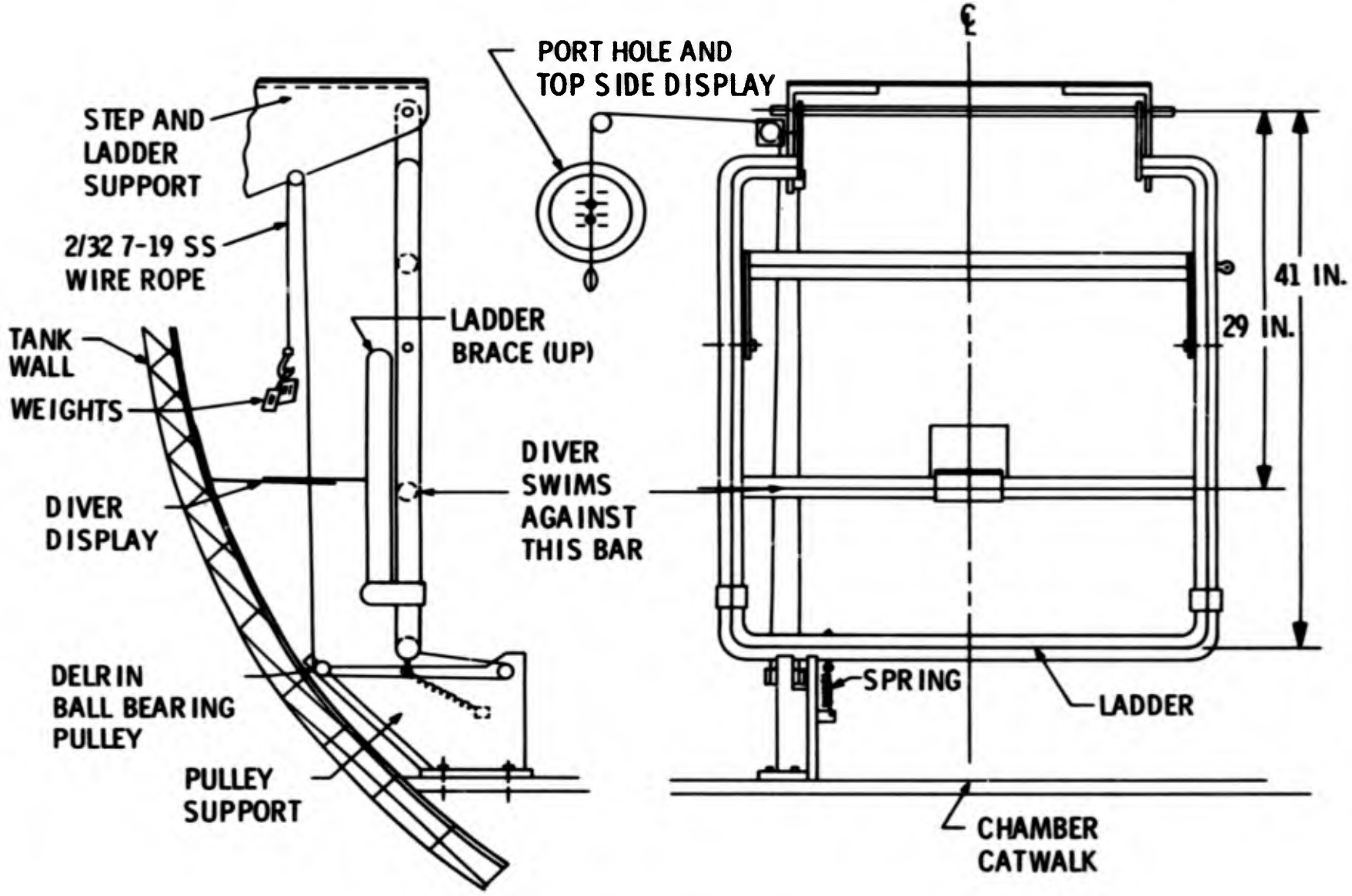

Figure 8. Ergometer Layout Drawings.

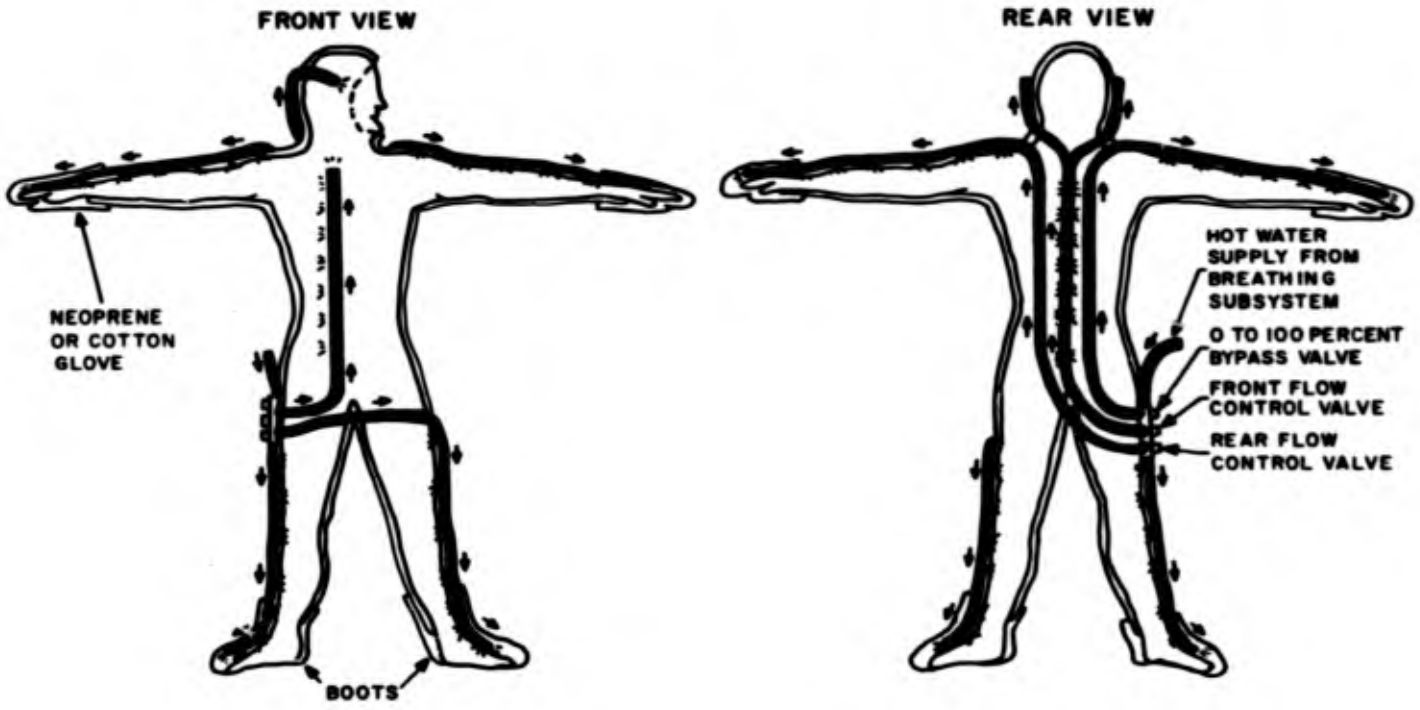

Figure 9. Hot Water Suit Flow Distribution.

size according to regional body hot water requirements. Soft flexible tubes extend beyond the wrists and ankles, and feed water to the hands and feet. The water exits the suit at the wrist, ankles, and neck in undetermined proportions.

Approximately 1/2 inch of clearance is required between the suit and the diver's body for efficient circulation of the hot water. Diver subjects were measured and suits ordered which would provide adequate clearance after a 5% shrinkage with compression. A nominal 1/8 inch neoprene foam suit consisting of pants and jacket was worn under the free flooding suit.

The suit manifold block consists of three valves for regulating the amount of umbilical water flow into the suit, to the front of the body, and to the back and head, respectively. During the test swims the valves were maintained in full open position. Hot water flow into the suit was maintained at 2.0-2.25 gallons per minute and inlet temperature to the suit at 105-107°F for the 450 and 650 feet runs and at 110°F for the 850 and 1000 feet runs. These water flow rates and temperatures were controlled topside.

Calculation of Respiratory Heat Loss

Heat lost from the respiratory tract due to heating and humidification of the breathing gas can be calculated using the following equation:

$$Q_r = V_g \quad \rho_g \, Cp_g \, (Te-Ti) + V_g \quad \rho_g \quad h_{fg} \, (We-Wi) \qquad (1)$$

Q_r = respiratory heat loss, Btu/hr.

V_g = Respiratory rate, ft^3/hr.

ρ_g = gas density, lbm/ft^3

Cp_g = gas specific heat, Btu/lbm °F

Te = temperature of expired gas, °F

Ti = temperature of inspired gas, °F

h_{fg} = latent heat of vaporization, Btu/lb_w

We = humidity ratio of expired gas, lb_w/lb_g

Wi = humidity ratio of inspired gas, lb_w/lb_g

lb_w = pounds of water vapor

lb_g = pounds of dry gas

The first group of terms, $V_g \rho_g Cp_g (Te-Ti)$, is the heat required to raise the temperature of the inspired gas to the expired temperature, and is known as sensible heat. The second group of terms, $V_g \rho_g h_{fg} (We-Wi)$, is the heat required to vaporize the water which is added to the gas from the respiratory epithelium and is known as insensible heat.

The humidity ratio, W, can also be expressed as a ratio of the products of the molecular weights and partial pressures of the water vapor and dry gas.

$$W = \frac{M_{H_2O} \; P_{H_2O}}{M_g \quad P_g} \quad \text{and,} \tag{2}$$

$$We-Wi = \frac{M_{H_2O}}{M_g} \frac{(P_{H_2O_e} - P_{H_2O_i})}{P_g} \tag{3}$$

Where

M_{H_2O} = molecular weight of water vapor

M_g = molecular weight of gas

$P_{H_2O_e}$ = expired vapor pressure, psi

$P_{H_2O_i}$ = inspired vapor pressure, psi

P_g = pressure of dry gas, psi

To utilize the quick response of the computer system (Univac 1108 and teletype terminals), and to facilitate computer program writing and debugging basic language), equation (1) was rewritten into three parts (1) sensible gas, (2) sensible water vapor, and (3) insensible water vapor:

$$\underset{(1)}{Q_r = V_g \; \rho_g \, Cp_g (Te-Ti)} + \underset{(2)}{V_g \; \rho_g \; W_i \; Cp_{H_2O} (Te-Ti)} +$$

$$\underset{(3)}{\frac{h_{fg} \; V_g \; \rho_g \; M_{H_2O} \; (P_{H_2O_e} - P_{H_2O_i})}{M_g \quad P_g}} \tag{4}$$

The composition of inhaled and exhaled gas was calculated using measured values for oxygen and carbon dioxide.

The nitrogen component of chamber atmospheric gas was estimated at 1.11 atmospheres absolute partial pressure. This was based upon an initial pressurization to 15 feet using air. This resulted in an oxygen partial pressure of 0.3 ata and a corresponding nitrogen partial pressure of 1.2 ata. During the dive the provisioning lock was pressurized using helium resulting in a loss of 0.4 ata nitrogen for the volume of gas in the lock. Make-up gas for the chamber was 100% helium. A main chamber atmosphere gas sample obtained on the final day at 850 feet showed an oxygen plus nitrogen percentage of 5.28%. Since chamber atmosphere oxygen composition was 1.12%, the nitrogen composition was 5.28 - 1.12 = 4.16%, and, at 850 feet, the nitrogen partial pressure therefore was 1.11 atmospheres absolute.

The density of the expired gas was calculated using:

$$\rho_g = \frac{(P_e - P_{H_2O_e})\,144}{T_e\,R_e}, \tag{5}$$

in which the subscript e stands for expired values, and Re is the expired gas constant which was calculated as follows:

$$R_e = \frac{\%O_2\,M_{O_2}\,R_{O_2} + \%CO_2\,M_{CO_2}\,R_{CO_2} + \%N_2\,M_{N_2}\,R_{N_2} + \%He\,M_{H_e}\,R_{H_e}}{\%O_2\,M_{O_2} + \%CO_2\,M_{CO_2} + \%N_2\,M_{N_2} + \%He\,M_{He}} \tag{6}$$

The expired gas specific heat is:

$$Cp_e = \frac{\%O_2\,M_{O_2}\,Cp_{O_2} + \%CO_2\,M_{CO_2}\,Cp_{CO_2} + \%N_2\,M_{N_2}\,Cp_{N_2} + \%He\,M_{He}\,Cp_{He}}{\%O_2\,M_{O_2} + \%CO_2\,M_{CO_2} + \%N_2\,M_{N_2} + \%He\,M_{He}} \tag{7}$$

Equations (6) and (7) convert volume percent to mass fraction.

The latent heat of vaporization was taken as 1045 Btu/lbm, corresponding to a vaporization temperature of 85°F.

Equations (8), (9), and (10) for specific heat of O_2, CO_2, and H_2O as a function of temperature were taken from Van Wylen (30). These equations were determined

for one atmosphere of pressure, and although they will change with pressure the overall effect on the specific heat of the gas mix is small:

$$Cp_{O_2} = \frac{1}{32}\left(11.515 - \frac{172}{\sqrt{T}} + \frac{1530}{T}\right) \tag{8}$$

$$Cp_{CO_2} = \frac{1}{44.01}\left(16.2 - \frac{6.53 \cdot 10^3}{T} + \frac{1.41 \cdot 10^6}{T^2}\right) \tag{9}$$

$$Cp_{H_2O} = \frac{1}{18.016}\left(19.86 - \frac{597}{\sqrt{T}} + \frac{7500}{T}\right) \tag{10}$$

A similar equation was given for nitrogen, but values calculated for low temperatures did not agree with corresponding values from other sources. Assuming a constant value of 0.247 Btu/lbm°F results in an error of less than 1% for the nitrogen fraction, or 0.04% for the mixture. The specific heat of helium is essentially constant at 1.24 Btu/lbm°F.

Since expired volume was measured with a dry gasometer a correction was made for the difference between the gasometer temperature and the expired temperature.

Vapor pressure was calculated using the formula for saturation pressure versus temperature from Smith, Keyes and Gerry (25):

$$\log_{10}\frac{218.167}{P_{H_2O}} = \frac{X}{T}\left[\frac{3.2437814 + 5.86826\ 10^{-3}\,X + 1.1702379.10^{-8}X^3}{1 + 2.1878462.10^{-3}X}\right] \tag{11}$$

where X = (647.27-T), °K P is in int. atm.

The computer could not solve this directly and an iteration procedure was used.

Units of the British Technical System were used for this calculation because of the abundance of data in engineering texts and references. Once heat loss is calculated in Btu/hr multiplying by 0.292833 converts the answer to watts, and mutiplying by 0.253 converts the answer to Kcal/hr. Similar conversions could be applied for density or specific heat if required.

The following assumptions were made:

1. Ideal gas laws apply for individual gases and ideal solutions are formed at every temperature and pressure. No data were found for thermodynamic properties of helium-oxygen mixtures and especially not for mixtures of helium-oxygen-nitrogen-carbon dioxide-water vapor.

2. Inspired gas is saturated at the inspired temperature. The temperature in the chamber was approximately 90°F and the relative humidity estimated at 50-80%. The resultant dew point was well above 55°F, the temperature of the warmest inspired gas.

3. Expired gas is saturated at the expired temperature.

4. Expired temperature is the mean expired temperature.

The complete computer program for calculating respiratory heat loss is included in Appendix 1.

SECTION 3

RESULTS

Respiratory Heat Loss

The 137 sets of measurements and the computed magnitudes of respiratory heat loss are listed consecutively, in Table I, in the order in which the data was obtained. Three sets of data are missing because the exposures were aborted voluntarily by the divers. The data number indicates the sequential data point in the total experiment and the run number indicates a diver-subject in the water. The next two columns index the data by depth in feet of seawater and by nominal water temperature in °F. TI and TE denote inhalation and exhalation temperature, respectively. Respiratory minute volume (RMV) is in liters per minute (BTPS). These values are slightly higher than the measured volumes exhaled, due to the correction to 37°C. Values of respiratory heat loss (RHL) were calculated using the respiratory minute volume at exhalation temperature. That portion of respiratory heat loss due to vaporization of water is shown as insensible heat loss in Kcal/hr. The final three columns are respiratory heat loss in units of Kcal/hr, Btu/hr and Watts.

Table I shows the essential components of the heat loss equation previously explained. The notable exceptions are the densities and specific heats of the breathing gases. Since these are relatively constant for a given depth, typical values are included below for the helium-oxygen-nitrogen-carbon dioxide mixes exhaled:

Depth (feet)	ρ (lb_m/ft^3)	Cp (Btu/lb_m-°F)	ρ Cp (Btu/ft -°F)
450	.292	.684	.199
650	.391	.715	.280
850	.491	.731	.358
1000	.565	.735	.415

Respiratory heat loss in Kcal/hr is illustrated as a function of respiratory minute volume in figures 10, 12, and 14. Figure 10 shows the calculated values derived from data acquired during the swims in 35°F water at depths of 450, 650, and 850 feet. Since the exhalation temperature did not vary significantly with depth, and the gas mixture was constant for a given depth, the relationship between RHL and RMV was expected to be linear. The magnitude of heat loss for a given RMV will be proportional to the density and specific heat of the gas mixture. This can be seen more clearly in Figure 11 which is the least squares regression for the data at each depth. The difference in heat capacity of the gas respired at 450 feet and at 650 feet is approximately the same as the heat capacity difference between the gas at 650 feet and 850 feet. This is seen in the regression coefficients for the different depths.

Figure 12 presents respiratory heat loss as a function of respiratory minute volume for data taken during swims in 45°F water. All data runs at 1000 ft were in 45°F water and these results are included in this figure. As anticipated, the difference between the slope of the 1000 ft data regression and the 850 ft data regression is less than slope differences for the other pairs of depths. The regression coefficients are shown in Figure 13.

Results at 850 feet are seen in Figure 14. The influence of changes in water (inhaled) temperature is also shown in Figure 15 (regression coefficients for RHL at 850 ft).

The insensible heat loss due to vaporization of water in the respiratory tract ranged between 5 and 26 Kcal/hr. This is plotted as percent of total respiratory heat loss (Figure 16). The respired gas was saturated at the inhalation temperature and assumed to be saturated at the exhalation temperature, which was considerably less than body core temperature. The variations in insensible heat loss with inhalation temperatures can be seen in Table I. Because the ranges of the different temperatures overlap considerably, the median and extreme values are marked for each depth.

Exhalation temperature as a function of inhalation temperature is shown in Figure 17. The exhalation temperature does not vary appreciably with depth and the total regression equation is TE = 22 + 0.649 TI. Figure 18 shows the inhalation-exhalation temperatures at 850 ft.

The mean respiratory minute volume for each diver-subject run was determined by dividing the total measured exhalation volume by the total elapsed time of the run. Since mean values of oxygen uptake and inhalation-exhalation temperature difference were required it was necessary to determine weighting factors for each of the four measurement periods, and for the rest periods during which no measurements were taken. The best correlation between measured mean RMV and the mean RMV calculated using weighting factors was found when the mean respiratory volume for the second and third rest periods equaled the respiratory volume for the light work period. Table II lists averaged measurements calculated using this weighting technique. The first three columns index the exposure according to run number, depth in feet and water temperature in °F and °C. Average Δ (TE-TI) is listed in column 5. The next three columns show the thermal imbalance of the diver's body as indicated by change in temperature. An average total body temperature is calculated using one third of the mean weighted skin temperature (Tmws) and two thirds of the rectal (core) temperature (Tr) (Burton, ref. 7). The change in total body temperature then becomes $\Delta T_b = 1/3\ \Delta Tmws + 2/3\ \Delta Tr$. The change in Tmws is listed in column 6, the change in Tr in column 7, and the change in T_b in column 8. The last two columns show the mean respiratory minute volume (LPM, BTPS) and mean respiratory heat loss in kilogram-calories per hour.

Body Heat Balance

The mean weighted skin temperatures for each diver exposure are presented in Table III. These were calculated according to the method of Teichner, described earlier.

TABLE I

Results Of Respiratory Heat Loss Calculations

DATA NO	RUN NO	DEPTH FT	TW F	TI C	TE C	RMV LPM	INSEN Q KCAL/HR	RHL KCAL/HR	RHL BTU/HR	RHL WATTS
1	1	450	45	7.1	24.5	11.2	5	40	159	47
2	1	450	45	6.7	23.8	20.1	9	71	279	82
3	1	450	45	6.7	24.5	22.8	11	83	329	96
4	1	450	45	6.5	23.8	35.1	16	124	489	143
5	2	450	45	6.3	23.0	15.8	7	54	214	63
6	2	450	45	6.3	23.6	23.5	11	85	334	98
7	2	450	45	6.1	23.8	26.5	12	97	382	112
8	2	450	45	6.1	23.8	28.4	13	103	407	119
9	3	450	45	5.9	25.7	22.0	12	90	356	104
10	3	450	45	5.9	27.6	27.7	18	125	495	145
11	3	450	45	5.9	26.0	34.6	19	143	567	166
12	3	450	45	5.9	26.0	44.6	25	184	729	213
13	4	450	35	2.1	22.3	7.1	3	29	114	33
14	4	450	35	2.3	23.8	14.8	8	64	254	75
15	4	450	35	2.3	24.5	29.0	16	130	512	150
16	4	450	35	2.1	26.0	42.1	26	203	802	235
17	5	450	35	1.7	26.0	14.1	9	71	279	82
18	5	450	35	1.7	27.6	17.1	12	91	361	106
19	5	450	35	1.9	26.0	18.1	11	89	353	103
20	5	450	35	1.9	26.0	23.9	14	118	467	137
21	6	450	35	2.1	21.5	24.0	10	93	369	108
22	6	450	35	2.1	20.8	30.5	12	115	454	133
23	6	450	35	2.1	20.8	32.5	13	122	483	141
24	6	450	35	1.7	23.8	36.3	18	162	641	188
25	7	650	35	1.9	23.8	11.7	6	70	279	82
26	7	650	35	2.6	24.5	19.5	10	119	468	137
27	7	650	35	1.7	24.5	35.5	19	222	879	258
28	7	650	35	2.1	25.3	39.1	22	250	988	289
29	8	650	35	2.3	23.8	16.8	8	99	392	115
30	8	650	35	3.0	22.3	20.5	9	108	429	126
31	8	650	35	3.4	21.5	23.1	9	114	452	132
32	8	650	35	3.0	23.0	26.5	12	146	576	169
33	9	650	35	2.6	26.0	14.1	8	91	361	106
34	9	650	35	2.6	26.0	22.8	14	148	585	171
35	9	650	35	2.1	25.3	28.0	16	178	704	206
36	9	650	35	2.6	24.5	34.4	18	207	818	239
37	10	650	45	6.7	26.0	9.2	5	50	197	58
38	10	650	45	7.1	25.3	17.6	9	89	353	103
39	10	650	45	6.5	26.0	29.2	16	159	627	184
40	10	650	45	7.9	28.0	40.3	25	228	900	263
41	11	650	45	5.9	27.6	13.6	9	83	327	96
42	11	650	45	6.7	26.0	18.5	10	100	394	116
43	11	650	45	6.7	26.0	19.1	10	104	410	120
44	11	650	45	6.3	26.0	24.6	13	135	536	157
45	12	650	45	6.7	26.8	18.0	10	101	400	117

TABLE I

Results Of Respiratory Heat Loss Calculations (Continued)

DATA NO	RUN NO	DEPTH FT	TW F	TI C	TE C	RMV LPM	INSEN Q KCAL/HR	RHL KCAL/HR	RHL BTU/HR	RHL WATTS
46	12	650	45	6.9	27.6	24.7	15	144	567	166
47	12	650	45	6.7	26.8	30.2	17	170	673	197
48	12	650	45	7.7	26.0	36.4	19	186	736	216
49	13	850	55	12.5	28.4	8.2	5	47	186	55
50	13	850	55	12.7	28.4	16.5	9	92	366	107
51	13	850	55	13.0	29.2	27.7	16	160	634	186
52	13	850	55	12.5	29.2	33.7	20	200	792	232
53	14	850	55	12.7	28.4	12.5	7	71	279	82
54	14	850	55	13.0	27.6	20.7	10	109	430	126
55	14	850	55	13.0	28.4	22.1	12	123	485	142
56	14	850	55	13.0	28.4	24.4	13	135	535	157
57	15	850	55	12.3	29.2	15.3	9	93	369	108
58	15	850	55	12.3	28.4	22.2	12	129	510	149
59	15	850	55	12.7	28.4	22.6	12	128	507	148
60	15	850	55	12.7	29.2	24.5	14	147	581	170
61	16	850	45	7.9	26.0	11.0	6	70	278	81
62	16	850	45	7.7	27.6	25.6	15	181	714	209
63	16	850	45	7.5	27.6	34.8	21	248	979	287
64	16	850	45	7.5	27.6	39.1	23	278	1098	321
65	17	850	45	7.3	27.6	16.7	10	120	475	139
66	17	850	45	7.3	26.8	28.0	16	193	761	223
67	17	850	45	7.3	26.8	31.8	18	219	864	253
68	17	850	45	6.9	26.0	34.8	18	234	924	271
69	18	850	45	7.1	28.4	19.5	13	147	582	170
70	18	850	45	6.9	28.4	28.0	18	213	842	247
71	18	850	45	7.5	27.6	35.0	21	248	979	287
72	18	850	45	6.7	26.8	36.0	21	254	1004	294
73	19	1000	45	7.1	26.8	11.1	6	89	354	104
74	19	1000	45	7.5	27.6	18.4	11	152	600	176
75	19	1000	45	6.9	26.4	30.3	20	265	1047	307
76	19	1000	45	7.5	28.4	34.0	22	290	1146	336
77	20	1000	45	7.5	26.8	15.3	9	120	475	139
78	20	1000	45	7.1	26.0	25.0	13	191	755	221
79	20	1000	45	7.1	26.8	28.8	16	231	913	267
80	20	1000	45	7.3	26.0	28.5	15	216	855	250
81	21	1000	45	6.7	28.4	19.9	13	177	698	205
82	21	1000	45	6.9	27.6	26.8	16	225	891	261
83	21	1000	45	7.1	28.4	29.2	19	254	1005	294
84	21	1000	45	7.1	28.4	36.4	23	316	1250	366
85	22	850	35	3.2	26.0	8.3	5	67	263	77
86	22	850	35	3.0	26.0	13.5	8	109	432	127
87	22	850	35	3.2	26.0	20.7	12	165	654	192
88	22	850	35	3.2	26.0	28.6	17	228	901	264
89	23	850	35	3.2	26.0	17.5	10	139	550	161
90	23	850	35	3.0	25.3	30.4	17	236	933	273

TABLE I

Results Of Respiratory Heat Loss Calculations (Continued)

DATA NO	RUN NO	DEPTH FT	TW F	TI C	TE C	RMV LPM	INSEN Q KCAL/HR	RHL KCAL/HR	RHL BTU/HR	RHL WATTS
91	23	850	35	3.0	26.8	41.0	26	341	1347	394
92	23	850	35	.0	.0	.0	0	0	0	0
93	24	850	35	2.7	27.6	19.6	13	172	679	199
94	24	850	35	2.7	26.8	31.1	19	262	1035	303
95	24	850	35	3.0	26.0	38.1	22	305	1207	353
96	24	850	35	.0	.0	10.1	0	0	0	0
97	25	850	35	2.7	26.0	.0	6	82	324	95
98	25	850	35	3.4	25.3	15.7	9	121	477	140
99	25	850	35	3.2	26.0	23.0	13	183	722	211
100	25	850	35	2.6	26.0	29.0	17	237	935	274
101	26	850	35	2.7	25.3	21.0	12	165	652	191
102	26	850	35	3.0	25.3	24.5	14	190	752	220
103	26	850	35	3.2	25.3	32.7	18	252	996	292
104	26	850	35	3.2	25.3	36.5	20	281	1111	325
105	27	850	35	2.7	27.6	22.8	15	200	788	231
106	27	850	35	3.2	27.6	35.4	23	303	1197	350
107	27	850	35	3.4	26.8	41.7	26	341	1349	395
108	27	850	35	.0	.0	7.7	0	0	0	0
109	28	850	35	3.8	26.0	13.3	4	60	237	69
110	28	850	35	3.0	25.3	.0	7	104	411	120
111	28	850	35	3.2	26.0	21.6	13	172	679	199
112	28	850	35	3.0	26.0	34.5	20	276	1092	320
113	29	850	35	3.4	26.0	24.4	14	191	755	221
114	29	850	35	3.2	25.3	24.3	14	187	739	216
115	29	850	35	3.2	25.3	31.7	18	243	959	281
116	29	850	35	2.6	24.5	37.7	20	286	1130	331
117	30	850	35	3.2	26.8	13.3	6	110	433	127
118	30	850	35	3.0	26.0	24.6	14	197	778	228
119	30	850	35	3.0	26.8	28.7	18	239	944	277
120	30	850	35	3.0	26.4	37.7	23	307	1212	355
121	31	850	45	7.9	27.6	4.7	3	33	132	39
122	31	850	45	7.9	26.8	11.9	7	80	315	92
123	31	850	45	7.9	26.8	18.8	10	125	495	145
124	31	850	45	7.5	26.8	21.4	12	145	575	168
125	32	850	45	7.3	28.4	9.9	6	75	295	86
126	32	850	45	7.1	26.8	19.8	11	138	544	159
127	32	850	45	7.1	26.8	24.7	14	172	679	199
128	32	850	45	7.5	27.6	29.9	18	213	841	246
129	33	850	35	3.0	25.3	8.5	5	66	262	77
130	33	850	35	3.0	25.3	17.2	10	133	526	154
131	33	850	35	3.0	26.0	25.8	15	207	819	240
132	33	850	35	3.0	26.0	30.7	18	246	973	285
133	34	850	35	3.2	26.0	15.0	9	120	474	139
134	34	850	35	3.2	25.3	25.0	14	192	758	222
135	34	850	35	3.2	25.3	21.5	12	165	653	191

TABLE I

Results of Respiratory Heat Loss Calculations (Continued)

DATA NO	RUN NO	DEPTH FT	TW F	TI C	TE C	RMV LPM	INSEN Q KCAL/HR	RHL KCAL/HR	RHL BTU/HR	RHL WATTS
136	34	850	35	3.2	25.3	28.1	15	217	856	251
137	35	850	35	2.6	27.6	16.1	11	141	559	164
138	35	850	35	3.0	26.0	26.6	16	213	842	247
139	35	850	35	3.2	26.0	35.6	21	282	1115	327
140	35	850	35	3.0	25.3	42.7	25	342	1350	395

NOW AT 130

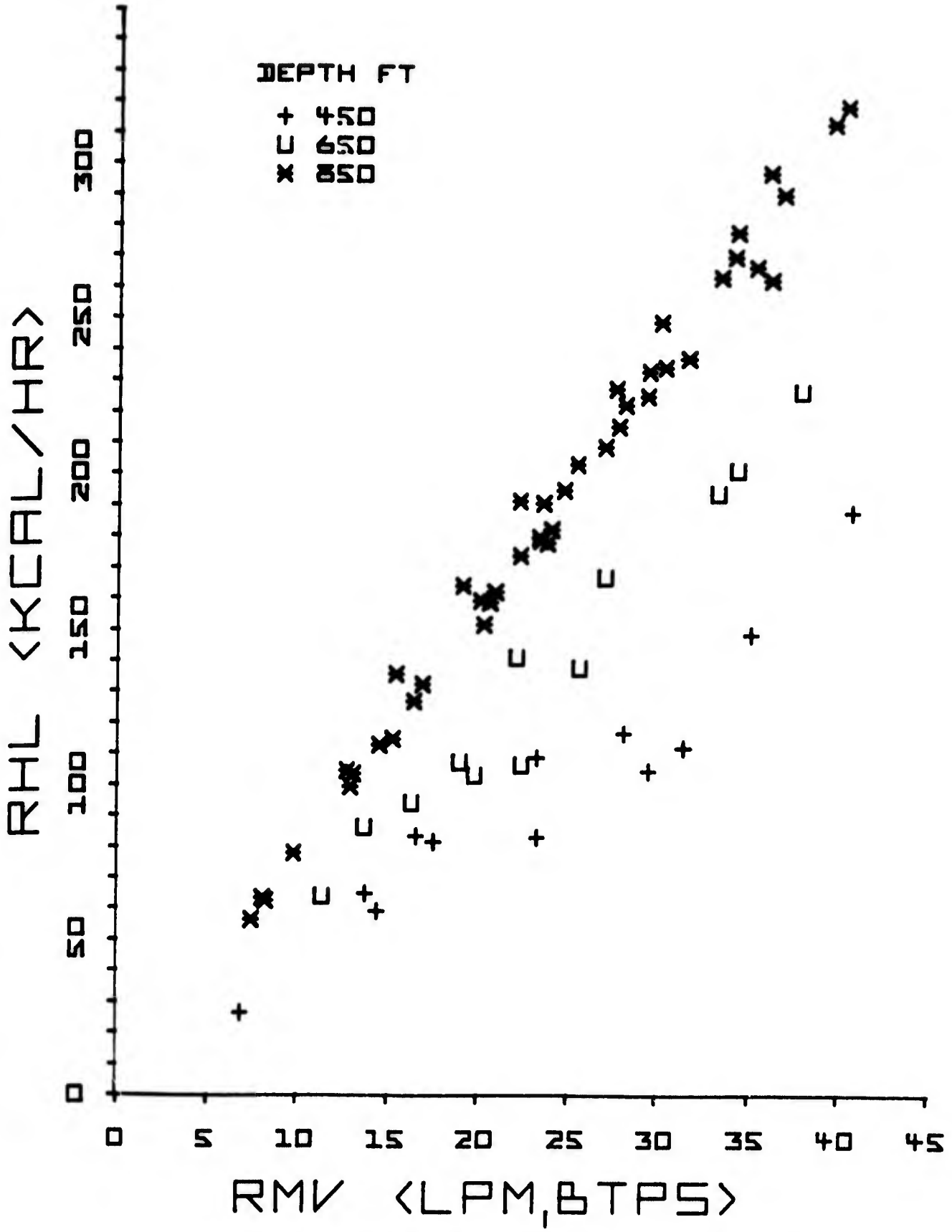

Figure 10. Water Temperature 35°F: Respiratory Heat Loss As A Function Of Ventilation During Data Runs At 450, 650, and 850 Feet.

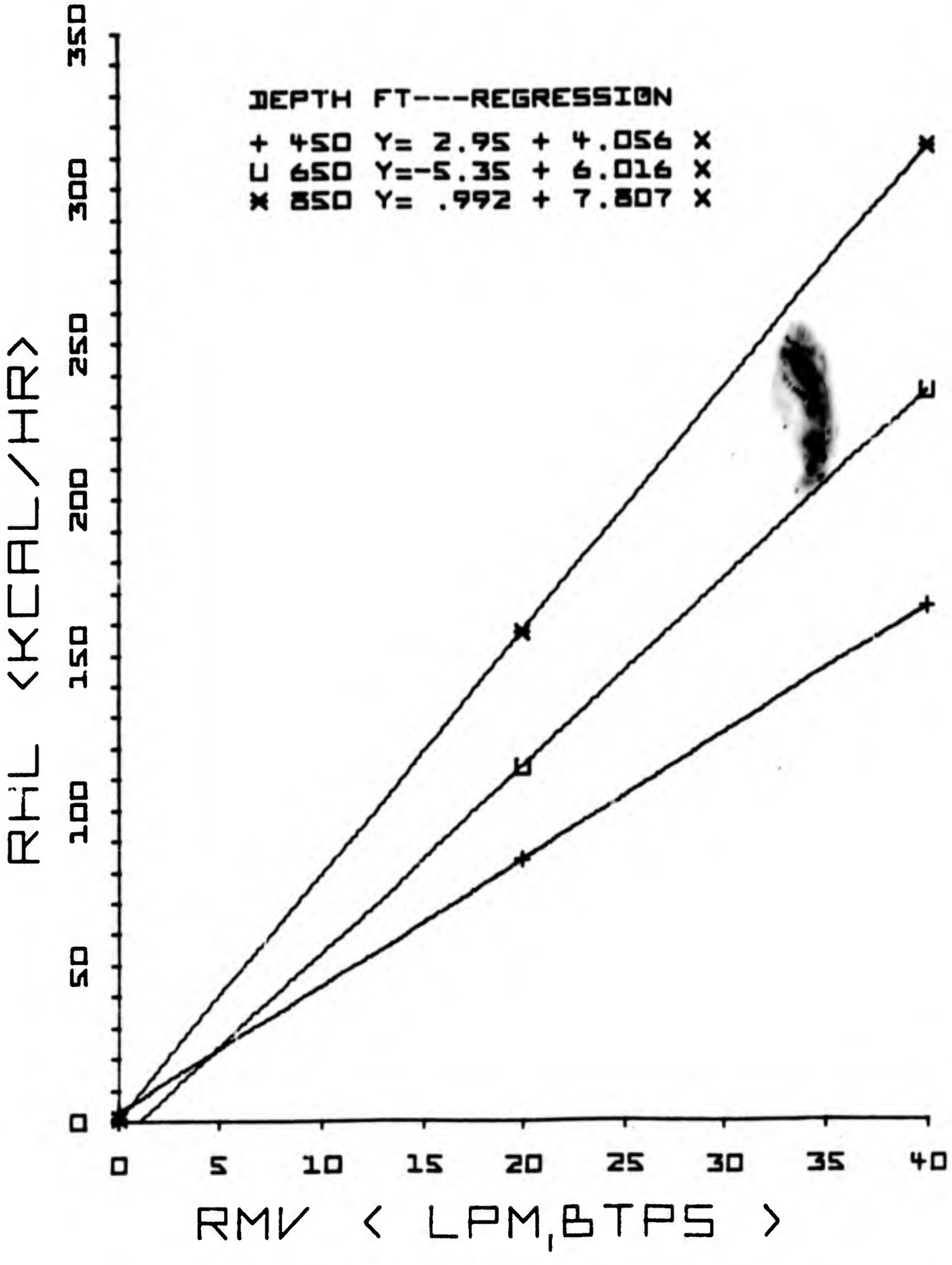

Figure 11. Water Temperature 35°F: Regression Lines For Respiratory Heat Loss As A Function Of Ventilation During Data Runs At 450, 650, and 850 Feet.

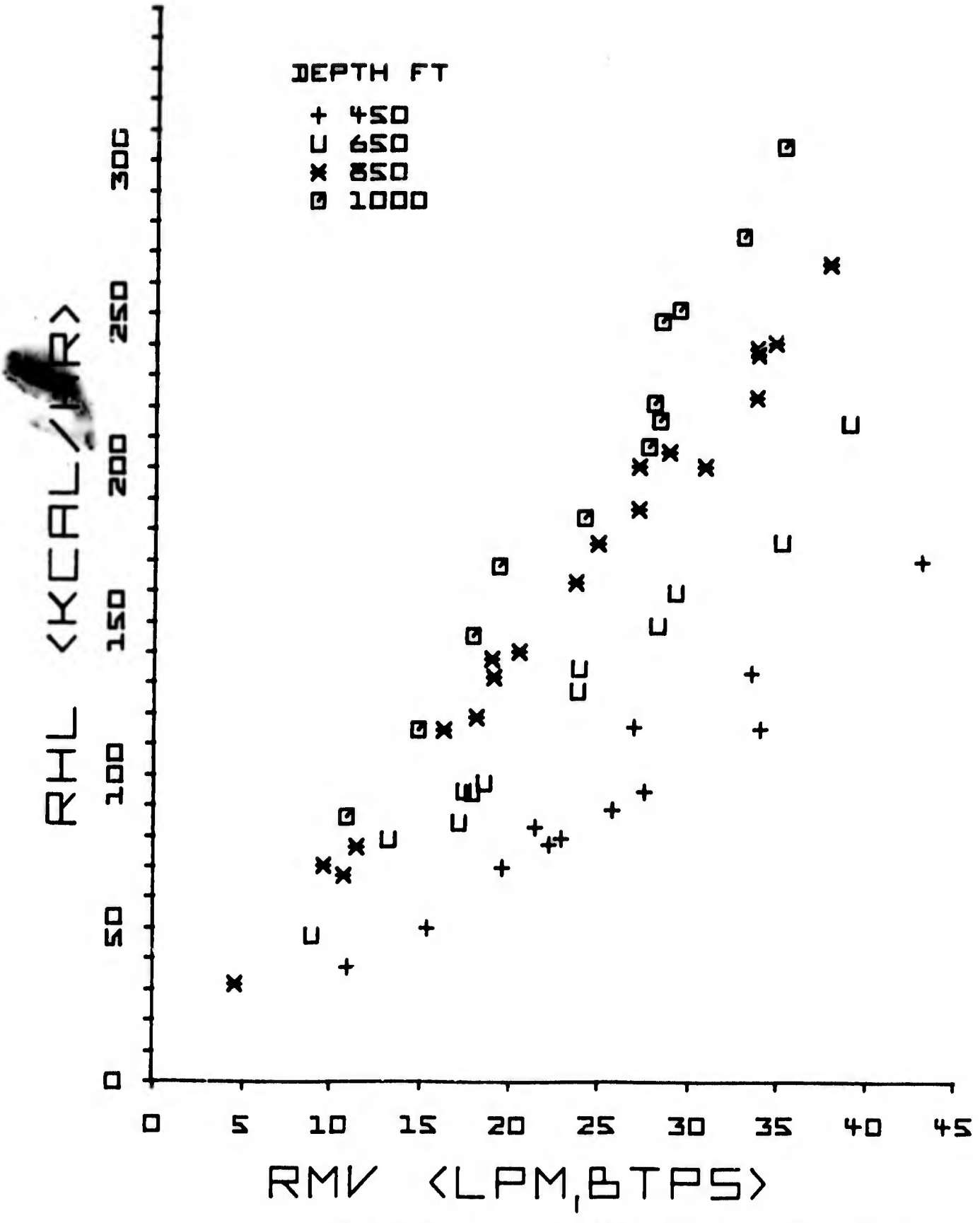

Figure 12. Water Temperature 45°F: Respiratory Heat Loss As A Function Of Ventilation During Data Runs at 450, 650 and 1,000 Feet.

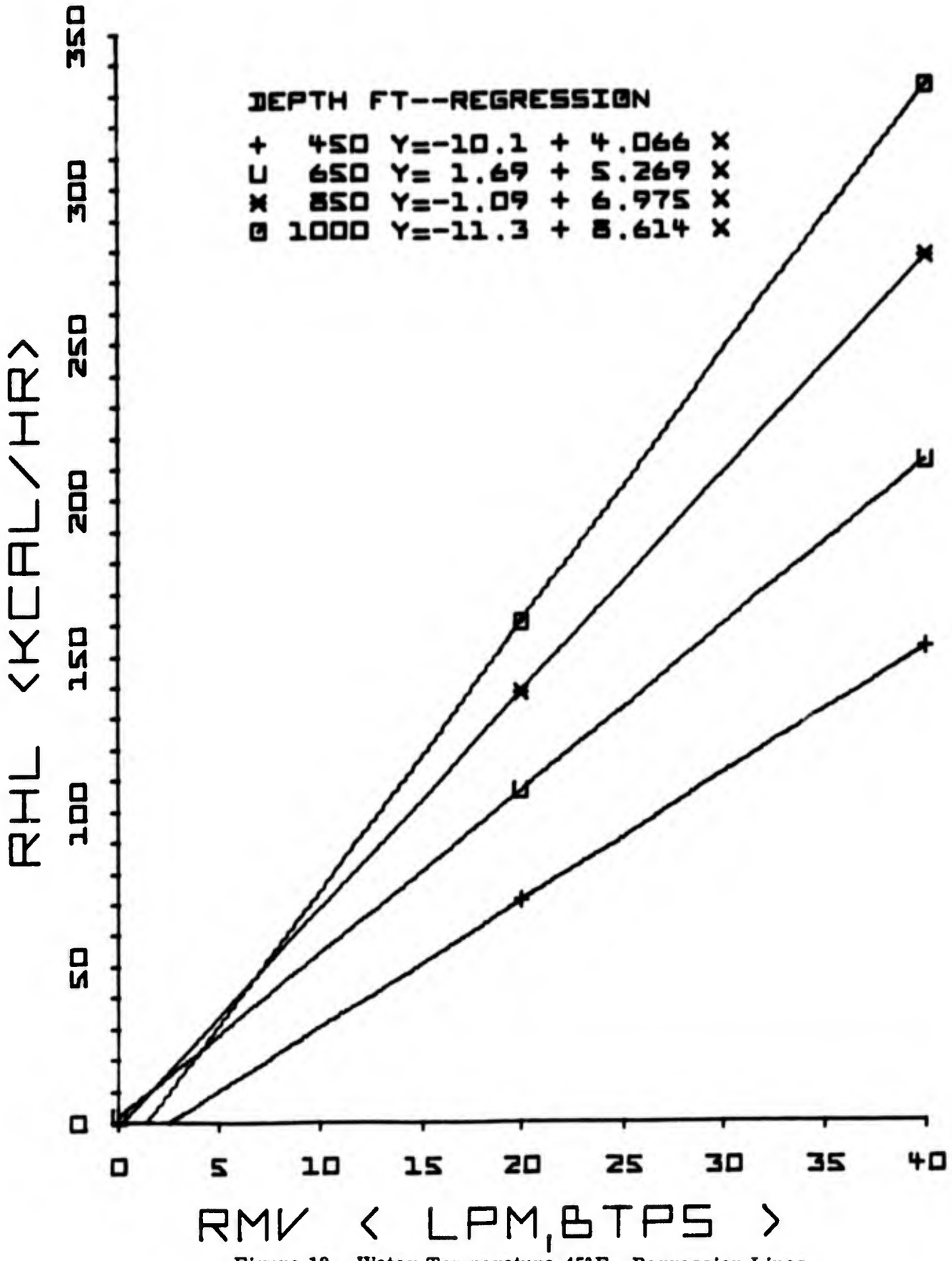

Figure 13. Water Temperature 45°F: Regression Lines For Respiratory Heat Loss As A Function Of Ventilation During Data Runs At 450, 650, 850 and 1,000 Feet.

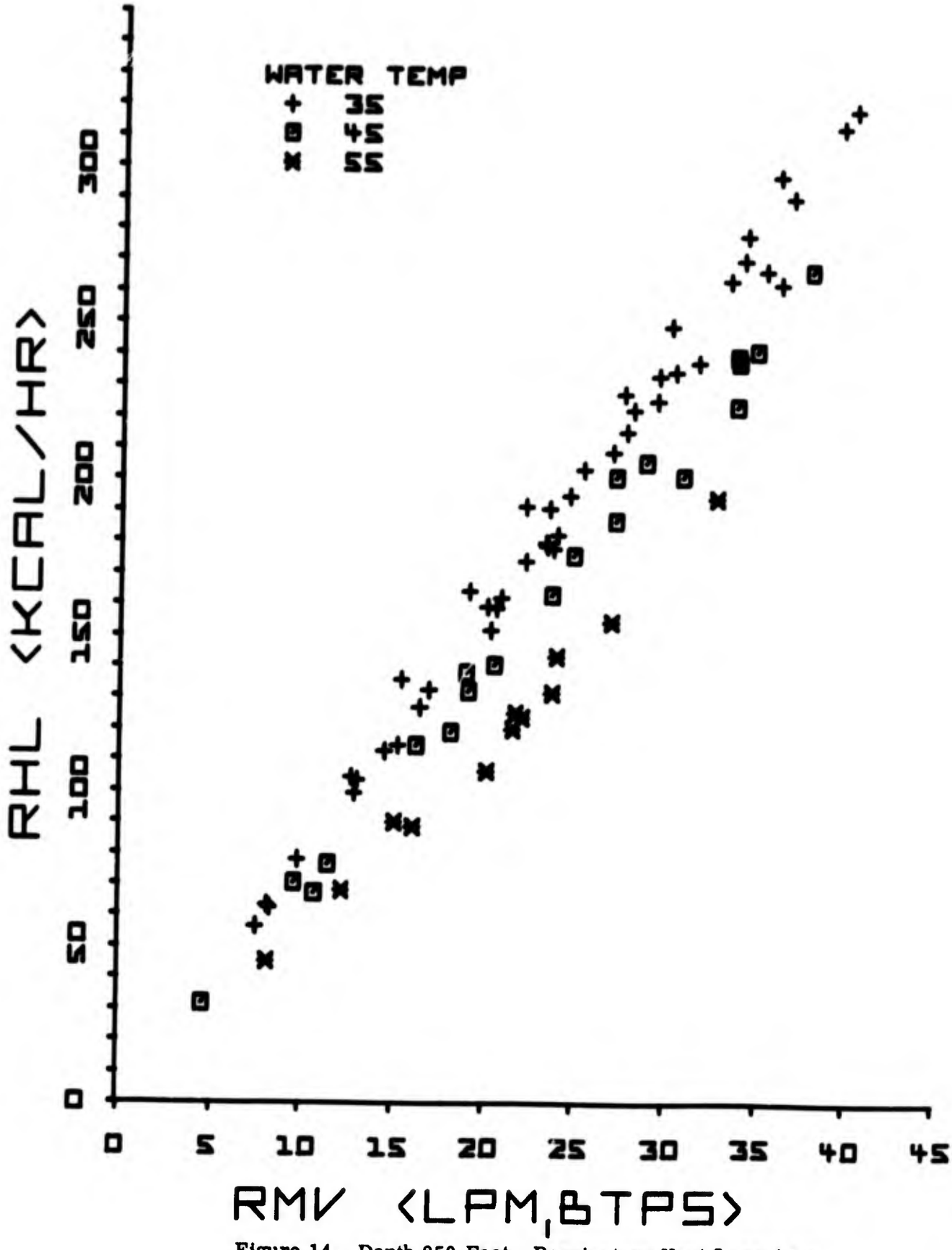

Figure 14. Depth 850 Feet: Respiratory Heat Loss As A Function Of Ventilation During Data Runs At Nominal Water Temperatures of 35°F, 45°F and 55°F.

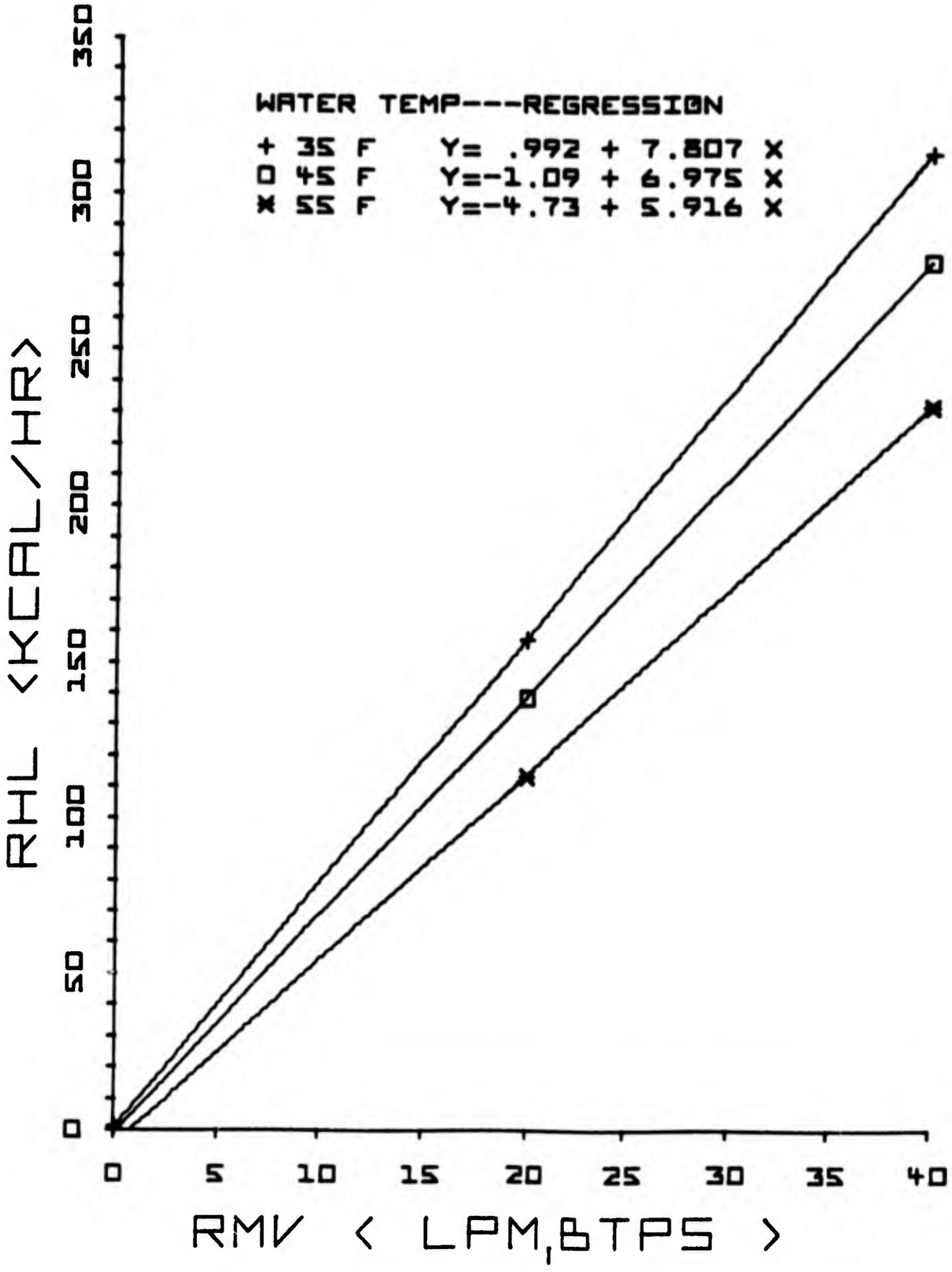

Figure 15. Depth 850 Feet: Regression Lines For Respiratory Heat Loss As A Function Of Ventilation During Data Runs At Nominal Water Temperatures of 35°F, 45° F and 55°F.

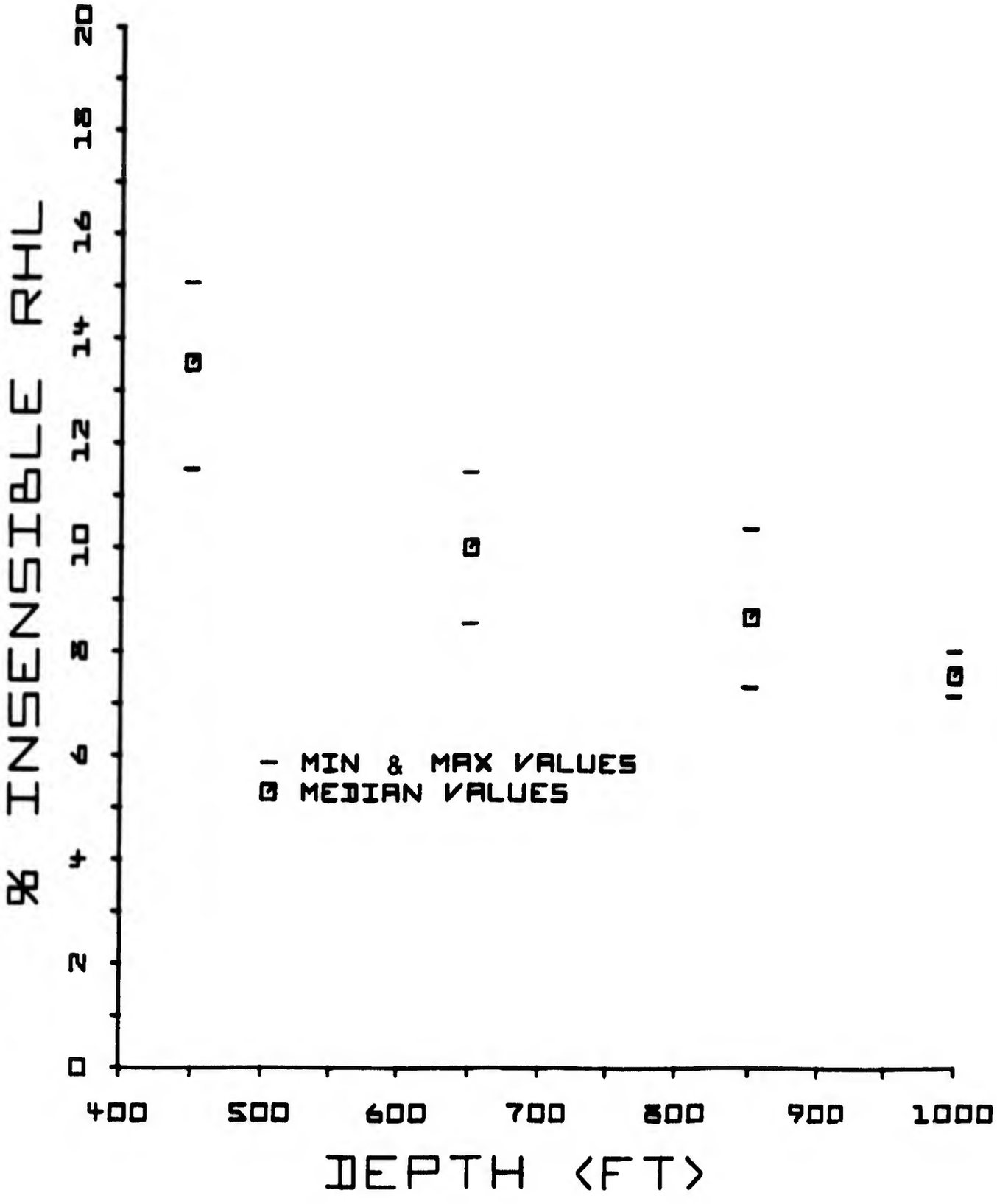

Figure 16. Insensible Heat Loss Fraction of Total Respiratory Heat Loss.

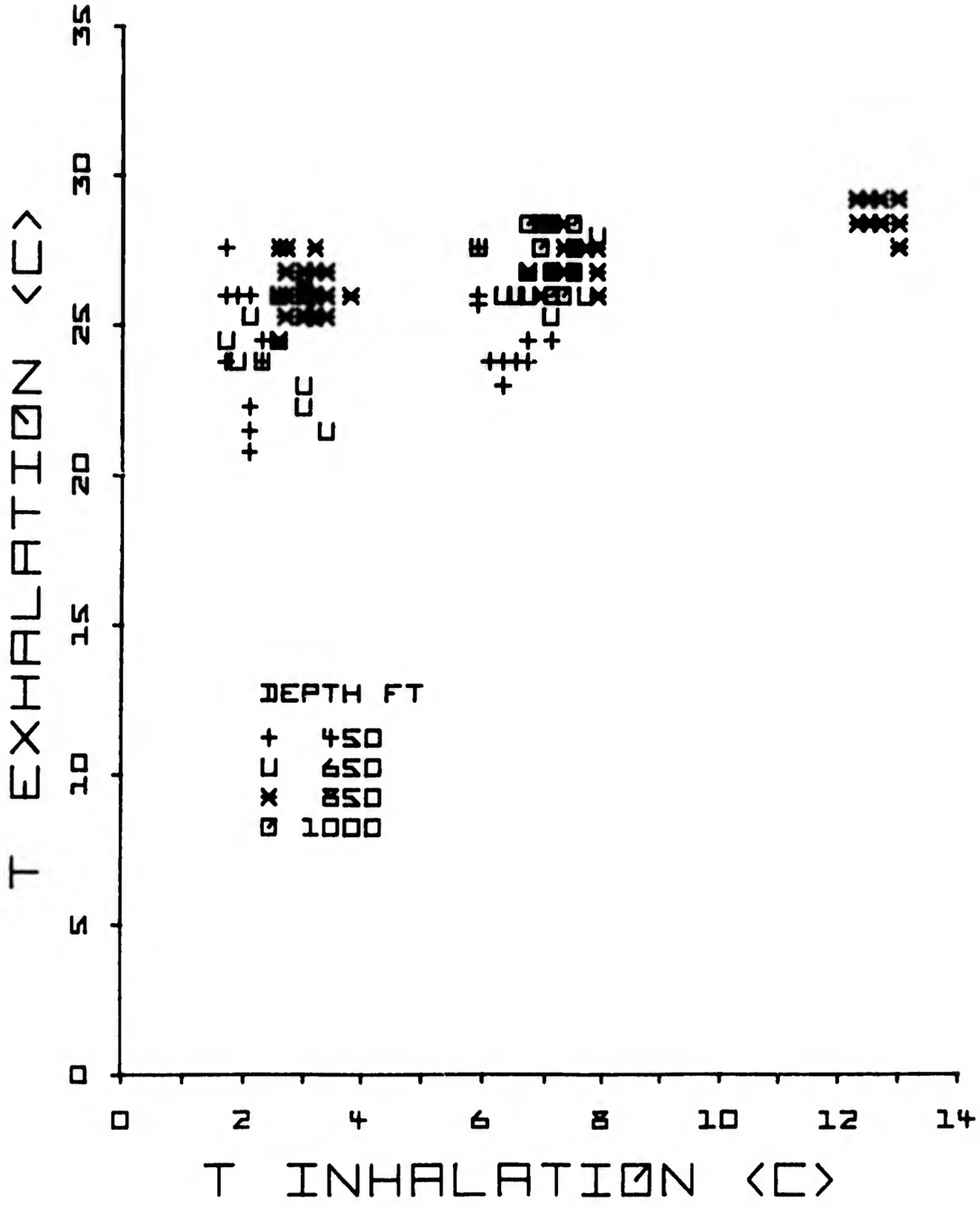

Figure 17. Relationship Between Observed Temperatures (°C) Of Inhaled and Exhaled Gases.

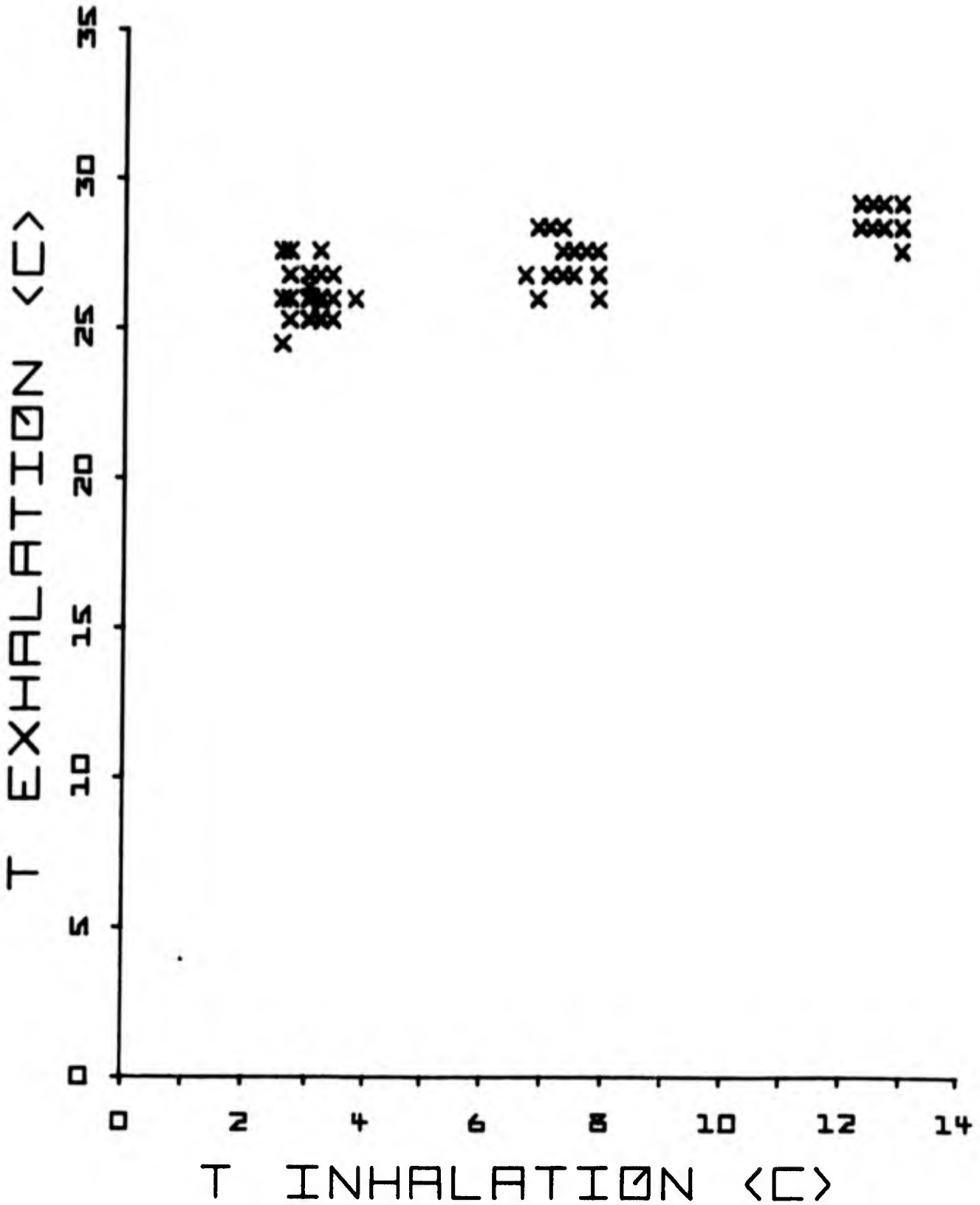

Figure 18. Depth 850 Feet: Relationship Between Observed Temperatures (°C) Of Inhaled And Exhaled Gases.

TABLE II

Averaged Parameters Of Respiratory Heat Loss And Thermal Balance For Each Immersion Exposure.

Run No	Depth Ft	T Water °F	T Water °C	TE-TI AVG °C	Δ T MWS °C	Δ T Rectal °C	Δ T Body °C	RMV-AVG LPM	RHL AVG Kcal/hr
1	450	45	7.2	17.3	+0.27	xx	xx	22.4	80
2	450	45	7.2	17.5	-0.38	-0.44	- .42	23.9	86
3	450	45	7.2	20.7	-1.29	-1.66	-1.53	31.2	136
4	450	35	1.7	21.9	-2.02	-0.32	-0.88	22.1	102
5	450	35	1.7	24.9	-1.56	-0.81	-1.04	18.1	93
6	450	35	1.7	19.5	-2.20	-1.61	-1.80	31.0	123
7	650	35	1.7	22.4	-3.22	-0.73	-1.55	25.4	161
8	650	35	1.7	19.5	-2.61	-0.49	- .90	21.6	116
9	650	35	1.7	23.0	-1.57	-1.44	-1.48	24.5	158
10	650	45	7.2	19.0	- .73	-0.31	-0.45	23.0	127
11	650	45	7.2	19.8	-2.20	-0.53	-1.09	18.8	105
12	650	45	7.2	20.0	-2.14	-1.21	-1.52	26.6	151
13	850	55	12.8	16.0	-1.22	-0.50	-0.74	20.7	122
14	850	55	12.8	15.1	-2.01	-0.81	-1.21	20.2	111
15	850	55	12.8	16.2	-0.85	-0.80	-0.82	21.6	127
16	850	45	7.2	19.7	-3.29	-0.47	-1.48	27.3	198
17	850	45	7.2	19.5	-1.83	-0.89	-1.20	27.7	195
18	850	45	7.2	20.9	-1.82	-0.93	-1.23	28.9	219
19	1000	45	7.2	20.5	-2.24	-0.46	-1.05	22.5	195
20	1000	45	7.2	19.1	-1.48	-0.94	-1.12	24.5	194
21	1000	45	7.2	21.1	-1.87	-0.94	-1.25	27.4	243
22	850	35	1.7	22.9	+0.84	-0.46	-0.59	17.1	139
23	850	35	1.7	22.6	-1.66	-0.71	-1.03	29.9	246
24	850	35	1.7	23.7	-0.87	-1.52	-1.29	29.8	254
25	850	35	1.7	22.6	-1.35	-0.62	-0.86	18.8	152
26	850	35	1.7	22.3	2.11	-1.00	-1.37	27.5	218
27	850	35	1.7	24.0	-1.96	-1.12	-1.40	33.4	291
28	850	35	1.7	22.5	-0.80	-0.91	-0.87	18.3	148
29	850	35	1.7	22.1	-1.44	-0.65	-0.91	27.9	220
30	850	35	1.7	23.3	-0.33	-1.21	-1.90	25.7	215
31	850	45	7.2	19.1	-0.61	-0.59	-0.60	14.0	96
32	850	45	7.2	20.0	-1.16	-0.70	-0.85	20.9	151
33	850	35	1.7	22.6	-2.41	-1.14	-1.56	20.0	162
34	850	35	1.7	22.2	-1.52	-0.82	-1.05	22.8	180
35	950	35	1.7	23.1	-2.46	-1.55	-1.85	29.7	243

TABLE III

Time Sequence For Mean Weighted Skin Temperature

RUN NO.	DEPTH FT	TW F	SUB	REST 1	LIGHT WORK 2	REST 3	MEDIUM WORK 4	REST 5	HARD WORK 6	7	MEAN TMWS F	C
1	450	45	KC	88.1	90.2	87.9	89.0	88.9	88.1	88.6	88.3	31.3
2	450	45	SZ	93.9	95.7	91.9	92.7	92.0	91.2	93.2	93.5	34.2
3	450	45	FA	94.4	92.3	91.6	91.3	92.3	91.7	92.1	93.2	34.0
4	450	35	KC	93.5	93.5	90.3	90.7	89.9	89.7	89.8	91.7	33.2
5	450	35	SZ	94.1	95.8	93.4	93.9	91.3	91.5	91.3	92.7	33.7
6	450	35	FA	93.8	93.1	91.4	91.8	90.2	91.5	89.9	91.8	33.2
7	650	35	KC	93.7	91.0	89.0	91.5	89.2	90.0	87.9	90.7	32.6
8	650	35	SZ	96.5	94.6	92.7	93.8	93.3	94.6	91.7	94.1	34.5
9	650	35	FA	96.1	96.9	95.5	96.7	94.9	95.6	93.2	94.7	34.8
10	650	45	KC	93.7	93.8	91.4	92.2	92.5	93.6	92.4	93.1	33.9
11	650	45	SZ	94.2	94.7	92.4	93.0	91.8	93.1	90.3	92.2	33.4
12	650	45	FA	95.8	95.3	92.4	92.5	92.3	94.3	92.0	93.9	34.4
13	850	55	KC	94.0	94.1	93.3	94.2	92.7	93.3	91.8	92.9	33.8
14	850	55	SZ	93.9	92.3	90.1	91.0	90.8	91.1	90.2	92.1	33.4
15	850	55	FA	97.0	99.2	96.6	98.6	96.9	98.5	95.4	96.1	35.6
16	650	45	KC	96.4	92.5	90.7	91.2	89.5	91.2	90.5	93.4	34.1
17	650	45	SZ	92.8	90.6	89.3	92.0	91.1	92.2	89.6	91.2	32.9
18	650	45	FA	94.3	95.5	92.6	95.1	91.2	93.5	91.0	92.7	33.7
19	1000	45	KC	99.1	98.0	95.8	97.4	95.7	96.4	95.1	97.1	36.2
20	1000	45	SZ	95.0	95.8	93.2	94.6	92.9	94.0	92.4	93.7	34.3
21	1000	45	FA	95.6	95.8	95.2	95.2	92.9	94.1	92.2	93.9	34.4
22	850	35	KC	92.1	94.3	92.6	93.2	95.0	95.8	93.6	92.8	33.8
23	850	35	SZ	94.5	92.4	93.6	91.5				93.0	33.9
24	850	35	FA	91.9	92.3	88.2	89.2	90.3			91.1	32.8
25	850	35	KC	93.9	92.5	93.4	92.1	92.8	92.9	91.5	92.7	33.7
26	850	35	SZ	93.6	96.1	93.0	95.4	93.6	91.3	89.8	91.7	33.2
27	850	35	FA	93.9	94.2	90.9	91.8	90.3			92.1	33.4
28	850	35	KC	94.8	95.5	93.6	93.7	93.2	92.3	93.4	94.1	34.5
29	850	35	SZ	93.3	91.4	90.8	90.3	90.6	90.6	90.7	92.0	33.3
30	850	35	FA	94.1	96.3	94.2	94.8	92.5	94.5	93.5	93.8	34.3
31	850	45	KC	95.3	96.8	94.5	96.7	95.1	95.6	94.2	94.7	34.8
32	850	45	FA	97.6	99.3	97.9	100.3	96.4	98.5	95.6	96.6	35.9
33	850	35	KC	97.6	97.2	95.0	95.2	94.2	94.6	93.3	95.4	35.2
34	850	35	SZ	93.8	91.8	91.5	91.0	95.2	91.1	91.1	92.3	33.5

NOW AT 540

15:51 RAN 0 MINS 0.75 SECS

READY

Oxygen consumption and carbon dioxide production were computed from the inhaled and exhaled gas composition and the exhalation volume. Oxygen consumption (STPD) is shown as a function of respiratory minute volume (BTPS) in Figures 19-22. The reasons for the scatter of this data at 850 feet are not evident. Carbon dioxide production (STPD) as a function of respiratory minute volume (BTPS) is plotted in Figures 23-28. The data at 850 feet, Figure 26, is again completely random. Without the 850 feet data there is a trend: $\dot{V}CO_2 = .045$ RMV (Fig. 28). Figures 29-33 are plots of oxygen consumption-carbon dioxide production. The 850 feet data (Fig. 32) which was scattered for both $\dot{V}CO_2$ and $\dot{V}O_2$ appear to correlate along a line of $\dot{V}CO_2 = 0.9\dot{V}O_2$. This correlation line also appears to be the best representation of the total data shown in Figure 29.

Other Ventilatory Data

Tidal volumes, respiratory frequency, inhalation and exhalation pressure drop and exhalation peak flow rate, as well as $\dot{V}O_2$, $\dot{V}CO_2$, and respiratory exchange ratio are presented in Table IV. Neither pressure drop, flow, nor respiratory resistance during exhalation appear to vary consistently as functions of depth (density) or inhalation temperature. The applicability of pneumotachography to diving research is the subject of Appendix 3.

Subjective Effects of Breathing Cold Hyperbaric Gas

The following paragraphs, and Table V, are from the test subjects' reports, and are, in fact, directly quoted (author: subject SSZ).

"The respiratory heat loss effects reported here are those noted by one test subject, myself, and partly those reported or observed from the other two test subjects. The data summarized in Table V are from 850 feet, 35°F water dives of May 12, 14, 15, 16, and 18, 1971. Factors which affected the heating and cooling of each test subject were the ability of the inner and outer wet suits to heat the subject and the level of muscular activity of the subject. These factors are discussed below. Both the sequence of appearance of the effects of respiratory heat loss and the magnitude of these effects were consistent in several of the experiments, despite variations in heating from the wet suits and in work rates used.

"Early in the experiments, loosely fitting inner wet suits caused cold skin areas on all the test subjects and inadequate hot water circulation from the outer wet suit caused cold skin areas on two subjects, FA and KC, throughout the experiments. Table V shows a correlation of cold skin areas with early onset of shivering, usually within the first few minutes of the first rest period. The third subject, myself, noted fewer cold skin areas and had a later onset of shivering. These data indicate that the onset of heat loss effects is somewhat dependent on external heating.

"Another effect of the inadequate circulation of the wet suits was that the feet and hands became cold if they were not in at least intermittent movement. Thus, the rest periods were actually periods of activity of about 30-50% of work rate 3 (lightest effort).

"Where heating from the wet suits was sufficient, the onset of chest muscle shivering occurred during either work rate 3 or the second rest period. Work rate 3 was a very light work rate, requiring only a slow, easy kick with the fins. This work rate was sufficient to increase the subjects' heart rate and breathing rate and to create some warmth from exercise.

"All test subjects had chest muscle shivering during the second rest period, indicating that the warmth lost from cessation of exercise, or the continued exposure caused the onset of shivering.

"A decrease in shivering in both limbs and torso occurred with the increased activity of the moderate and the heavy work rates, indicating that the warmth produced by exercise somewhat affects the heat lost to the large volumes of cold gas that are breathed at these work rates.

"The first respiratory symptom was a flow of saliva, starting within the first minute of exposure and increasing to a steady rate within a few minutes at each work rate. These steady rates seemed to be proportional to the volumes of gas breathed. The total flow was about four to eight ounces of saliva per subject per dive, estimated from the drainage from the water trap and transparent hose for all three subjects.

"The second symptom was nasal drainage, beginning in the first work period and continuing at a slow, steady rate throughout each dive. The total flow was about 0.5 to 1 ounce per subject per dive. This flow is estimated from observations of all three subjects.

"Another symptom was shivering in the torso, beginning in the skeletal chest muscles. The following estimates of frequency and magnitude of shivering are only for one test subject, myself. The initial frequency of shivering was about once every three breaths, or approximately every 9 to 12 seconds, for a duration of about two seconds. The frequency would decrease to once every four or five breaths during heavy work with about the same duration.

" Shivering would usually spread over the skeletal muscles of the chest and abdomen, then over the back muscles from shoulders to thighs. This shivering was involuntary and uncontrollable.

"The fourth symptom was shivering of the muscles of the limbs, starting with the upper arms and thighs. This symptom usually began in the second rest period, decreased or stopped during the second work period, recurred in the third rest period, and usually stopped during heavy work. Thus, warmth from exercise apparently decreased this shivering.

"The shivering of the upper limbs spread to the hands and feet during two of the five dives, during the second and third rest periods. The rate of shivering was approximately

once every three breaths, for a duration of about two seconds. This shivering was involuntary and uncontrollable. The amplitude at the fingers was about one-quarter inch, estimated by holding the trapeze firmly and watching the work rate indicator. This symptom also includes shivering of the jaw and neck muscles, which caused difficulty retaining the mouthpiece. Shivering of the hands never became severe enough to prevent holding any object.

"Other symptoms, such as chest pain, headache, coughing, visual disturbance and breathing difficulty occured occasionally, with no appreciable repeatability or consistency among all three subjects."

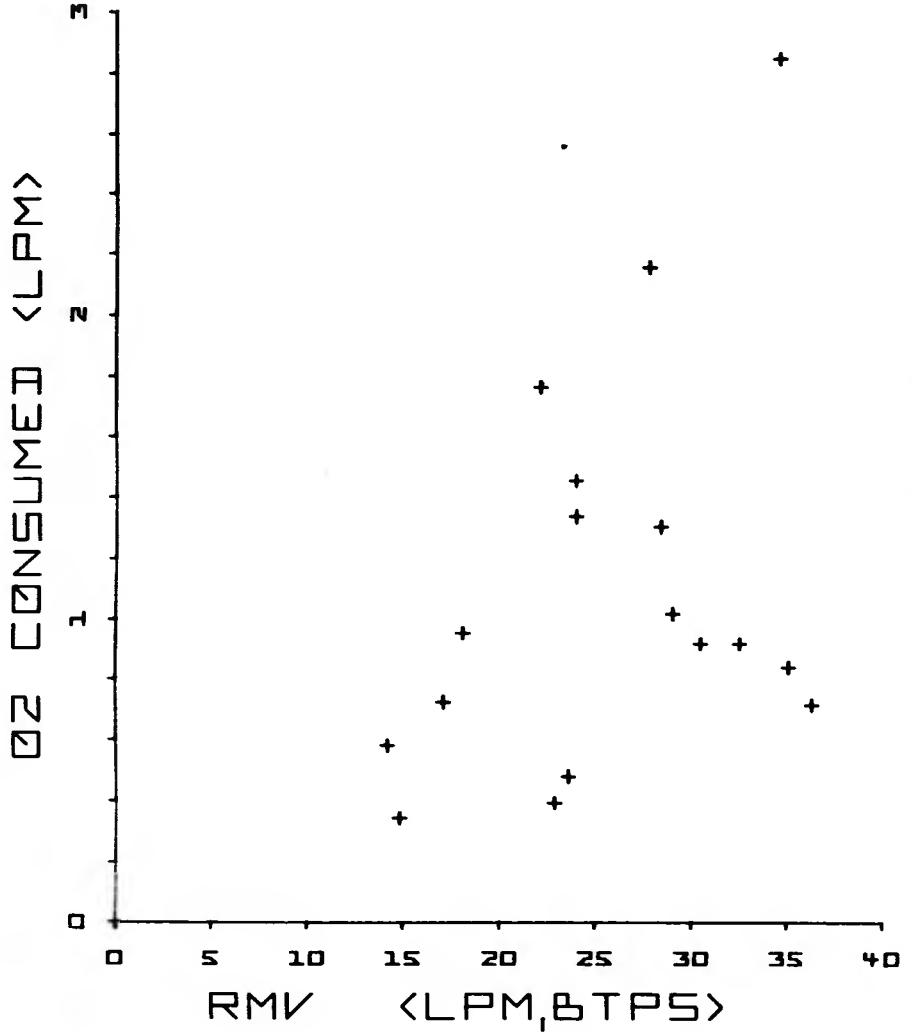

Figure 19. Oxygen Consumption (LPM, STPD) During Data Runs At 450 Feet.

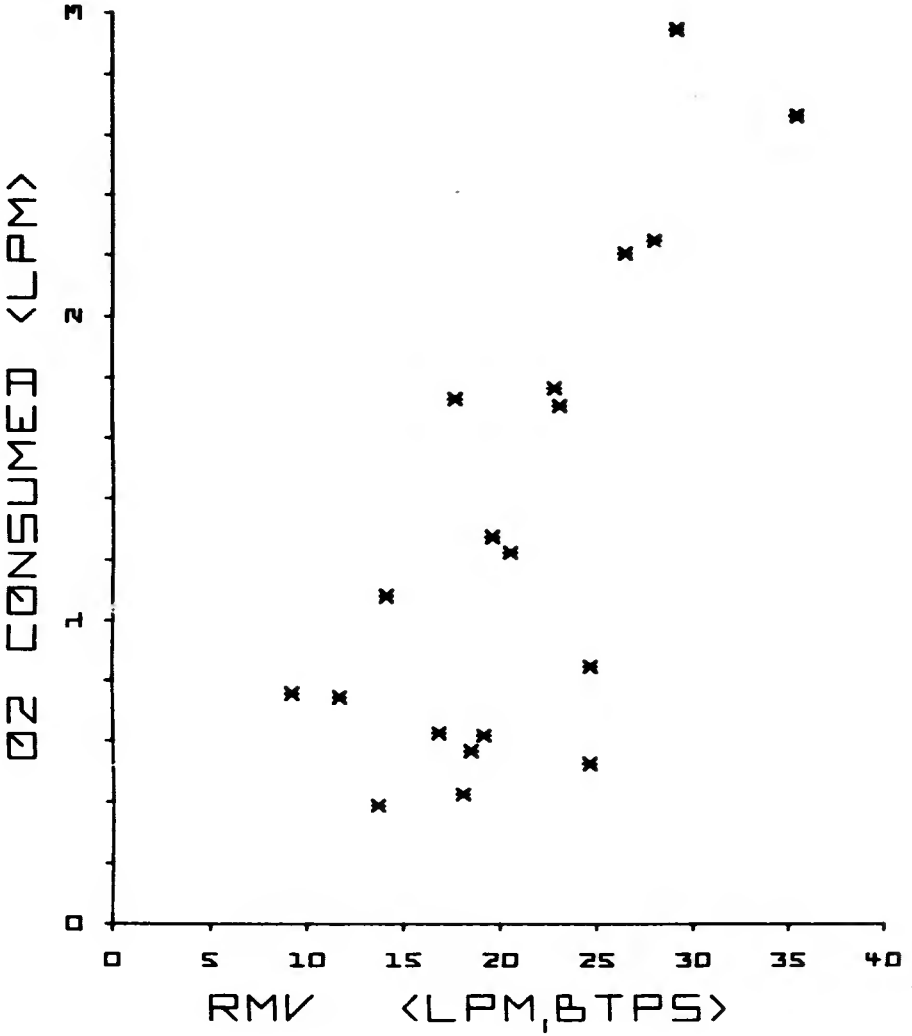

Figure 20. Oxygen Consumption (LPM, STPD) During Data Runs At 650 Feet.

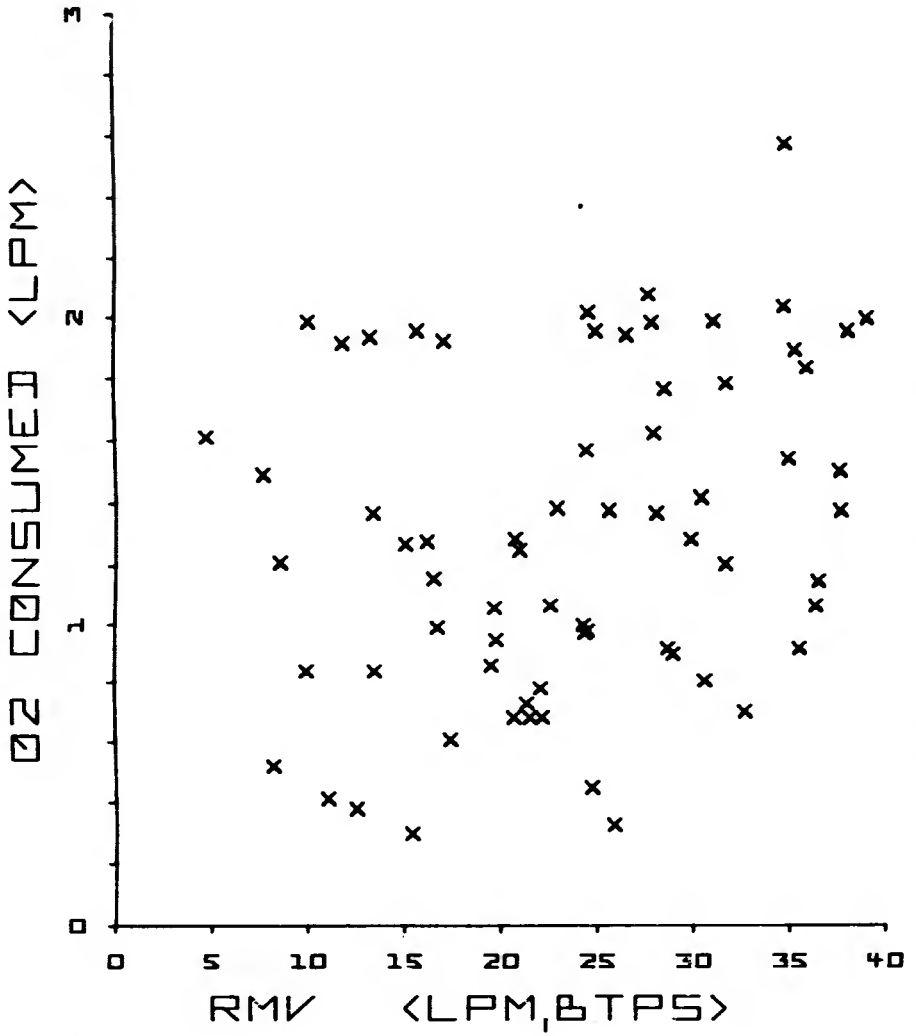

Figure 21. Oxygen Consumption (LPM, STPD) During Data Runs At 850 Feet.

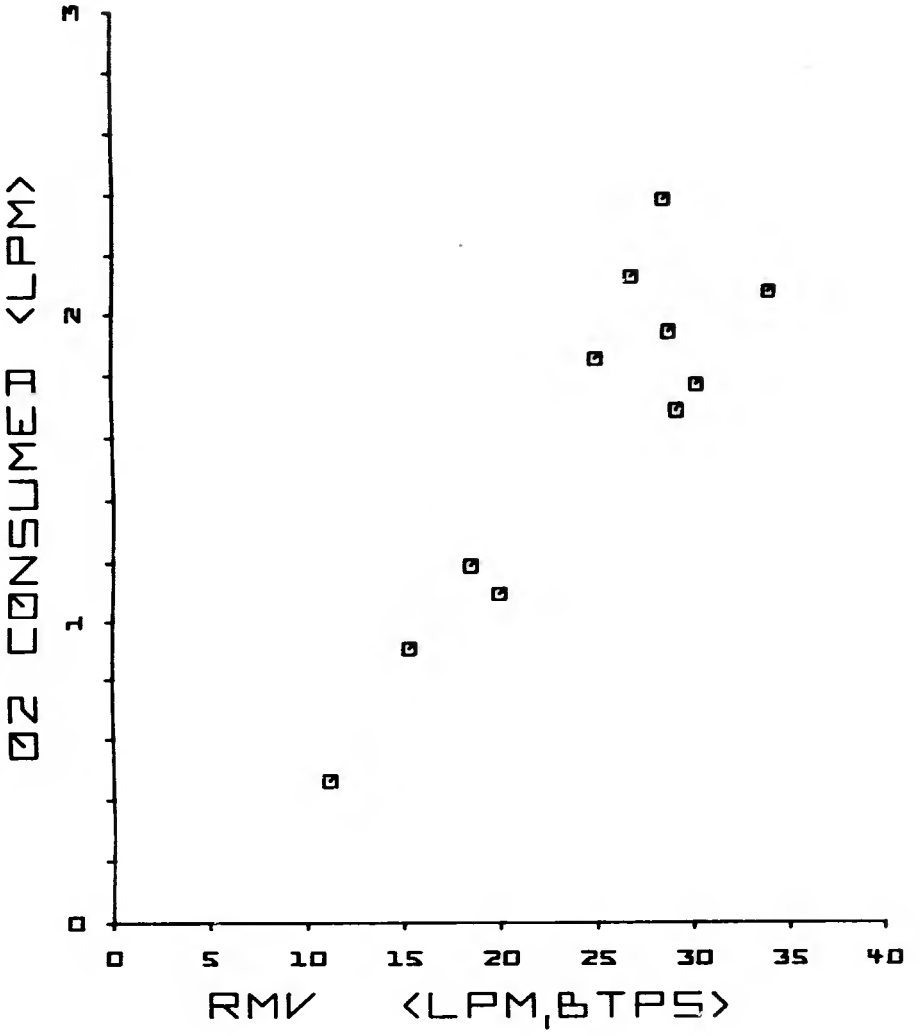

Figure 22. Oxygen Consumption (LPM, STPD) During Data Runs At 1,000 Feet.

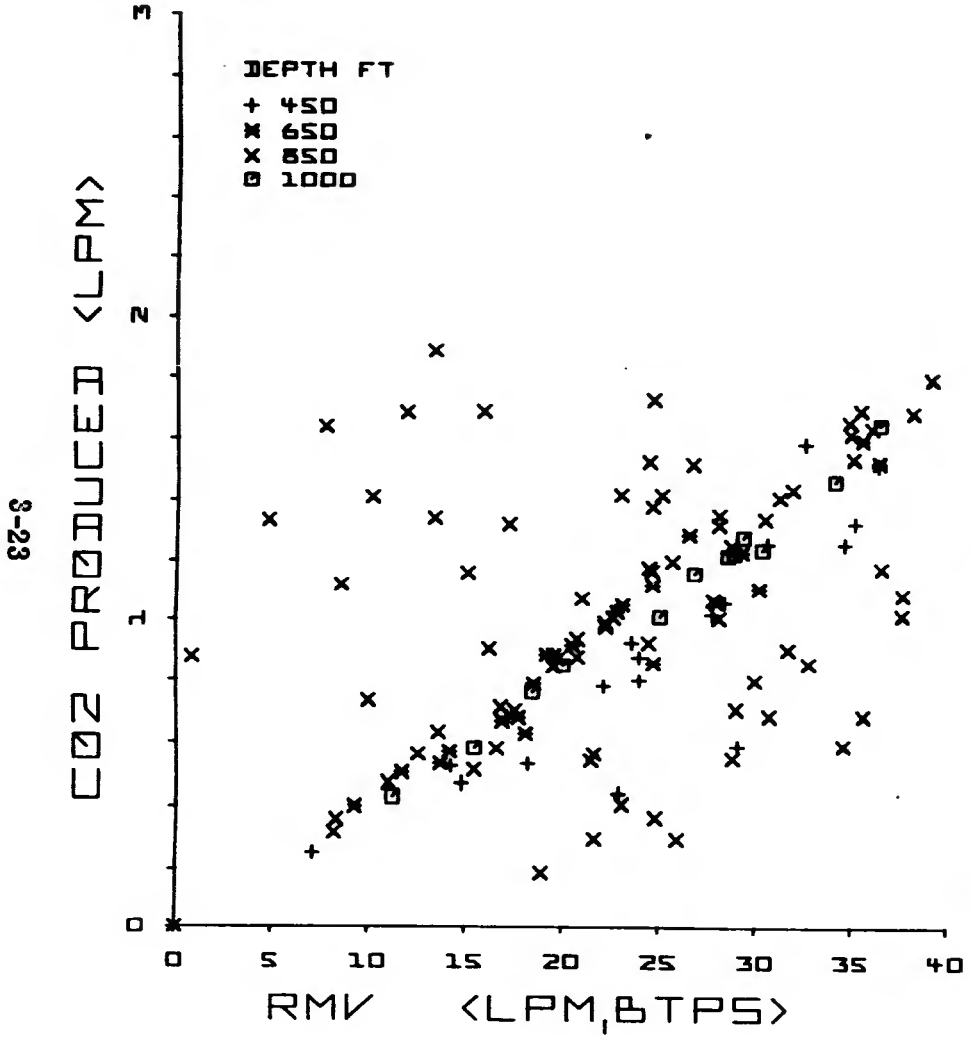

Figure 23. Plot Of All Values For Carbon Dioxide Production (LPM, STPD), As Functions Of Respiratory Minute Volume.

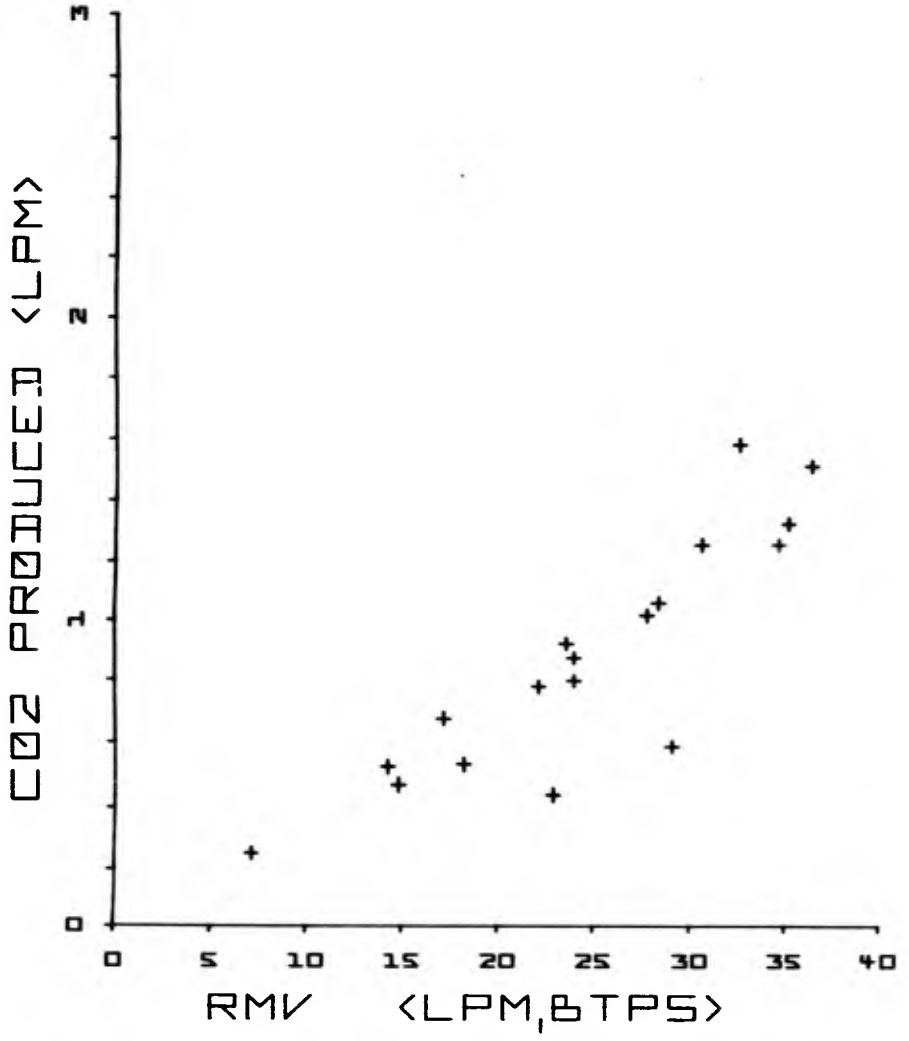

Figure 24. Carbon Dioxide Production (LPM, STPD) During Data Runs At 450 Feet.

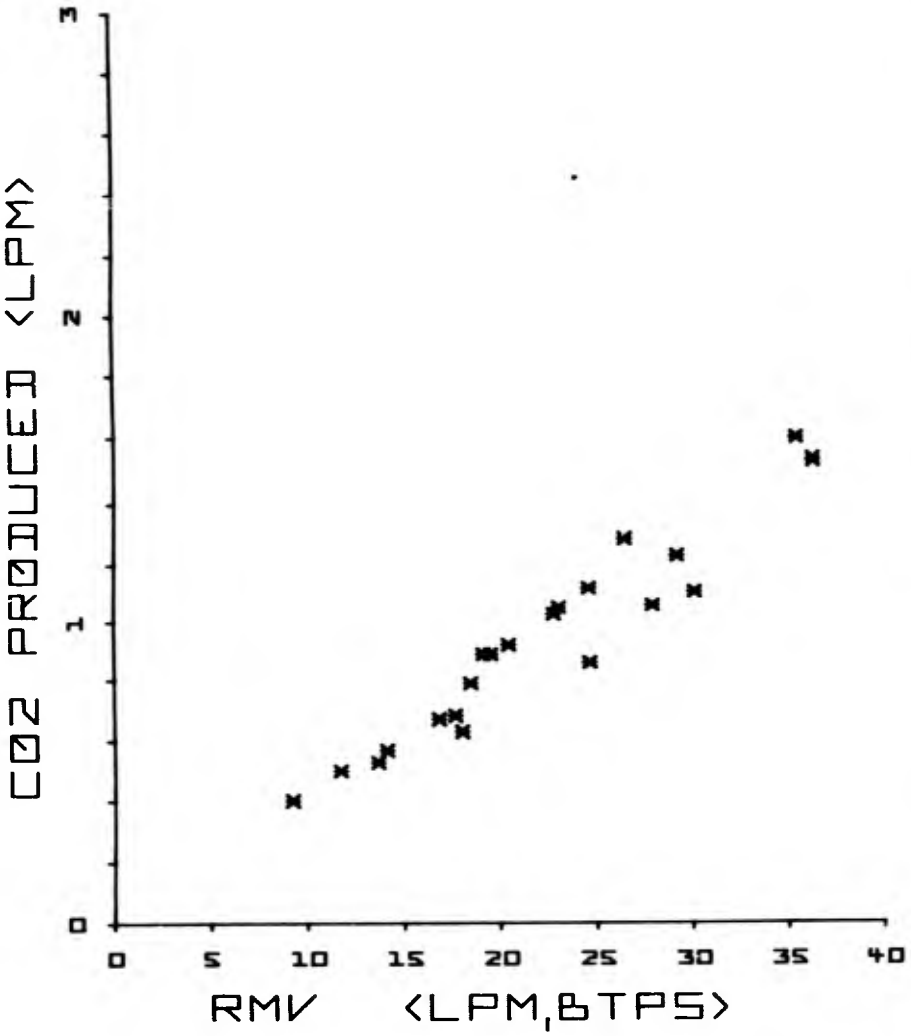

Figure 25. Carbon Dioxide Production (LPM, STPD) During Data Runs At 650 Feet.

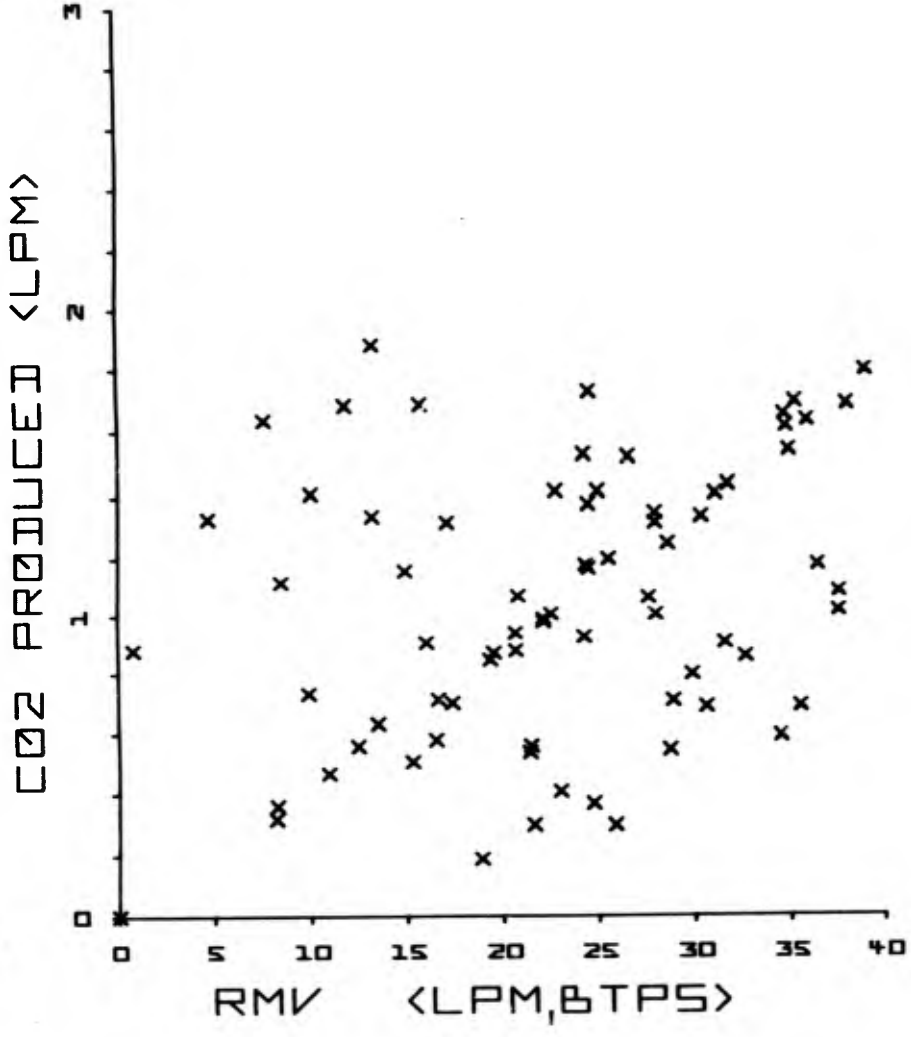

Figure 26. Carbon Dioxide Production (LPM, STPD) During Data Runs At 852 Feet.

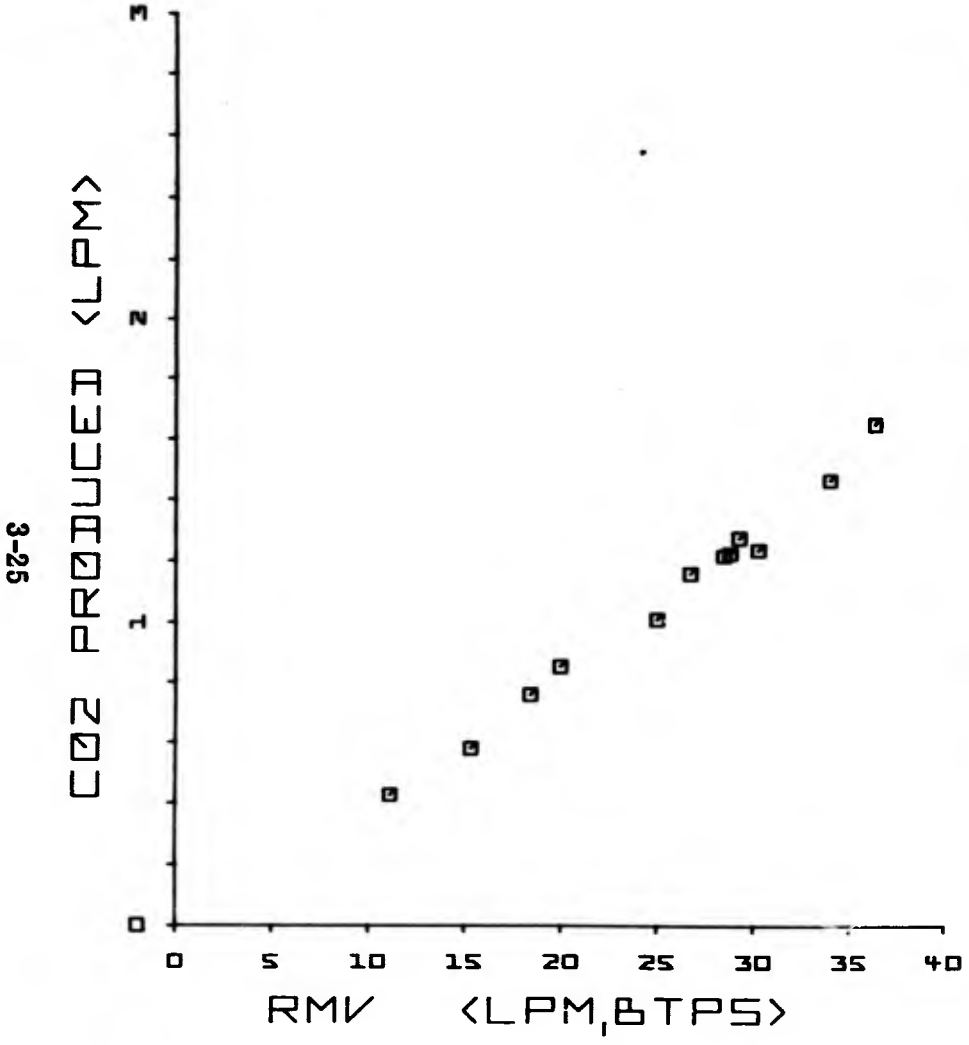

Figure 27. Carbon Dioxide Production (LPM, STPD) During Data Runs At 1,000 Feet.

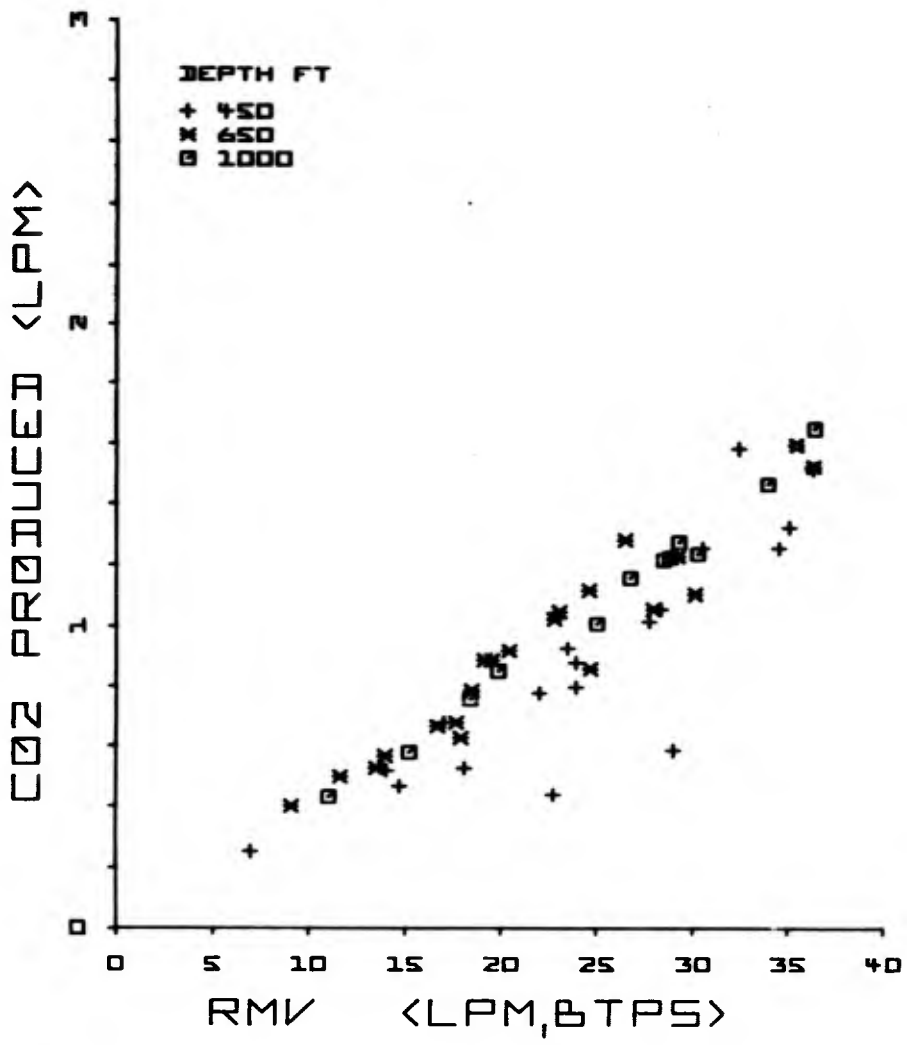

Figure 28. Carbon Dioxide Production As A Function Of Ventilation: Same As Figure 23, Without Data For 852 Feet.

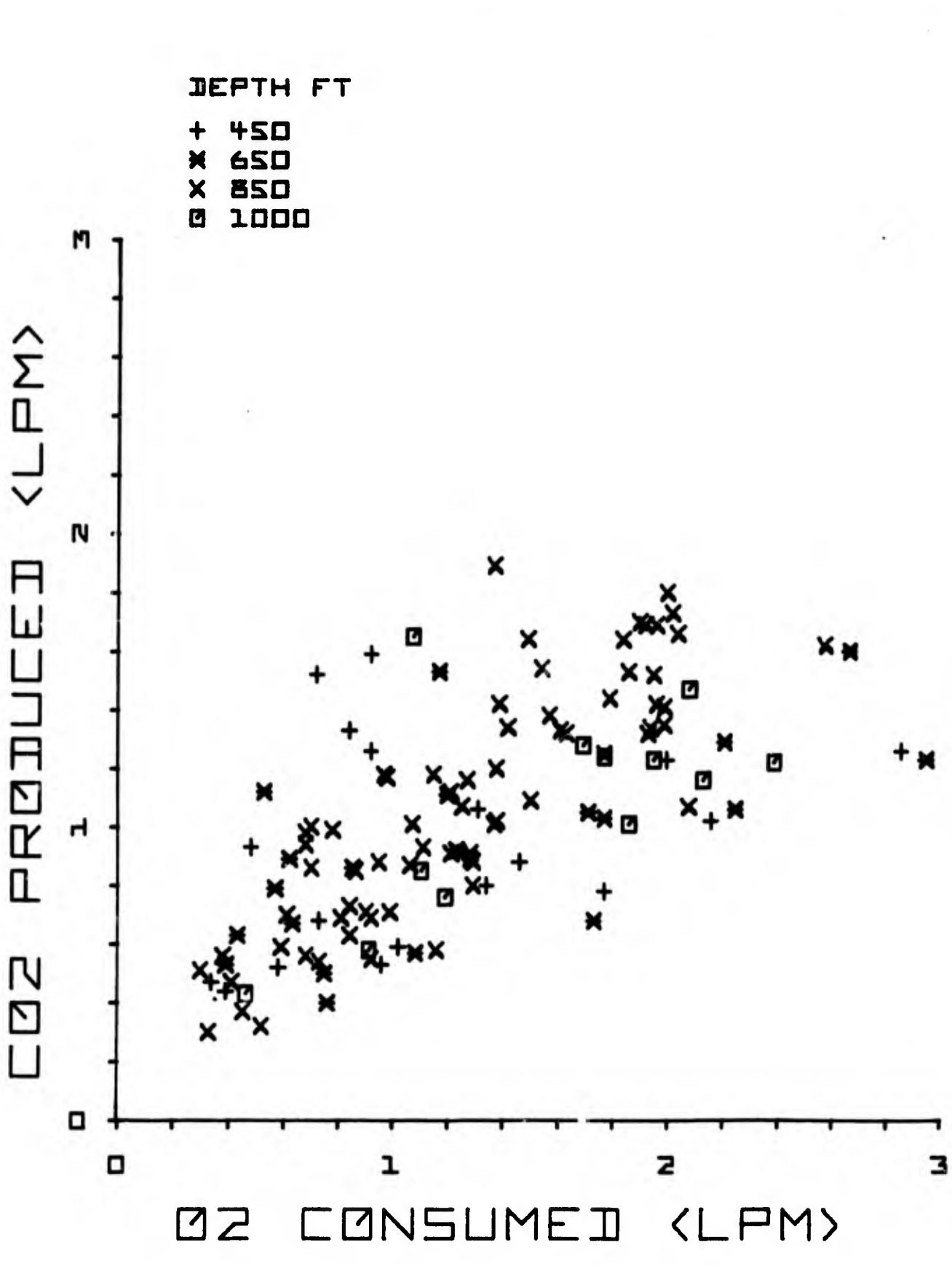

Figure 29. Relationship Of Oxygen Consumed To Carbon Dioxide Produced (V_{CO_2}/V_{O_2} = Respiratory Exchange Ratio).

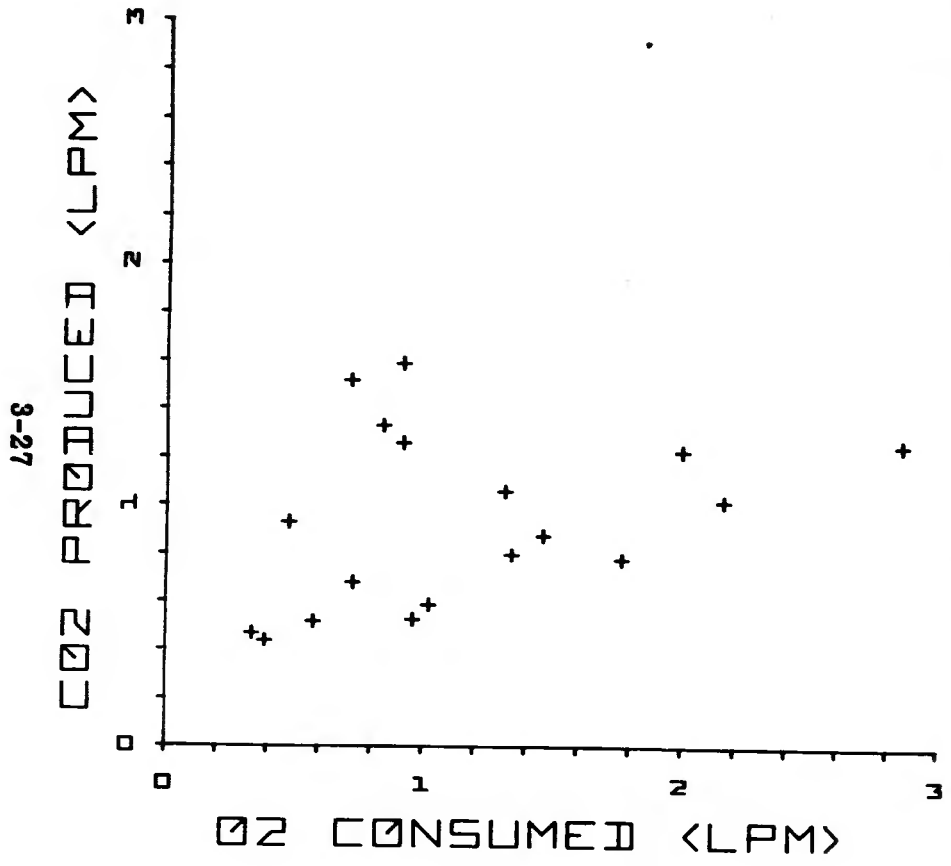

Figure 30. Depth 450 Feet: Relationship Of Oxygen Consumption And Carbon Dioxide Production.

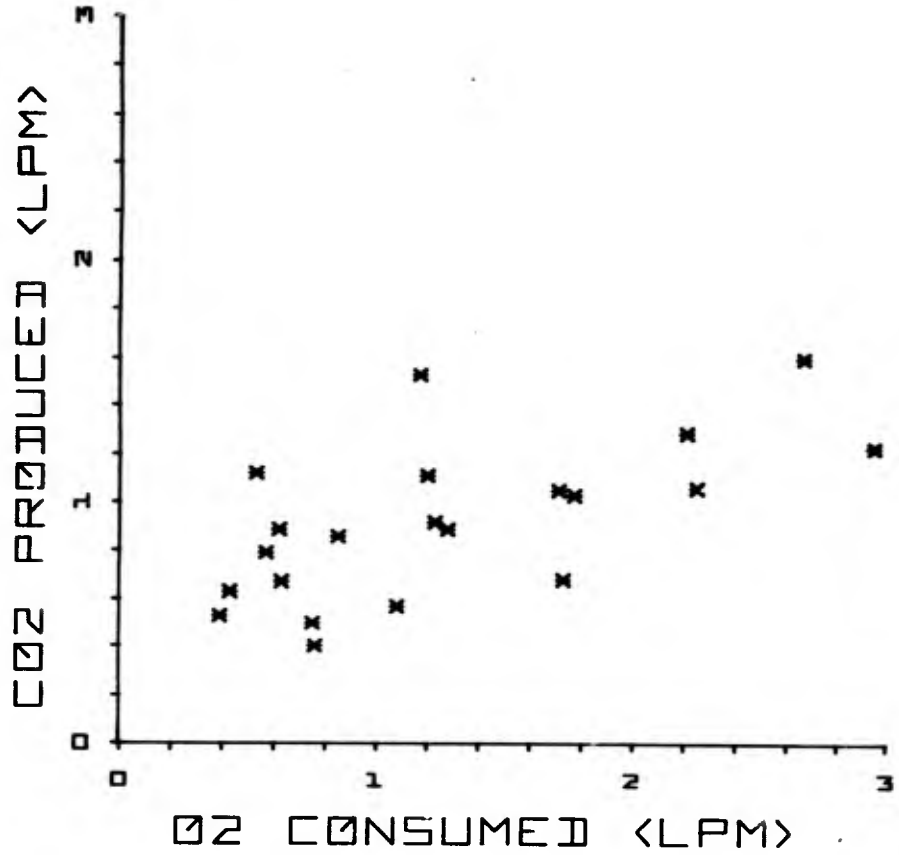

Figure 31. Depth 650 Feet: Relationship Of Oxygen Consumption and Carbon Dioxide Production.

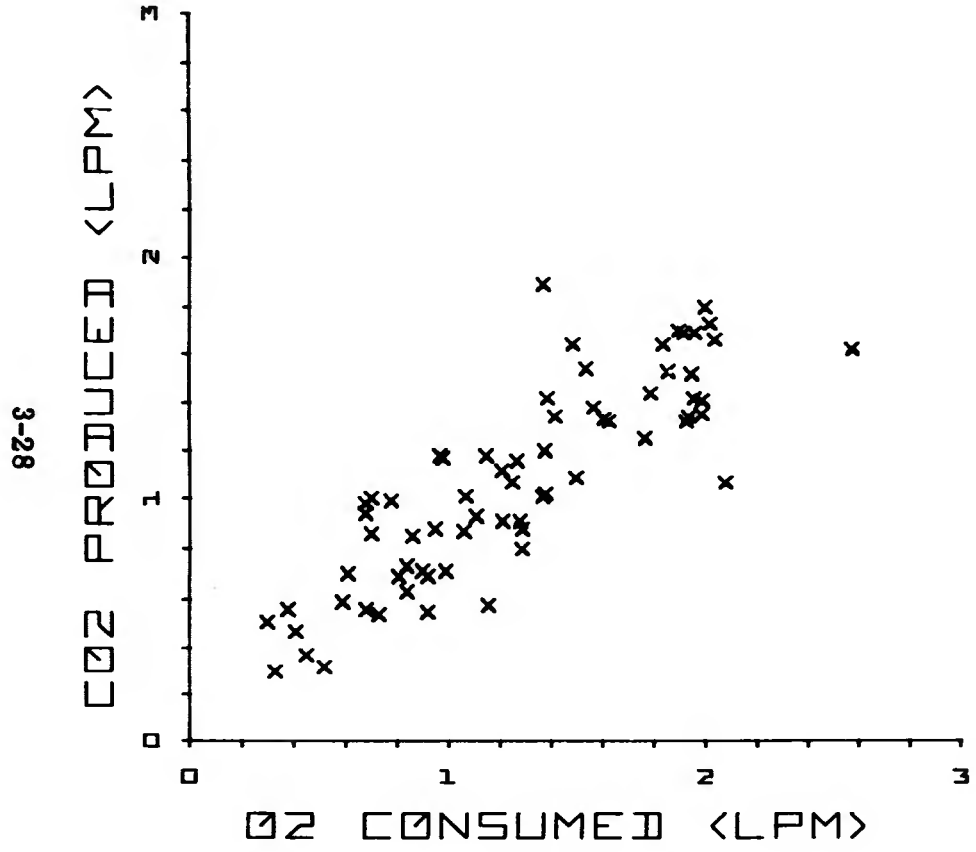

Figure 32. Depth 850 Feet: Relationship Of Oxygen Consumption and Carbon Dioxide Production.

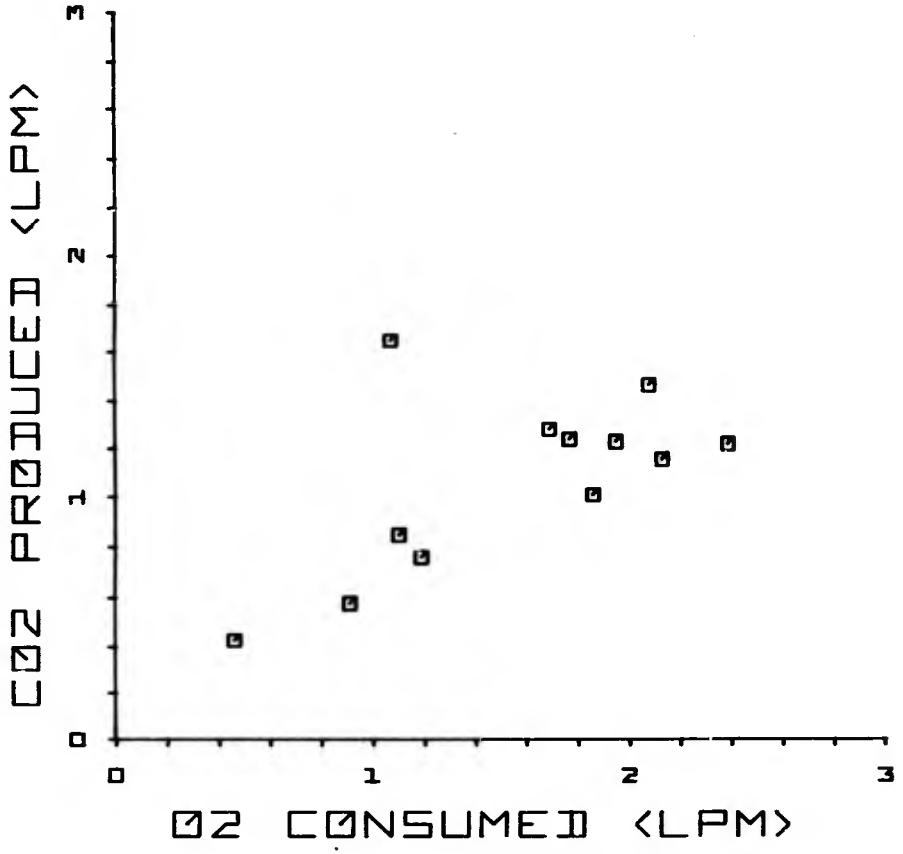

Figure 33. Depth 1,000 Feet Relationship of Oxygen Consumption and Carbon Dioxide Production.

TABLE IV

Ventilatory Parameters

DATA NO	RMV LPM,BTPS	VT L,BTPS	F	P(CMH2O) IN	P(CMH2O) EX	FLOW L,SEC	V02 LPM	VC02 LPM	RER
1	11.189	.9	13.0	0	0	.5	2.283	.280	.12
2	20.138	1.4	14.4	3	5	.7	4.010	.520	.13
3	22.816	1.4	16.6	8	8	1.2	.393	.437	1.11
4	35.136	1.6	21.3	8	10	1.8	.844	1.328	1.57
5	15.778	.8	19.6	2	3	.6	2.584	.564	.22
6	23.543	1.4	17.4	2	5	1.0	.479	.925	1.93
7	26.537	1.6	17.0	4	6	1.2	3.977	1.016	.26
8	28.359	1.8	16.2	7	8	1.2	1.313	1.057	.80
9	22.035	1.9	11.9	4	4	.7	1.768	.775	.44
10	27.722	1.9	14.3	6	8	1.0	2.164	1.017	.47
11	34.573	1.7	20.4	7	10	1.2	2.864	1.257	.44
12	44.610	1.8	24.3	8	12	1.8	3.220	1.671	.52
13	7.052	.6	12.0	0	0	.4	.235	.252	1.07
14	14.751	1.1	13.7	3	4	.8	.341	.466	1.37
15	29.033	1.8	16.4	14	17	2.2	1.015	.586	.58
16	42.103	3.6	11.8	15	35	2.5	2.000	1.235	.62
17	14.148	.7	19.0	3	3	.4	.575	.520	.90
18	17.092	.9	18.8	3	3	.7	.733	.680	.93
19	18.087	1.1	17.2	3	5	.9	.964	.534	.55
20	23.946	1.6	15.0	6	12	1.3	1.456	.882	.61
21	23.959	1.7	14.0	0	0	1.0	1.344	.804	.60
22	30.498	1.9	15.8	6	8	1.4	.917	1.261	1.37
23	32.505	1.8	18.2	0	8	1.6	.924	1.586	1.72
24	36.299	1.7	21.0	0	0	1.8	.724	1.520	2.10
25	11.656	.7	16.5	0	0	.6	.749	.503	.67
26	19.545	1.0	19.4	0	0	.9	1.283	.888	.69
27	35.471	2.1	17.0	7	10	1.8	2.672	1.604	.60
28	39.111	3.1	12.8	11	18	3.5	3.111	1.106	.36
29	16.816	.7	22.8	4	4	.6	.635	.668	1.05
30	20.466	.9	22.9	2	8	.9	1.231	.918	.75
31	23.062	1.0	22.8	4	5	1.0	1.706	1.053	.62
32	26.465	1.2	23.0	4	4	1.0	2.209	1.292	.58
33	14.080	1.2	11.8	0	0	.8	1.077	.571	.53
34	22.809	1.6	14.6	0	0	1.0	1.772	1.027	.58
35	27.964	1.5	18.5	0	0	1.2	2.251	1.061	.47
36	34.378	1.5	22.2	10	12	1.6	3.112	1.447	.46
37	9.170	.7	13.0	2	3	.5	.758	.395	.52
38	17.644	1.4	13.0	4	5	1.0	1.729	.678	.39
39	29.184	2.8	10.4	10	12	3.0	2.952	1.227	.42
40	40.277	3.4	12.0	12	35	3.6	4.325	1.650	.38
41	13.632	.6	21.0	4	4	.5	.394	.526	1.34
42	18.476	1.0	18.6	3	7	.8	.565	.795	1.41
43	19.133	1.1	18.2	4	5	.9	.617	.888	1.44
44	24.566	1.3	19.4	6	8	1.2	.533	1.119	2.10
45	18.031	1.4	12.7	3	4	.7	.425	.629	1.48
46	24.678	1.6	15.1	5	8	1.0	.849	.864	1.02

TABLE IV

Ventilatory Parameters (Continued)

DATA NO	RMV LPM,BTPS	VT L,BTPS	F	P(CMH2O) IN	P(CMH2O) EX	FLOW L,SEC	V02 LPM	VC02 LPM	RER
47	30.159	1.8	17.0	0	0	1.2	1.201	1.110	.92
48	36.364	1.9	18.7	0	10	1.8	1.174	1.534	1.31
49	8.213	.7	11.5	2	2	.4	.516	.319	.62
50	16.520	1.4	11.5	3	4	.8	1.165	.580	.50
51	27.750	3.3	8.4	7	15	2.0	2.083	1.066	.51
52	33.686	4.1	8.3	10	25	3.0	1.732	1.532	.88
53	12.484	.8	16.0	0	0	.6	.382	.556	1.45
54	20.732	1.0	21.0	6	7	.9	.681	.940	1.38
55	22.148	1.0	22.0	10	12	1.1	.779	.994	1.28
56	24.366	1.1	22.5	10	20	1.2	.967	1.176	1.22
57	15.315	1.3	11.6	0	0	.7	.303	.512	1.69
58	22.176	1.7	12.8	0	0	1.0	.682	.981	1.44
59	22.583	1.9	11.7	0	0	1.3	1.069	1.009	.94
60	24.526	1.6	15.8	9	22	1.6	.977	1.165	1.19
61	10.978	.7	15.2	2	2	.6	.413	.470	1.14
62	25.606	2.0	13.0	4	6	1.2	1.376	1.203	.87
63	34.826	3.0	11.5	5	8	2.2	2.035	1.661	.82
64	39.140	3.6	10.8	6	12	3.1	2.004	1.801	.90
65	16.708	1.0	16.6	2	3	.9	.990	.707	.71
66	27.975	1.5	18.2	5	6	1.6	1.990	1.347	.68
67	31.805	1.6	20.2	0	0	1.9	1.791	1.439	.80
68	34.843	1.5	23.0	0	0	2.0	2.579	1.623	.63
69	19.508	1.6	12.2	2	4	1.2	.863	.850	.98
70	28.006	1.8	15.5	3	5	1.4	1.633	1.321	.81
71	35.002	2.2	16.1	8	13	2.0	1.544	1.536	.99
72	35.974	2.1	17.1	8	13	2.4	1.843	1.641	.89
73	11.118	.8	14.7	0	0	.4	.464	.430	.93
74	18.431	2.2	8.5	0	0	.9	1.195	.761	.64
75	30.261	3.4	8.8	5	16	2.6	1.765	1.243	.70
76	34.022	3.8	9.0	9	21	3.5	2.076	1.465	.71
77	15.339	.7	21.0	0	0	.7	.910	.576	.63
78	24.975	1.1	23.3	5	5	1.1	1.860	1.011	.54
79	28.834	1.3	22.0	0	0	1.4	1.952	1.226	.63
80	28.469	1.4	21.0	5	9	1.3	2.395	1.224	.51
81	19.921	1.5	13.0	3	5	.7	1.099	.850	.77
82	26.750	1.8	14.5	0	0	1.1	2.134	1.163	.54
83	29.249	2.0	14.3	0	0	1.3	1.688	1.280	.76
84	36.401	2.2	16.5	0	0	1.9	1.072	1.650	1.54
85	8.283	.8	10.8	0	0	.4	.213	.364	1.71
86	13.498	1.2	11.0	3	3	.7	.837	.626	.75
87	20.735	2.6	8.0	7	11	2.3	1.292	.882	.68
88	26.632	3.0	9.5	8	14	2.7	1.771	1.248	.70
89	17.451	1.1	16.2	2	3	.7	.615	.700	1.14
90	30.413	1.6	18.5	3	6	1.4	1.421	1.341	.94
91	41.017	1.7	24.3	5	7	2.2	5.736	.336	.06
92	.000	.0	.0	0	0	.0	.000	.000	.00

TABLE IV

Ventilatory Parameters (Continued)

DATA NO	RMV LPM,BTPS	VT L,BTPS	F	P(CMH2O) IN	P(CMH2O) EX	FLOW L,SEC	VO2 LPM	VCO2 LPM	RER
93	19.641	1.7	11.3	4	4	1.0	1.062	.874	.82
94	31.097	2.0	15.3	5	7	1.6	1.988	1.407	.71
95	38.120	2.4	16.0	0	0	2.2	1.961	1.693	.86
96	10.052	.0	.0	0	0	.0	1.988	1.407	.71
97	.000	.0	12.8	2	3	.4	.000	.000	.00
98	15.745	1.3	11.8	3	4	.7	1.961	1.693	.86
99	22.976	2.9	7.8	7	16	2.1	.174	.409	2.35
100	28.992	2.6	11.0	6	20	2.3	.904	.706	.78
101	20.956	.9	23.9	3	4	.8	1.251	1.074	.86
102	24.503	1.2	21.0	4	6	1.2	1.575	1.378	.87
103	32.726	1.3	24.6	5	7	1.4	.699	.858	1.23
104	36.531	1.6	23.2	7	14	1.8	1.153	1.175	1.02
105	22.844	1.8	12.4	4	5	1.1	1.391	1.417	1.02
106	35.400	2.2	16.2	5	8	1.8	1.898	1.701	.90
107	41.749	2.2	19.2	5	8	1.9	.700	.998	1.43
108	7.694	.0	.0	0	0	.0	1.488	1.644	1.11
109	13.344	1.2	11.3	0	0	.4	1.369	1.889	1.38
110	.000	.0	11.2	0	0	.7	.000	.000	.00
111	21.597	2.6	8.4	4	9	2.6	.184	.299	1.63
112	34.513	3.1	11.0	8	14	2.4	.594	.590	.99
113	24.387	1.1	22.4	3	6	1.2	1.114	.934	.84
114	24.349	1.1	21.8	3	7	1.4	1.856	1.531	.83
115	31.672	1.4	22.9	4	8	1.6	1.208	.910	.75
116	37.682	1.7	22.8	5	9	2.2	1.378	1.020	.74
117	13.266	1.3	10.6	0	0	.7	1.944	1.338	.69
118	24.560	1.7	14.6	5	6	1.3	2.023	1.733	.86
119	28.743	1.9	15.1	7	9	1.7	.922	.550	.60
120	37.673	1.8	21.2	8	11	1.9	1.503	1.089	.72
121	4.747	.4	10.7	0	0	.4	1.605	1.329	.83
122	11.874	1.0	11.4	0	0	.6	1.924	1.694	.88
123	18.828	2.7	7.0	0	0	2.3	.146	.188	1.29
124	21.384	3.1	6.9	0	0	2.6	.730	.538	.74
125	9.947	1.2	8.2	0	0	.7	.841	.727	.86
126	19.832	1.6	12.3	0	0	1.0	.951	.878	.92
127	24.714	1.8	14.0	0	0	1.5	.448	.368	.82
128	29.897	1.6	18.2	0	0	1.7	1.289	.800	.62
129	8.511	.7	11.7	0	0	.4	1.211	1.117	.92
130	17.160	1.3	12.8	0	0	.8	1.926	1.324	.69
131	25.843	2.8	9.3	0	0	1.7	.326	.305	.94
132	30.655	2.9	10.5	0	0	2.0	.812	.689	.85
133	15.012	1.0	14.7	0	0	.8	1.269	1.161	.92
134	24.976	1.2	20.6	0	0	1.7	1.963	1.417	.72
135	21.528	1.4	15.2	0	0	1.9	.681	.562	.83

TABLE IV

Ventilatory Parameters (Continued)

DATA NO	RMV LPM,BTPS	VT L,BTPS	F F	P(CMH2O) IN	P(CMH2O) EX	FLOW L,SEC	VO2 LPM	VCO2 LPM	RER
136	28.079	1.3	22.3	0	0	1.7	1.366	1.012	.74
137	16.140	1.5	10.7	0	0	1.2	1.280	.906	.71
138	26.595	1.9	14.0	0	0	2.1	1.949	1.517	.78
139	35.569	2.0	18.0	7	13	1.9	.917	.685	.75
140	42.710	2.0	21.2	9	15	2.3	1.775	1.172	.66

TABLE V

TEST SUBJECT RESPONSES TO COLD WATER - COLD GAS EXPOSURES

ACTIVITY	RESTING			LIGHT WORK			RESTING			MODERATE WORK			RESTING			HEAVIEST WORK		
SUBJECT	F.A.	K.C.	S.Z	F.A.	K.C.	S.Z.	F.A.	K.C.	S.Z.	F.A.	K.C.	S.Z.	F.A.	K.C.	S.Z.	F.A.	K.C.	S.Z.
Cold Torso, Skin	100	100	50	100	100	50	100	100	50	100	100	25	100	100	0	100	75	0
Cold Extremity, Skin	100	100	50	100	100	50	100	75	25	100	75	25	100	75	0	100	25	0
Headache	0	0	0	0	0	0	0	0	0	0	0	25	0	0	25	0	0	25
Chest Pain	0	0	0	0	0	50	0	0	0	0	0	75	0	0	0	0	0	75
Shivering, Chest	100	100	75	100	100	75	100	100	100	100	100	75	100	100	100	100	75	50
Shivering, Limbs	100	75	25	100	75	0	100	75	100	100	75	50	100	75	75	100	75	50
Salivating	100	100	100	100	100	100	100	100	100	100	100	100	100	100	100	100	100	100
Nasal Drainage	100	100	100	100	100	100	100	100	100	100	100	100	100	100	100	100	100	100
Coughing	0	0	0	0	0	0	0	0	0	0	0	0	0	0	0	0	25	0
Breathing Difficulty	0	0	0	25	0	0	0	0	0	100	0	0	0	0	0	100	25	0

BLANK PAGE

SECTION 4

DISCUSSION

Temperature of Exhaled Gas

Unless there are reliable measurements of the temperature of the gas as it is exhaled, projections of the heat loss through respiration remain speculative. With respect to the mathematical expressions for respiratory heat loss, one can define the magnitudes of the gas properties, density and specific heat, and assign sample values to inhaled gas temperature and pulmonary ventilatory rate, but, as Webb (35) has stated, "the only unknown is the temperature of the air as it leaves the oronasal portal in expiration." The effect of presuming that the exhaled air is at core temperature has already been reviewed (see Introduction). Thus, the most important quantitative information acquired during this study is the temperature data for exhaled gas. The extensive engineering efforts in support of this data acquisition have been documented in Appendix 2.

The results listed herein for respiratory heat loss will be approximately 60 - 80% of theoretical values calculated assuming exhalation temperature equals core temperature. Also, these results are based upon a gas saturated at inhalation temperature and saturated at exhalation temperature, not core temperature. This will produce a lower value of insensible heat loss of 30 to 60% depending upon the water temperature.

Diver-Subject Heat Balance

The energy generated by metabolism is thermally stored in the body or lost to the environment by work and thermal conduction, convection, evaporation, and radiation heat transfer. The rates of energy flow are given in the energy flow equation for a body, as shown by Nevins (23)

$$M = S + W + K + C + E + R$$

where:

M is rate of metabolic energy produced within the body. It varies with the level of physical activity and is calculated using the measured oxygen consumption.

S is rate of heat stored into the body. It is calculated by the technique of Burton described earlier

$$S = m_b \, Cp_b \, (2/3 \, \Delta T_r + 1/3 \, \Delta T_{mws})$$

m_b is mass of the body

Cp_b = .83 Btu/lb - °F (0.83 Kcal/Kgm °C) is the most acceptable mean value of specific heat of the body (17).

ΔT_r is change in rectal temperature

ΔT_{mws} is change in mean weighted skin temperature

In this study the temperatures decrease so we have a negative value of stored heat, S, or a positive value of (-S).

W is rate of work done by the body on the environment. For the swimmer working against the ergometer described herein, his body motion work energy is converted into ambient water kinetic energy and finally dissipated in the ambient water as viscous energy loss.

K is rate of heat loss conducted into a solid surface touching the skin.

$C = C_s + C_r$ is rate of heat conducted and convected away from the body by a gas or a liquid medium touching the skin, C_s, or breathing gas in the respiratory tract, C_r.

$E = E_s + E_r$ is rate of heat loss by evaporation from the skin, E_s, and from the respiratory tract, E_r.

R is net rate of heat radiated from the skin.

The total heat loss through the skin (Q_s) is

$$Q_s = + K_s + C_s + E_s + R$$

and, the heat loss from the respiratory tract (Qr) is

$$Q_r = C_r + E_r$$

C_r and E_r are calculated from changes in temperature and composition of the breathing gas, utilizing the equation shown in Section 2 and Appendix 1.

In the case of a fully submerged diver wearing a free flooding hot water suit the radiation term, R, and skin evaporation term, E_s, are assumed to be zero, and the energy flow equation for the diver subjects of this study becomes

$$M = S + W + Q_s + Q_r.$$

The heat balance, thus computed on a run basis, is shown in Table VI.

A rough estimate of the diver-subjects mean work rate is W = 0.1 hp or 64 Kcal/hr. This value was obtained assuming a maximum work rate of 0.4 hp and scaling the work rates according to the diver-subjects reported effort levels. The reference for this estimate is the Bioastronautics Data Book (36) which summarizes the sustainable work levels on a time and subject fitness basis. This value is used to calculate Q_s in Table VI.

Metabolic rates of the diver subjects were calculated from measured compositions of mixed exhaled gas. To obtain an average value for each diver-subject run the values of oxygen uptake were averaged using the technique described earlier for respiratory minute volume. These values were then converted to units of energy (1 liter per minute O_2 uptake = 1158 Btu/hr or 293 Kcal/hr) and are listed in column 2 of Table VI. The wide range in metabolic rates for the individual data points resulted in average metabolic rates which did not allow a heat balance analysis of any consistency. Therefore two assumptions were made: (1) that the average respiratory quotient for all data was 0.9; (2) that CO_2 production was 0.045 liters CO_2 produced per liter exhaled gas. Oxygen consumption was then estimated by assuming that 0.05 liters of O_2 were produced per liter of gas exhaled. The metabolic rates thus calculated (M_c) are listed in column 3 of Table VI.

Columns 4 and 5 of Table VI list respiratory heat loss and body heat storage respectively. The storage term is negative indicating that the body is in negative thermal balance. The magnitude of the storage term indicates the rate that the energy leaving the body exceeds the metabolic rate.

TABLE VI

HEAT BALANCE ANALYSIS								
Run No.	Metabolic Rate M Kcal/hr	Adjusted Metabolic Rate Mc Kcal/hr	RHL (Qr) Kcal/hr	S Storage Kcal/hr	Qr/Mc %	Q_s	Heat Transfer Coefficient H_s Kcal/hr M^2C	W Kcal/hr
1	180	328	79	--	24	—	--	64
2	262	350	86	-21	25	221	42.2*	64
3	721	457	135	-48	30	306	50.6*	64
4	238	324	101	-37	31	196	25.3	64
5	265	265	93	-53	35	161	21.5	64
6	276	454	122	-64	27	332	49.0*	64
7	547	372	160	-65	43	213	25.3	64
8	421	316	116	-60	37	196	31.7	64
9	597	359	157	-53	44	191	49.0*	64
10	694	337	126	-19	37	166	26.5	64
11	158	275	105	-54	38	160	18.7	64
12	270	390	151	-54	39	228	46.4*	64
13	374	303	122	-31	40	148	23.3	64
14	208	295	111	-61	38	182	22.4	64
15	223	316	127	-29	40	154	—	64
16	436	400	197	-62	49	201	35.1	64
17	558	406	195	-60	48	207	22.5	64
18	448	423	218	-44	51	185	29.1	64
19	404	330	194	-44	59	116	53.6*	64
20	548	359	193	-56	54	158	26.0	64
21	482	401	242	-54	60	150	27.0	64
22	301	250	139	-11	55		9.2	64
23	334	438	245	-75	56	204	27.2	64
24	510	437	254	-68	58	186	25.0	64
25	293	275	152	-36	55	95	13.4	64
26	376	403	218	-68	54	189	24.4	64

TABLE VI (Continued)

Run No.	Metabolic Rate M Kcal/hr	Adjusted Metabolic Rate Mc Kcal/hr	RHL (Qr) Kcal/hr	S Storage Kcal/hr	Qr/Mc %	Q_s	Heat Transfer Coefficient H_S Kcal/hr M^2C	W Kcal/hr
27	367	490	290	-73	59	208	29.9	64
28	264	268	147	-36	55	175	39.6	64
29	469	408	219	-46	54	172	21.6	64
30	444	376	214	-68	57	166	33.8	64
31	206	205	96	-25	47	70	16.3	64
32	372	306	159	-31	49	123	75.0*	64
33	313	293	161	-65	55	133	38.6	64
34	397	334	179	-52	54	143	19.4	64
35	548	435	242	-66	56	195	158.5*	64

The percentage of metabolic heat lost through respiratory heat loss is shown in column 6. In all cases but two at 850 feet and deeper this value exceeds 50%, including each case that was diver aborted.

Theoretically, reducing the respiratory heat loss by an amount equal to or greater than the value of negative thermal storage would restore thermal balance. Unpublished results of prior dives in 35°F water at 650 ft. with the diver subject wearing the identical hot water suit described herein showed divers in thermal balance over a four-hour period. The breathing apparatus worn by the diver was semi-closed circuit and featured a hot-water-heated CO_2 absorbent canister. These divers also used full face masks with inner oro-nasal masks. At that time the inhalation temperature (not measured) was estimated to be water temperature. Subsequent unpublished tests with this breathing apparatus and face mask indicate that actual inhalation temperature was much higher, possibly 65°F. This, of course, has a considerable influence on the magnitude of respiratory heat loss, and evidently allowed thermal balance.

The remaining factor in the heat balance expression is the heat lost through the skin. Heat lost through the skin of the diver-subjects depended on mean temperatures, and on characteristics of the diver, the water heated suit, and the ambient wet pot water. Figure 34 shows a schematic cross section of diver's skin, suit, and wet pot water with a hypothetical mean temperature profile and mean heat flows. The complex shape of the human body and the unknown distribution of hot water within the suit make it difficult to directly calculate this heat loss. However, since the other components of the heat balance are measured, the energy loss through the skin can be calculated indirectly. The results of solving the equation, $Q_s = M-S-W-Q_r$, are shown in column 8 of Table VI. The amount of heat lost by the body at the skin surface must equal the heat flowing to the skin from the deep body tissues. This heat flow can be expressed as follows:

$$Q_s = h_s A_b (T_r - T_{mws})$$

where

h_s = mean heat transfer coefficient for the skin and body tissues, and

A_b = body surface area according to the method of Dubois (15):

$$A_b = \left[0.108\right] \left[W^{0.425}\right] \left[H^{0.725}\right] ,$$

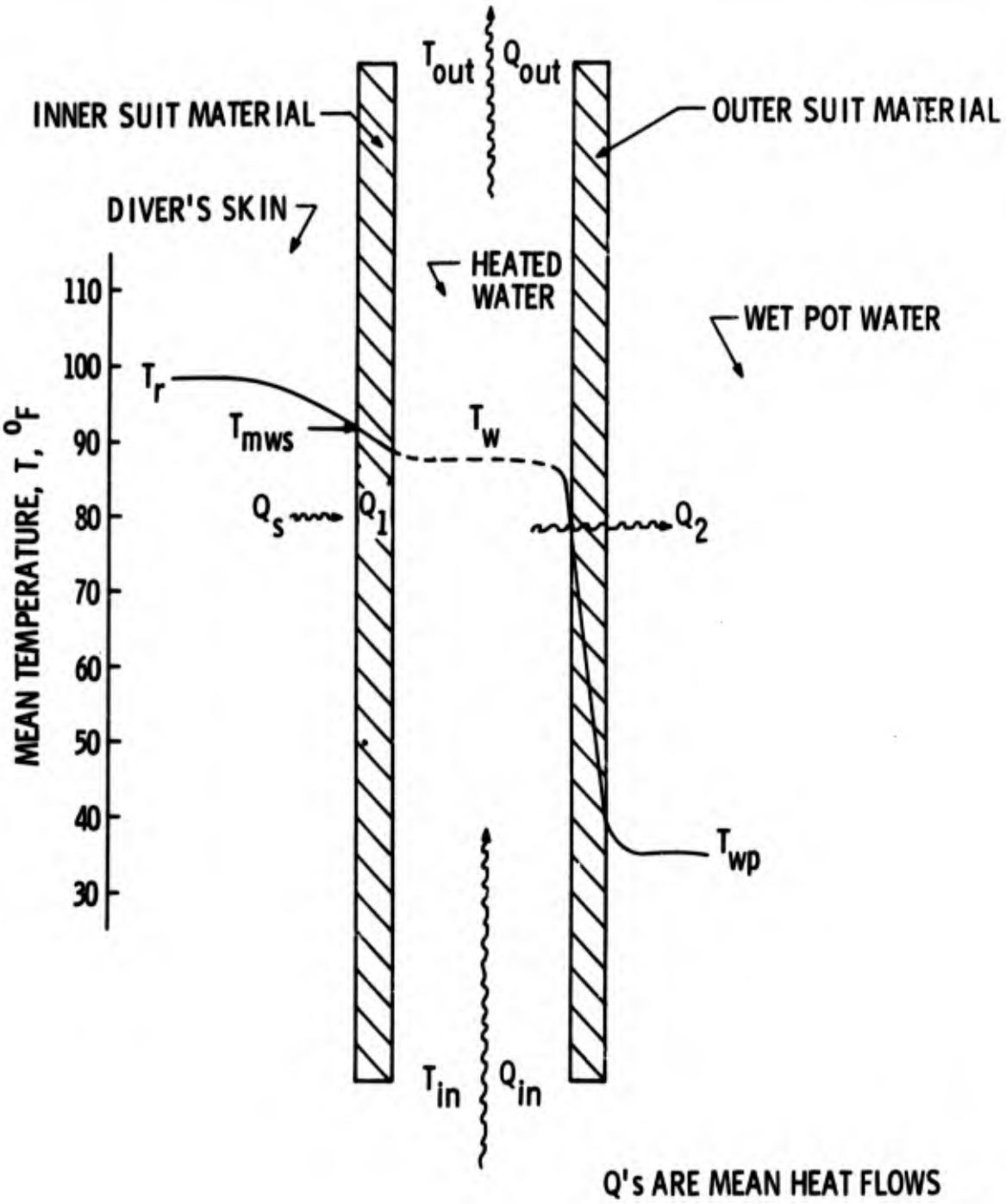

Figure 34. Hypothetical Mean Temperature Profile Across A Diver's Skin And Water Heated Suit.

with weight (W) in pounds and height (H) in inches.

The values for BSA as computed for our subjects are as follows:

Subject	Body Surface Area (M^2)	Data Runs
SZ	2.14	2, 5, 8, 11, 14, 17, 20, 23, 26, 29, 34
KC	1.93	1, 4, 7, 10, 13, 16, 19, 22, 25, 28, 31, 33
FA	1.84	3, 6, 9, 12, 15, 18, 21, 24, 27, 30, 32, 35

This equation can be rearranged, and the unknown term h_s calculated using

$$h_s = \frac{Q_s}{A_b (T_r - T_{mws})} = \frac{M-S-E-W}{A_b (T_r - T_{mws})}$$

Results of this equation are given in Table VI for all runs except the first, for which a value of mean corrected heat flow out of the skin was not obtainable.

Calculated values of heat transfer coefficient, h_s, show 24 of the 33 values are grouped between h_s = 9.2 and 38.6 Kcal/hr m^2°C. The remaining values seemed higher than possible. Nine of the calculated values of h_s are much greater than the approximate range of skin heat transfer coefficients found in the literature. For example, an approximate range of skin conductance is given as 9-30 Kcal/hr m^2°C by Webb (36). References (9) (24) indicate that heat transfer coefficients are greatest for high work rates, high skin temperatures, and thin subjects. These sources report variation in h_s between 2.2 and 33 Kcal/hr m^2°C, for immersed subjects. The variation in skin heat transfer coefficient is mainly due to differences in fat skin fold thicknesses and the variation in vasoconstriction of the peripheral blood vessels. It is not surprising therefore that six of the nine high values of h_s were for runs by the thinnest diver, F.A.

The divers mean weighted skin temperatures were in the range normally considered to be comfortable (38) (39). This indicates that the peripheral vessels were not constricted, and that the heat transfer coefficient was high.

The measured mean weighted skin temperatures and their correlation with reported comfort zones are contradictory to the divers subjective reports. The method of Teichner, which was selected for calculating mean weighted skin temperatures to allow direct

comparisons with earlier results (3), does not include extremity temperatures. Some sample calculations were made with the DuBois formula which includes extremity temperatures, and the results for mean weighted skin were about 0.8°C (1.4°F) lower. Also it is characteristic of this hot water suit that the extremities are maintained warmer than they are under conditions of thermal comfort in air. A 1°C lower skin temperature is not significant since all the measurements except one indicate that skin temperature is in the comfort range. Also the drop in skin temperatures is much less than would be expected from either the subjective responses or the fall in rectal temperature. Two of the exceptions are runs 23 and 27, which were aborted by the divers.

One explanation for the discrepancy between reported comfort levels and that indicated by the skin temperatures is that the extreme local discomfort of breathing the cold gas interferes with appreciation of warm skin areas. Another may be that sections of the diver's suits trapped and held water, causing cold skin temperatures in areas not under thermistor monitoring. This would cause the measured mean skin temperature to be greater than actual skin temperature, thus producing unreasonably high calculated values of h_s. Cold water within the suit could be due to wet pot water flushing in and out, or to low flow of heating water as a result of flow restrictions.

To determine the effectiveness of the water heated diving suit, the heat flow, Q_s, through the diver's skin for a typical run is compared to the theoretical heat flow, Q'_s, if the diver had been wearing a hypothetical suit with a uniform flow of heating water in it. The hypothetical suit is assumed to have rectangular shape with a length of L, a breadth of B, and a heating water gap of D_1. The heated water is assumed to have a uniform velocity and a constant temperature at each distance, x, of the total flow length, L. The typical run chosen for the comparison is run 29. The value of h_s for this run is 21.6 Kcal/hr m^2°C, which is about the mean value of the grouped values of h_s. The heat flow out through the skin, calculated from test data is 681 Kcal/hr as compared to the heat flow into the skin from the hypothetical suit, 43 Kcal/hr. The heat flow into the hypothetical suit is found from

$$Q'_s = \frac{1}{\frac{1}{h_s} + \frac{D_1}{K_m}} A_b (T_r - T_w) = -170 \text{ Btu/hr } (-43 \text{ Kcal/hr})$$

where

D_1 = thickness of inner suit

K_m = thermal conductivity of inner suit material, Btu/hr ft^2°F

T_w = mean water temperature inside the suit

The heat transfer coefficient of the skin, h_s = 4.4 Btu/hr ft^2°F, for run 29 is considerably less than the heat transfer coefficient of the inner suit material, K_m/D_1 = .1/.00833 = 12 Btu/hr ft^2°F. This indicates that the inner suit material does not significantly contribute to the thermal insulation.

The mean water temperature (T_w) used to calculate the heat flow through the skin of the diver with the hypothetical suit is 101°F. This was calculated by assuming heat flow only across the outer suit material. Such a simplification results in little error because the heat flow across the outer suit material is much greater than the heat flow across the inner suit material. Heat flow across an incremental length, dx, of the outer suit material would be

in which $$dQ_2 = K_m (T - T_{wp}) B dx/D_0$$

T_{wp} = wet pot water temperature.

Heat flow from an incremental length of water in the suit would be

$$dQ_2 = Cp\rho\ V\ dT$$

Equating the heat flows,

$$K_m (T - T_{wp})\ B\ dx/D_0 = -Cp\rho\ V\ dT \quad \frac{K_m B}{D_2 Cp\rho V} dx = \frac{dT}{T-T_{wp}}$$

Integrating across the water flow length, L,

$$\int_0^L \frac{K_m B}{D_2 Cp\rho V} dx = -\int_{T_{in}}^{T_{out}} \frac{dT}{T-T_{wp}}$$

Since

$\rho V = w$, i.e., density multiplied by volume flow equals mass flow,

$$\frac{K_m}{D_2 \, Cp \, w} + -\ln \frac{T_{out} - T_{wp}}{T_{in} - T_{wp}}$$

Using (area) A = BL (breadth - length) and rearranging in exponential form, results in the equation of outlet water temperature:

$$T_{out} = T_{wp} + (T_{in} - T_{wp}) \, e^{-\frac{K_m A}{D_2 \, Cp \, w}}$$

Evaluating T_{out}:

$$T_{out} = 35 + (110 - 35) \, e^{-\frac{.1 \, (23.0)}{.00833 \, (1.0) \, 1044}}$$

$$= 92.5°F$$

The temperature distribution is a function of water flow path length and surface area, resulting in a mean water temperature in the suit of

$$T_w = \frac{1}{A} \int_0^A T dA$$

For the case of even distribution, T_w can be approximated by $T_w = (T_{in} + T_{out})/2$. For the example just described $T_w = 101°F$.

The mean skin temperature for the diver wearing the hypothetical suit is about 100°F and the suit is adding heat to the diver's body. This was not the case during this study since the skin temperatures were always below core temperature, and the thermal gradient indicates heat flow from the body. This is corroborated by the correlation between values of h_s derived from the heat balance and those reported in the literature. The suits therefore did not heat the body, but by maintaining a warm skin temperature did decrease the magnitude of heat flow from the body core.

Respiratory Effects

It must not be thought that the subjects were able, uniformly, to swim and endure their exposures in 35°F water at 850 feet to completion. In three such instances the diver elected to discontinue the run, and thus we present 137 sets of data rather than 140. Often it was necessary for the divers to interrupt the swimming tasks because the accumulating fluids within the breathing valve and their mouths inhibited respiration gas flow. Of course, in the simulation scenario of a wet pot, in contradistinction to a real operation in the water, the diver is never more than a few feet away from a refuge. And the applied stresses of these experiments repeatedly forced them to utilize it, even in the runs which they swam to completion.

Diver reports (also refer to Table V) filed subsequent to the aborted runs are of particular interest in this context. Following are brief exerpts:

(1) "By the end of work no. 2 it was constant moderate to severe shaking. During the rest period it remained same. Right after start of work number 1 I started constant severe shaking with difficulty in holding work load. When I quit I was unable to even come close to holding work load and was experiencing difficulty in taking breaths."

(2) "At the time I aborted today's dive I was in bad shape. Due to neck and jaw hurting I was having a very hard time holding the mouthpiece. Experiencing severe shakes with ice cold back and chest."

(3) "Torso shivering on work number 3 and rest period, stopped as I started work rate 2. Began shivering while cleaning thermistor, waited for a couple of minutes while shivering, decided the situation was unhealthy at least and possibly dangerous, and bailed out. I really thought I was in jeopardy."

Miscellaneous Discussion

The chamber atmosphere oxygen partial pressure was increased to 0.5 atm. abs. just prior to the excursion dive to 1,000 feet. The length of the swimming-work periods and

interspersed rests was reduced to 15 and 5 minutes, respectively, so that all three subject immersion exposures could be completed within the allotted four hour span of the excursion. Subsequent decompression to 850 feet was gradual, over a period of 10 hours, and was uneventful. There were, likewise, no incidents of decompression sickness during the final ascent from 850 feet to the surface.

SECTION 5

CONCLUSIONS

Computed magnitudes of respiratory heat loss, observations of progressively decreasing core (rectal) temperatures, and subjective responses (diver reports and observations of their behavior) have been used in formulating the following conclusions which relate to operational diving:

(1) Dives to 850 feet for exposure durations in excess of 90 minutes in water of 45°F (or colder), i.e., with 215 kilogram-calories/hour (250 watts) respiratory heat loss are, in this context, hazardous without supplemental heating of the inhaled gas;
(2) Dives to 650 feet, or deeper, for exposure durations in excess of 90 minutes in water of 35°F, i.e., with 150 kilogram-calories/hour (about 175 watts) respiratory heat loss are, in this context, liable to be discomforting to the point of distraction and task performance degradation.

SECTION 6

REFERENCES

1. Albano, G. Principles and Observations on the Physiology of the Scuba Diver. ONR Report DR-150, 1970.

2. Armstrong, J., A. Burton and G. Hall. The physiological effects of breathing cold atmospheric air. J. Aviat. Med. 29: 593-597, 1958

3. Bondi, K. R. and J. F. Tauber. Physiological evaluation of a free-flooding diver heat replacement garment. Project MF 12.524.014-1004, Report No. 17, Naval Medical Research Institute, 1969

4. Brebbia, O., R. Goldman and E. Buskirk. Water vapor loss from the respiratory tract during outdoor exercise in the cold. J. Appl. Physiol. 11: 219-222, 1957

5. Burch, G. Study of water and heat loss from the respiratory tract of man. Arch. Int. Med. 76: 308-314, 1945

6. Burch, G. Rate of water and heat loss from the respiratory tract of normal subjects in a subtropical climate. Arch. Int. Med. 76: 315-328, 1945

7. Burton, A. C. Human calorimetry. II. The average temperature of the tissues of the body. J. Nutrition, 9: 261, 1935

8. Carlson, L. D. Man in cold environment. A study in physiology. Arctic Aeromedical Laboratory, 1954

9. Carlson, L. D., A.C.L. Hsieh, F. Fullington, and R. W. Elsner. Immersion in cold water and body tissue insulation. J. Aviation Medicine 29: 145-152, 1958

10. Cole, P. Some aspects of temperature, moisture and heat relationships in the upper respiratory tract. J. Laryng. 67: 449-456, 1953

11. Cole, P. Recordings of respiratory air temperature. J. Laryng Otol. 68: 295-307, 1954

12. Corlette, C. E. On the calculation of the heat and moisture dissipated from the body by respiration, with a table designed to make the calculation easy at any temperature, any humidity, and any pressure of air. Med. J. Australia 2: 198-203, 1942

13. Cramer, I. Heat and moisture exchange of respiratory mucus membrane. Ann. Oto. Rhinol. & Laryng. 66: 327-343, 1957

14. Day, R. Regional Heat Loss, in, Newburgh, L. H. (editor).Physiology of Heat Regulation and the Science of Clothing. Philadelphia: W. B. Saunders Co., 1949

15. DuBois, E. F. and D. DuBois. Formula to estimate the approximate surface area if height and weight are known. Arch. Int. Med. 17: 863, 1916

16. Hardy, J. D. and E. F. Dubois. Basal metabolism, radiation, convection, and evaporation at temperatures of 22-35°C. J. Nutrition 15: 477, 1938

17. Hart, J. S. Calorimetric determination of average body temperature of small laboratory animals and its variation with environmental conditions. Can. J. Biology 29: 224, 1951

18. Ingelstedt, S. and N. G. Toremalm. Air flow patterns and heat transfer within the respiratory tract. A new method for experimental studies on models. Acta. Physiol. Scand. 51: 1-14, 1961

19. Jackson, D. C. and K. Schmidt - Nielson. Countercurrent heat exchange in the respiratory passages. Proc. Nat. Acad. Sci. 51: 1192-1197, 1964

20. McCutchan, J. W. and C. L. Taylor. Respiratory heat exchange with a varying temperature and humidity of inspired air. AF Tech rept. 6023, ATI 92232, 1950

21. McCutchan, J. W. and C. L. Taylor. Respiratory heat exchange with varying temperature and humidty of inspired air. J. Appl. Physiol. 4: 121-135, 1951

22. Moritz, A. and J. Weisiger. Effects of cold air on the air passages and lungs, an experimental investigation. Arch. Int. Med. 75; 233-240, 1945

23. Nevins, R. G., F. W. Holm, and G. H. Advani. Heat loss analysis for deep-diving oceanauts. Am. Soc. Mech Engrs. Paper 65-WA/HT-25, 1965

24. Pugh, L. G. C. and O. G. Edholm. Physiology of channel swimmers. Lancet 2: 761-768, 1955

25. Rawlins, J. F. P. and R. Tauber. Thermal balance at depth, in C. Lambertsen (editor). Proceedings of the 4th Symposium on Underwater Physiology. New York: Academic Press, 1971

26. Seeley, L. E. Study of changes in the temperature and water vapor content of respired air in the nasal cavity. Heating, Piping and Air Conditioning 12: 377-388, 1940

27. Smith, L. B., F. G. Keyes and H. T. Gerry. Proc. Am. Acad. Arts and Sci. 69: 137, 1934

28. Spealman, C., N. Pace and W. A. White, Jr. Heat exchange by way of the respiratory tract. I. Theoretical considerations. II. Relative efficacy for conserving heat loss of the (1) Salathiel Breath Heat Exchanger, (2) A-14 rubber mask, (3) wool scarf. U.S. Naval Medical Research Institute Research project X-163, 1944

29. Teichner, W. H., Assessment of mean body surface temperature J. Appl. Physiol. 12: 169-176, 1958

30. Van Wylen, G. J., Thermodynamics, p. 551, New York: John Wiley & Sons Inc., 1961

31. Walker, J., R. Wells, Jr. and E. Merrill. Heat and water exchange in the respiratory tract. Amer. J. Med. 26: 259-267, 1961

32. Webb, P. Air temperatures in respiratory tracts of resting subjects in cold. J. Appl. Physiol. 4: 378-382, 1951

33. Webb, P. The measurement of respiratory air temperature. Rev. Sci. Inst. 23: 232-234, 1952

34. Webb, P. Heat loss from the respiratory tract in cold. Arctic Aeromedical Laboratory project 7-7951, report No. 3, 1955

35. Webb, P. Body heat loss in undersea gaseous environments. Aerospace Med. 41: 1282-1288, 1970

36. Webb, P. (ed.) Bioastronautics Data Book. Washington, D. C.: U. S. Government Printing Office, 1964

37. Webb, P. and J. Annis, Respiratory heat loss with high density gas mixtures. Final rept. Contract Nonr 4965(00), ONR, 1966

38. Winslow, C.E.A., L. P. Harington, and A. P. Gagge. Relationship between atmospheric conditions, physiological reactions and sensations of pleasantness. Am. J. Hyg. 26: 103-115, 1937

39. Yaglou, C. P. A method for improving the effective temperature index. Trans. ASHVE 53: 307, 1947

BLANK PAGE

SECTION 7
ADDITIONAL BIBLIOGRAPHY

Andrews, A.H., Jr., J.C. Ross and S.B. Osenar. Significance of water in exhaled air. Ann. Oto. Rhin. Laryn. 78: 499-511, 1969.

Atkins, A. and C. Wyndam. A study of temperature regulation in the human body with the aid of an analog computer. Pflügers Archiv. European J. Physiol. 307: 104-119, 1969.

Bazett, H., L. Love, M. Newton, L. Eisenberg, R. Day and R. Forster. Temperature changes in blood flowing in arteries and veins in man. J. Appl. Physiol. 1: 3-19, 1948.

Beckman, E. Thermal protection during immersion in cold water. NMRI report MR 005.13-4001.06, No. 1, 1964.

Beckman, E. Thermal protective suits for underwater swimmers. AIAA paper 66-716, 1966.

Beckman, E. Thermal protective suits for underwater swimmers. Mil. Med. 132:195-209, 1967.

Beckman, E. and E. Reeves. Physiological implications as to survival during immersion in water at 75°F. Aerospace Med. 37: 1136-1142, 1966.

Behnke, A.R. and C.P. Yaglou. Physiological responses of men to chilling in ice water and to slow and fast rewarming. J. Appl. Physiol. 3: 591-602, 1951.

Benzinger, T. Clinical temperature. J.A.M.A. 209: 1200-1206, 1969.

Bowen, H. M. Diver performance and the effects of cold. BSD Technical Rept. No. 67-441, 1967.

Bowen, H. M. and J. W. Miller. Man as an undersea inhabitant and worker. Ergonomics 10: 611-615, 1967.

Bowers, R.W. and E.L. Fox. Metabolic and thermal responses of man in various helium-oxygen and air environments. J. Appl. Physiol. 23: 561-565, 1967.

Brebbia, O., R. Goldman and E. Buskirk. Water vapor loss from the respiratory tract during outdoor exercise in the cold. J. Appl. Physiol. 11: 219-222, 1957.

Bullard, R.W. and G.M. Rapp. Problems of body heat loss in water immersion. Aerospace Med. 41: 1269-1277, 1970.

Butler, H.S. Jr. and R.H. Payne, Jr. Thermal conductance of diver wet suit materials under hydrostatic pressure. Naval Ship Res. and Development Center R&D interim rept. 2903, 1969.

Caldwell, P., D. Gomez and H. Fritts, Jr. Respiratory heat exchange in normal subjects and in patients with pulmonary disease. J. Appl. Physiol. 26: 82-88, 1969.

Cannon, P. Cold immersion. J. Royal Nav. Med. Serv. 49: 88-92, 1963.

Carlson, L. D., A.C.L. Hsiek, F. Fullington and R.W. Elsner. Immersion in cold water and body tissue insulation. J. Aviat. Med. 29: 145-152, 1958.

Case, E. and J. Haldane. Human physiology under high pressure. 1. Effects of nitrogen, carbon dioxide and cold. J. Hygiene 41: 225-249, 1941.

Chambers, A. B. A psychrometric chart for physiological research. J. Appl. Physiol. 29: 406-412, 1970.

Christie, R. and A. Loomis. The pressure of aqueous vapor in the alveolar air. J. Physiol. 77: 35-48, 1933.

Costill, D., T. Cahill and D. Eddy. Metabolic responses to submaximal exercise in three water temperatures. J. Appl. Physiol. 22: 628-632, 1967.

Craig, A., Jr. and M. Dvorak. Thermal regulation of man exercising during water immersion. J. Appl. Physiol. 25: 28-35, 1968.

Cuthrell, C. and R. Buzhardt. Evaluation of one-piece wet suit. United States Coast Guard Office of Engineering, Field Testing and Development Center Rept. No. 481, 1968.

Dery, R., J. Pelletier, A. Jacques, M. Clavet and J. Houde. Humidity in anesthesia: I. A modified dew-point hygrometer. Can. Anaes. Soc. J. 14:104-111, 1967.

Dery, R., J. Pelletier, A. Jacques, M. Clavet and J. Houde. Humidity in anesthesia: III. Heat and moisture patterns in respiratory tract during anesthesia with a semi-closed system. Can. Anaes. Soc. J. 14: 287-298-, 1967.

Fischer, B.A. and X.J. Musacchia. Responses of hamsters to helium-oxygen at low and high temperatures: induction of hypothermia. Amer. J. Physiol. 215: 1130-1136, 1968.

Frey, H.R. Electrically-heated pressure-compensated wet suits for Sealab II. U.S. Rubber Co., Final report, contract No. N600(168)63855, 1966.

Fulton, H., W. Welham, J. Dwyer and R. Dobbins. Preliminary report on protection against cold water. U.S. Navy Experimental Diving Unit Report 5-52, 1952.

Gagge, A., J. Hardy and G. Rapp. Proposed standard system of symbols for thermal physiology. J. Appl. Physiol. 27: 439-446, 1969.

Gagge, A.P., A.C. Burton and H.C. Bazett. A practical system of units for the description of the heat exchange of man with his environment. Science 94: 428-430, 1941.

Gagge, A.P., J.A. Stolwijk and B. Saltin. Comfort and thermal sensations and associated physiological responses during exercise at various ambient temperatures. Environmental Res. 2:209-229, 1969.

Glickman, N., H. Mitchell, R. Keeton and E. Lambert. Shivering and heat production in men exposed to intense cold. J. Appl. Physiol. 22: 1-8, 1967.

Goff, L., H. Brubach, H. Specht and N. Smith. Effect of total immersion at various temperatures on oxygen uptake at rest and during exercise. J. Appl. Physiol. 9: 59-61, 1956.

Good, A. and A. Sellers. Temperature changes in the blood of the pulmonary artery and left atrium of dogs during exposure to extreme cold. Amer. J. Physiol. 188: 447-450, 1957.

Green, I. and M. Nesarajah. Water vapor pressure of end tidal air of normal and chronic bronchitics. J. Appl. Physiol. 24: 229-231, 1968.

Greenfield, A.D., G.A. Kernohan, R.J. Marshall, J.T. Shepherd and R.F. Whelan. Heat loss from toes and fore-feet during immersion in cold water. J. Appl. Physiol. 4: 37-45, 1951.

Guleria, J., J. Talwar, O. Malhotra and J. Pande. Effect of breathing cold air on pulmonary mechanics in normal man. J. Appl. Physiol. 27: 320-322, 1969.

Hair, G., N. Fischer and M. Preslar. Humidification of air by nasal mucosa. A method of study. Laryngoscope 79: 375-381, 1969.

Hanna, J. A comparison of laboratory and field studies of cold response. Amer. J. Phy. Anthro. 32: 227-232, 1970.

Hardy, J.D. Physiology of temperature regulation. Physiol. Rev. 41: 521-606, 1961.

Hardy, J. and J. Stolwijk. Partitional colorimetric studies of man during exposures to thermal transients. J. Appl. Physiol. 21: 1799-1806, 1966.

Hellstrom, B., K. Berg and F. Vogt Lorentzen. Human peripheral rewarming during exercise in the cold. J. Appl. Physiol. 29: 191-199, 1970.

Horvath, S.M. and H. Golden. Observations on men performing a standard amount of work in low ambient temperatures. J. Clin. Invest. 26: 311-319, 1947.

Josenhans, W.T., G.N. Melville and W.T. Ulmer. The effect of facial cold stimulation on airway conductance in healthy man. Canad. J. Physiol. & Pharm. 47: 453-457, 1969.

Josenhans, W., G. Melville and W. Ulmer. Effects of humidity in inspired air on airway resistance and functional residual capacity in patients with respiratory diseases. Resp. 26: 435-443, 1969.

MacDonald, D.K. and C.H. Wyndham. Heat transfer in man. J. Appl. Physiol. 3: 342-364, 1950.

Mather, G., G. Nahas and A. Hemingway. Temperature changes of pulmonary blood during exposure to cold. Amer. J. Physiol. 173: 390-392, 1953.

Melville, G.N., W.T. Josenhans and W.T. Ulmer. Changes in specific airway resistance during prolonged breathing of moist air. Can J. Physiol. & Pharmacol. 48: 592-597, 1970.

Meryman, H. Tissue freezing and local cold injury. Physiol. Rev. 37: 233-251, 1957.

Miller, M.R. and A.J. Miller. Physiological effects of brief periods of exposure to low temperatures. J. Aviat. Med. 20: 179-185, 1949.

Mitchell, D. and C. Wyndham. Comparison of weighting formulas for calculating mean skin temperature. J. Appl. Physiol. 26: 616-622, 1969.

Molnar, G.W. Survival of hypothermia by men immersed in the ocean. J.A.M.A. 131: 1046-1050, 1946.

Morris, R. and B. Wilkey. The effects of ambient temperature on patient temperature during surgery not involving body cavities. Anesth. 32: 102-107, 1970.

Nielsen, B. Thermoregulation in rest and exercise. Acta Physiol. Scand. Suppl. 323: 1-74, 1969.

O'Hanlon, Jr., J. and S. Horvath. Changing physiological relationships in man under acute cold stress. Can. J. Physiol. & Pharmacol. 48: 1-10, 1970.

Pittman, J., W. Kaufman and C. Harris. Physiologic evaluation of sea survival equipment. Aerospace Med. 40: 378-381, 1969.

Provens, K. and R. Clarke. The effect of cold on manual performance. J. Occupat. Med. 2: 169-175, 1960.

Pugh, L., O. Edholm, R. Fox, H. Wolff, G. Hervey, W. Hammond, J. Janners and R. Whitehouse. A physiological study of channel swimming. Clin. Sci. 19: 257-273, 1960.

Raven, P.B., I. Niki, T.E. Dahms and S.M. Horvath. Compensatory cardiovascular responses during an environmental cold stress, 5°C. J. Appl. Physiol. 29: 417-421, 1970.

Raymond, L.W. Physiologic mechanisms of maintaining thermal balance in high-pressure environments. J. Hydronautics 1: 102-107, 1967.

Raymond, L.W., W.H. Bell, K.R. Bondi and C.R. Lindberg. Body temperature and metabolism in hyperbaric helium atmospheres. J. Appl. Physiol. 24: 678-684, 1968.

Reeves, E., M.P. Stephens and E.L. Beckman. An evaluation of the foamed neoprene diver's wet suit as a survival garment for helicopter air pilots. Aerospace Med. 38: 599-606, 1967.

Robinson, S., E. Turrell and S. Gerking. Physiologically equivalent conditions of air temperature and humidity. Amer. J. Physiol. 143: 21-32, 1945.

Rochelle, R. and S. Horvath. Metabolic responses to food and acute cold stress. J. Appl. Physiol. 27: 710-714, 1969.

Ross, E.M. Bioenergetics of space suits for lunar exploration. NASA SP-84, 1966.

Rowell, L.B., J.A. Murray, G.L. Brengelmann and K.K. Kranning. Human cardiovascular adjustments to rapid changes in skin temperature during exercise. Circulation Res. 24: 711-714, 1969.

Roy, P., W. Josenhans and C. Miller. Variations in air viscosity due to changes in water vapor pressure for isothermal conditions at temperatures below 40°C. Canad. J. Physiol. & Pharmacol. 48: 50-53, 1970.

Selawry, O.S., H.S. Selawry and J.S. Holland. The use of liquid cholesteric crystals for thermographic measurement of skin temperature in man. Molecular Crystals, Volume 1: 495-501. Gordon and Breach Science Publishers, 1966.

Shumway, G. and J. Beagles. Arctic SCUBA diving, 1958. U.S.N. Electronics Laboratory R&D report 916, 1959.

Skreslet, S. and F. Aarefjord. Acclimatization to cold in man induced by frequent SCUBA diving in cold water. J. Appl. Physiol. 24: 177-181, 1968.

Takagi, Y., D. Proctor, S. Salman and S. Evering. Effects of cold air and carbon dioxide on nasal air flow resistance. Ann. Oto. Rhinol. & Laryng. 78: 40-48, 1969.

Vandam, L.D. and T.K. Burnap. Hypothermia. New Eng. J. of Med. 261: 546-553; 595-602, 1959.

Volkert, W.A. and X.J. Musacchia. Blood gases in hamsters during hypothermia by exposure to He-O_2 mixture and cold. Amer. J. Physiol. 219: 919, 1970.

Wells, Jr., R., J. Walker and R. Hickler. Effects of cold air on respiratory airflow resistance in patients with respiratory tract disease. N. Eng. J. Med. 263: 268-273, 1960.

Whipp, B. and K. Wasserman. Effect of body temperature on the ventilatory response to exercise. Resp. Physiol. 8: 354-360, 1970.

Whitby, J.D. and L.J. Dunkin. Temperature differences in the esophagus. Brit. J. Anaesth. 41: 615-618, 1969.

Whyte, H.M. Measurement of heat loss from the skin. J. Appl. Physiol. 7: 263-269, 1951.

Wyndham, C. and A. Atkens. A physiological scheme and mathematical model of temperature regulation in man. Pflügers Archiv. European J. Physiol. 303: 14-30, 1968.

APPENDIX 1

COMPUTER SYSTEM

This section describes the computer system used to calculate respiratory heat loss, mean weighted skin temperature, oxygen uptake, exhalation resistance, and several other parameters. A system with a punched IBM card input capability was chosen to facilitate the loading of data from several sets of manually constructed tables each having 137 entries, and from 35 machine printed paper tapes with 70 entries.

Although OR&EC does not have an in-house computer, access to several large computers via telephone link is available through two communications terminals as shown in Figure 1 to this appendix.

Some of the chief characteristics of the components of these terminals are listed below:

EQUIPMENT	MFR.	CHARACTERISTICS
Card Reader	UNIVAC Mod No. 711-00	80 cols 400 cards/min
Card Punch	UNIVAC Mod No. 603-04	80 cols 75-200 cards/min
Line Printer	UNIVAC Mod No. 3030/ F0868-01	120 Print Positions 100-250 line/min
Computer	UNIVAC 1108	36 bit words 0.750 msec memory access
Digital Plotter	ZETA 230	10 mil Resolution
Teletype	ASR-33	72 Print Positions 8-100 line/min

The high speed terminal possesses a large volume of input/output capability. Data and computer programs to perform mathematical analysis on the data are entered via punched IBM cards, interpreted by the card reader and sent via the telephone link to the computer. The results of the computation are returned via the link to the high speed printer.

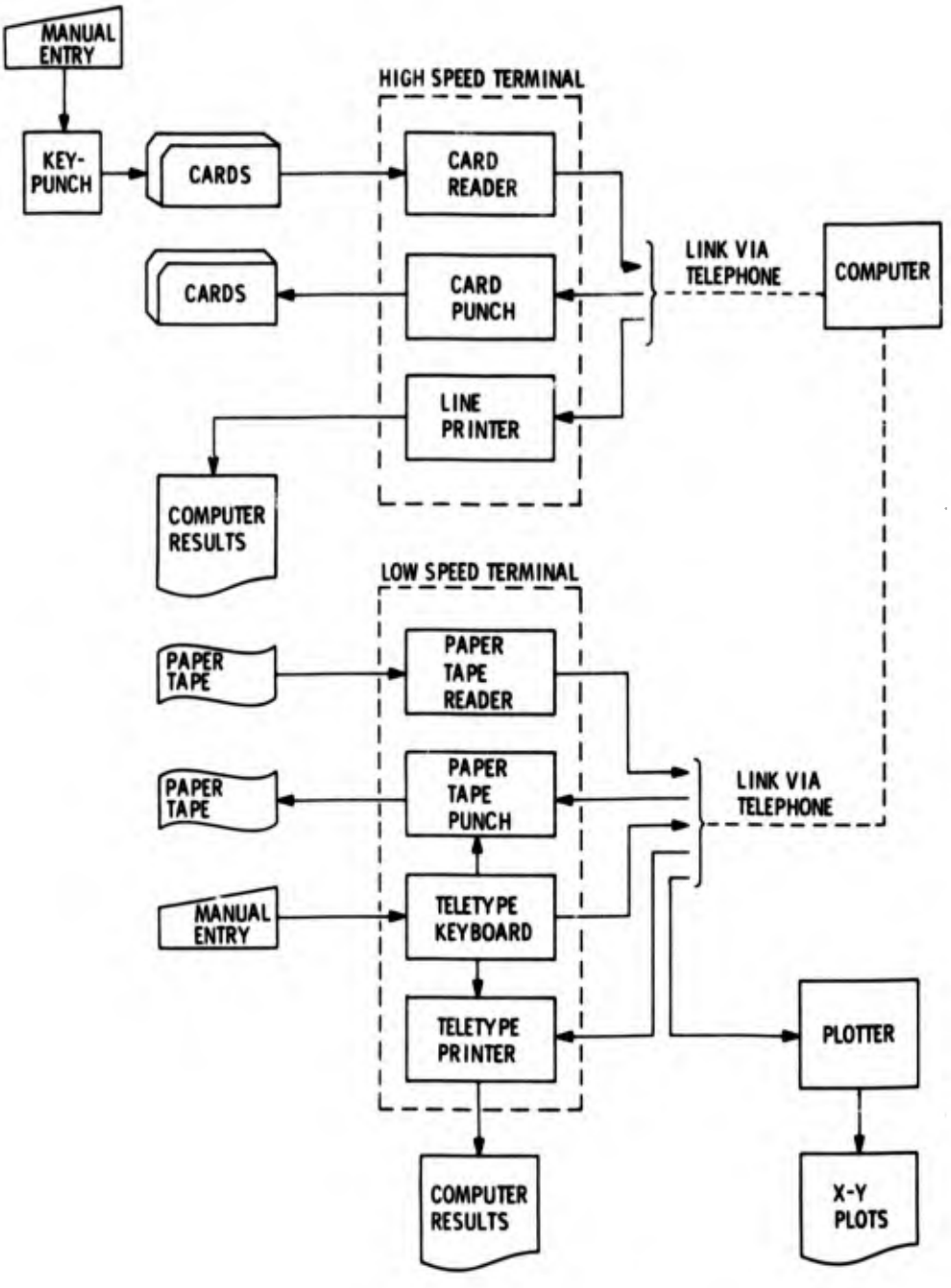

Figure 1. Computer System.

The low speed terminal presents an alternate access to the computer. Here the data and programs are entered directly to the computer through the teletype keyboard or by way of the paper tape reader. The punched paper tape is analogous to the punched cards and can be prepared via the teletype keyboard. Computational results are returned to the teletype printer or to the X-Y plotter or both.

There are advantages and disadvantages associated with both types of terminals. The high speed terminal possesses fast printout capability, rapid data via cards, but access to the computer is far more limited due to loading schedules.

The low speed terminal though slower in its input/output capability has almost unlimited immediate access to the computer because of its keyboard entry, particularly important during the checkout phase of computer programs. An additional bonus is its plotting capability.

Approximately fifteen computer programs were written to read data into the computer, combine data into useful files, scale the data, make calculations and print out and plot results. Of these programs only the program for calculation of respiratory heat loss (RHX1) is included and explained.

Program RHX 1

100	Calls files to be used
110	Sets up QRHX (file No. 4) for entry
120-140	Sets limits for entry from files 1-3
150	States heading for printed output
160-330	Reads files 1-3 and adds decimal points
340	R8 = gas constant for nitrogen
350	M8 = molecular weight of nitrogen
360	M4 = molecular weight of oxygen
370	M5 = molecular weight of carbon dioxide
380	M6 = molecular weight of helium
390	R4 = gas constant for oxygen
400	R5 = gas constant for carbon dioxide
410	R6 = gas constant for helium
420	M7 = molecular weight of water vapor
430	K3 = specific heat of helium

440 K4 = specific heat of nitrogen

450 Begins for/next loop.

460 V0 = gasometer volume flow, ALPM

470 P0 = correction for barometric pressure

480 T2 = gasometer mean temperature, °C

490 P5 = diver depth, ft.

500 T3 = inhalation temperature, °C

510 T5 = maximum exhalation temperature, °C

520 T1 = average exhalation temperature, °C

530 $\phi 1$ = volume % mixed exhaled CO_2 - Scholander analysis

540 $\phi 3$ = volume % mixed exhaled O_2 - Scholander analysis

550 $\phi 5$ = volume % mixed exhaled CO_2 - Beckman IR 315

560 $\phi 6$ = volume % mixed exhaled O_2 - Beckman E-2

570-590 Convert temperatures from Celsius to Rankine

600 $\phi 4$ = volume fraction nitrogen

610 converts depth (feet) to pressure (psia)

620 $\phi 2$ = volume fraction helium, found by subtraction

630 V1 = exhaled minute volume - corrected for temperature difference between mouthpiece thermister and gasometer temperature, also converted to ft^3/min

640-670 Z1-Z7 multiply the volume fractions, molecular weights and gas constants for O_2, CO_2, He, and N_2

680-710 Z4-Z8 divide the Z1-Z7 values by the respective gas constants

720 M2 = molecular weight of exhaled gas

730 R9 = gas constant of exhaled gas

740-900 This sub-program calculates the partial pressure of water vapor for the inhaled and exhaled temperatures. The computer cannot solve the equation directly therefore an iterative procedure is used. Starting with a low value of vapor pressure the equation is arranged to result in a negative number. The trial vapor pressure is then increased in steps of .0001 until the result of the equation is a

positive number. Values of vapor pressure calculated in this manner are accurate to the fourth decimal place. Line 880 converts the answer from international atmospheres to psia.

910-930 P1 = saturation vapor pressure for corresponding temperatures

940 sets T equal to the expiration temperature for the following equations

950 K1 = specific heat of oxygen

960 K2 = specific heat of carbon dioxide

970 R = density of the exhaled gas

980-1010 Y1 to Y4 multiply the volume fractions, molecular weights and specific heats for O_2, CO_2, He, and N_2.

1020 C1 = specific heat of the exhaled gas

1030 C2 = specific heat of water vapor

1040 A1 = sensible dry gas heat loss

1050 X1 = mass of inhaled gas

1060 A2 = sensible water vapor heat loss

1070 A3 = insensible water vapor heat loss

1080 Q = total respiratory heat loss, Btu/hr.

1090 W = total respiratory heat loss, Watts

1100 D = inhalation-exhalation temperature difference

1110 V5 = respiratory minute volume, converts V1 (ft^3/hr) to ALPM (BTPS)

1112 Q2 = total respiratory heat loss, Kcal/hr.

1120 Outputs Q, W, D, V5 into file No. 4 QRHX

1130 Tells computer to print out J, Q, W, D, V5

1140 Tells computer to make next calculation

```
100 FILES LPMFTG,TINTEX,XC0202,ORHXB
110 SCRATCH#4
114 V7=V0*310.16/(N(J)+270.16)
120 DIM F(150),H(150),I(150),K(150)
130 DIM L(150),M(150),N(150)
140 DIM O(150),P(150),U(150),V(150)
150 PRINT USING 151
151:    J        W        Q       Q2       V7       R        C1       R*C1
160 FOR J=1TO 140
170 INPUT #1,F(J),H(J),I(J),K(J)
180 F(J)=F(J)/1000
190 H(J)=H(J)/10000
200 I(J)=I(J)/100
210 IF END #1 GO TO 220
220 INPUT #2,L(J),M(J),N(J)
230 L(J)=L(J)/10
240 M(J)=M(J)/10
250 N(J)=N(J)/10
260 IF END #2 GO TO 270
270 INPUT #3,O(J),P(J),U(J),V(J)
280 IF END #3 GO TO 290
290 O(J)=O(J)/10000
300 P(J)=P(J)/10000
310 U(J)=U(J)/10000
320 V(J)=V(J)/10000
330 NEXT J
340 R8=55.15
350 M8=28.016
360 M4=32
370 M5=44.01
380 M6=4.003
390 R4=48.28
400 R5=35.1
410 R6=386
420 M7=18.016
430 K3=1.24
440 K4=.247
450 FOR J=1 TO 140
460 V0 =F(J)
470 P0=H(J)
480 T2=I(J)
490 P5=K(J)
500 T3=L(J)
510 T5=M(J)
520 T1=N(J)
530 O1=O(J)
540 O3=P(J)
550 O5=U(J)
```


RHXI Computer Program For Calculation Of Respiratory Heat Loss

```
560 D6=V(J)
570 T1=T1*1.8+491.67
580 T2=T2*1.8+491.67
590 T3=T3*1.8+491.67
600 D4=35/(P5+33)
610 P5=(P5+(33*P0))*14.696/33
620 D2=1-D6-D4-(D5/(P5/14.696))
630 V1=V0*T1*60/(28.32*T2)
640 Z1=D6*M4*R4
650 Z2=D5*M5*R5
660 Z3=D2*M6*R6
670 Z7=D4*M8*R8
680 Z4=Z1/R4
690 Z5=Z2/R5
700 Z6=Z3/R6
710 Z8=Z7/R8
720 M2=(Z4+Z5+Z6+Z8)
730 R9=(Z1+Z2+Z3+Z7)/M2
740 S(1)=T1
750 S(2)=T2
760 S(3)=T3
770 FOR Z=1 TO 3
780 T=S(Z)
790 T=(T-491.67)*5/9+273.16
800 X=(647.27-T)
810 FOR G=.006 TO .068 STEP .0001
820 A=(LOG(G)-LOG(218.167))/2.3025851
830 B=X*(3.2437814+.00586826*X+1.1702379E-8*(X↑3))
840 C=(1+X*2.1878462E-3)
850 E=A+(B/C)/T
860 IF E>0 THEN 880
870 NEXT G
880 G=G*14.696
890 P(Z)=G
900 NEXT Z
910 P1=P(1)
920 P2=P(2)
930 P3=P(3)
940 T=T1
950 K1=(11.515-172/SQR(T)+1530/T)/32
960 K2=(16.2-6530/T+1410000/(T↑2))/44.01
970 R=(P5-P2)*144/(R9*T1)
980 Y1=Z4*K1
990 Y2=Z5*K2
1000 Y3=Z6*K3
1010 Y4=Z8*K4
1020 C1=(Y1+Y2+Y3+Y4)/M2
1030 C2=(19.86-597/SQR(T)+7500/T)/18.016
1040 A1=V1*R*C1*(T1-T3)
1050 X1=V1*R*M7*P3/(M2*(P5-P3))
```

RHXI Computer Program For Calculation Of Respiratory Heat Loss (Continued)

```
1060 A2=X1*C2*(T1-T3)
1070 A3=(1045*V1*R*M7*(P1-P3))/(M2*(P5-P1))
1080 Q=A1+A2+A3
1090 W=Q*.292833
1100 D=(T1-T3)
1110 V5=V0*T1/T2
1112 Q2=Q*.253
1114 V7=V0*310.16/(N(J)+270.16)
1120 OUTPUT #4 USING 1132,A3,W,Q,Q2,V7,R,C1,R*C1
1130 PRINT USING 1132,J,W,Q,Q2,V7,R,C1,R*C1
1132:###.#  ###.#   ####.#  ###.#  ##.##  #.###  #.###  #.###
1140 NEXT J
1150 END
READY
```


RHXI Computer Program For Calculation Of Respiratory Heat Loss (Continued)

APPENDIX 2

CONSIDERATIONS FOR DESIGN OF AN INHALATION/EXHALATION THERMOMETER FOR DIVERS

Requirements for measuring minimum and maximum inhaled and exhaled gas temperatures of a diver were given as follows: accuracy of 0.5°F in 0.5 seconds for a range of 32-100°F; measurements to be made with air at approximately one atmosphere absolute, and 96% helium at approximately twenty-six atmospheres absolute; anticipated size of each step was 50-60°F; the diver to be in cold water, inhaling cold gas and exhaling it at an elevated temperature through a mouthpiece.

Measurement of temperature to the above accuracy is not of itself a problem; however, introduction of the time requirement for the desired accuracy introduces problems of transducer selection (most transducers, thermistors, resistance thermometers, thermocouples, etc., have time constants larger than desired) and considerations of reduced excitation level to avoid self heating of transducers. The transducer then must be mounted in and thermally isolated from the mouthpiece, which is in approximate thermal equilibrium with the surrounding water. Additionally, the gas being measured is very moist and the walls of the gas conductor are wet with saliva and mucous. At times, airborne saliva or mucus may impinge on the transducer or its mounting.

Transducer selection was rapidly narrowed to thermistors due to the requirements for speed, relatively large signal, and independence from special leads or lead resistance problems.

The time constant required was determined to be 0.094 seconds for 0.5% in 0.5 seconds; however, this did not leave any tolerance for other uncontrollable errors. A time constant of 0.075 seconds would leave an error of 0.125% at the end of 0.5 seconds, and a thermistor (VECO "Thinistor", free standing) was available with this time constant for still air. An analysis by Dr. W.A. Stewart of Westinghouse Research Laboratories indicated an improvement by a factor of ten in helium at 26 atmospheres absolute and a flow velocity of 100 ft/min. A derivation from that analysis indicates a factor of two improvement for air at 1 atmosphere absolute and 100 ft/min. Information in the Conax Corporation's catalog

no. 3000 supports the factor of two improvement. (In actual application, the "Thinistors" thus selected were not obtainable. A thermistor with a time constant in still air of 0.12 seconds (0.06 seconds in air at 1 atmosphere absolute and 100 ft/min and 0.01 seconds at depth) was obtained and was utilized in the design.)

The consideration of moisture, saliva and mucous on and about the thermistor was given some quantitative limitations when laboratory tests with pieces of fine wire immersed in a mixture of saliva and water displayed resistance of 6-10 megohms between wires configured to simulate the thermistor mounting. This resistance, which is high, is a function of the impressed voltage (30-50 millivolts) on the thermistor. A decision was made not to attempt to insulate the fine wire suspending and connecting the thermistor because: (1) the wires were too fine (0.75 mil diameter) to apply a conformal coating; (2) any insulation would have a heat capacity and a thermal conductivity which could affect the temperature of the thermistor bead; (3) the effect of short circuits of saliva would amount to errors of a small and predictable nature. The effect of a 9 megohm shunt on a thermistor with resistance of 1000 ohms at 25°C and a beta[1] of 2800°K is an error of 0.007°C at 0°C and 0.003°C at 40°C. A thermistor with a lower resistance at 25°C would be less affected; however, one thousand ohms was the lowest value available for the thermistor type with the necessary short time constant. (See Attachment 1)

Thermal isolation of the thermistor was accomplished by mounting the unit by its lead wires (0.75 mil dia.) according to the manufacturer's recommendations in a transistor type header. The mounted thermistor was protected from physical damage by a guard made of a pair of crossed loops of No. 24 wire approximately sixteen diameters from the thermistor bead. (Figure 1)

Design considerations for the signal conditioning bridge included optimizing the linearity of the bridge, minimizing self-heating errors, accounting for lead resistance from the thermistor to the bridge, consideration of the thermistor's aging or drift characteristics, drift of the resistors used in the bridge and changes in battery voltage during the experiment.

---

[1] Beta is a material constant of the thermistor used to relate resistance to temperature.

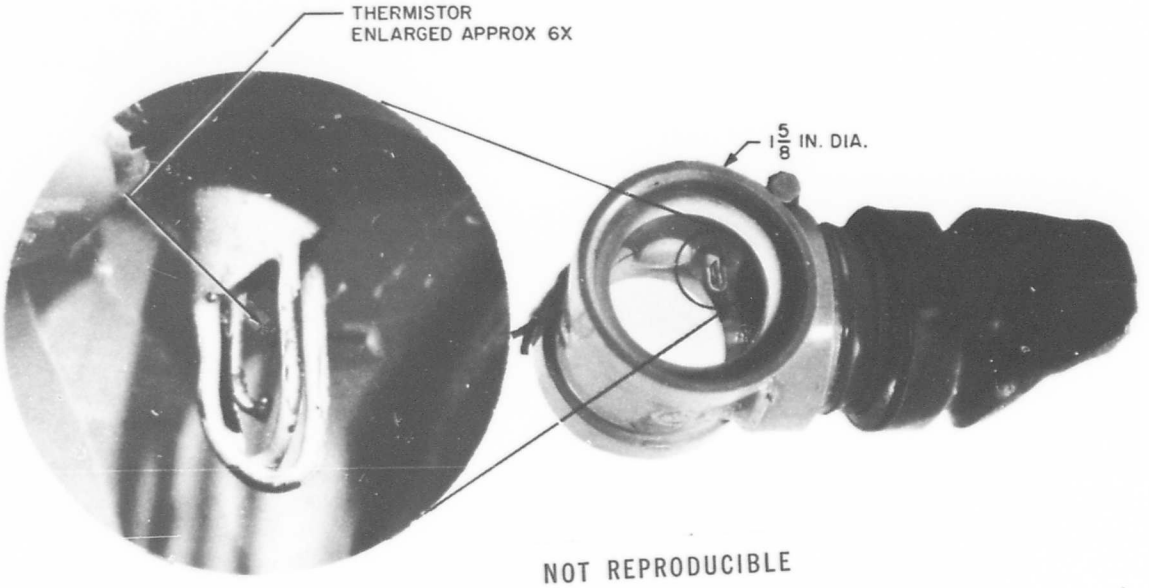

Figure 1. (To Appendix 2)

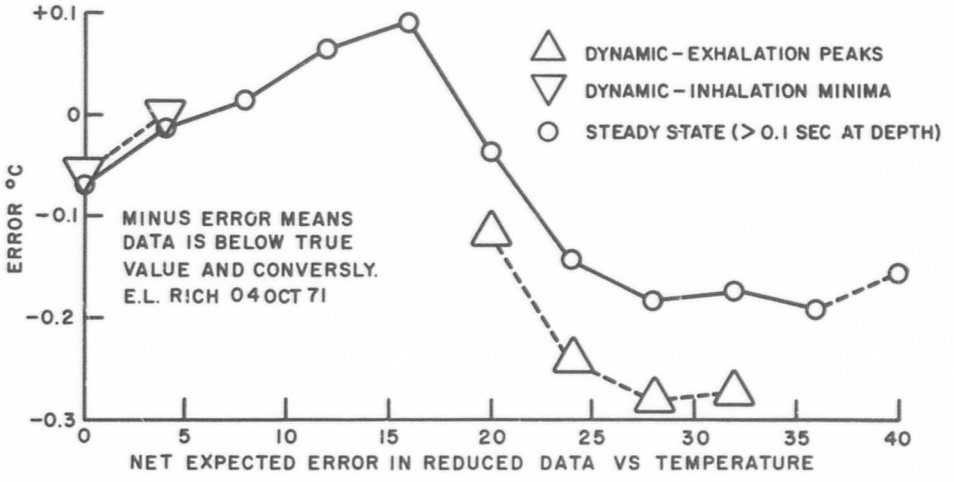

Figure 2. (To Appendix 2)

Optimization of linearity was accomplished using linearization criteria supplied by the manufacturer (Victory Engineering Corp.) and solved using computer data processing to enhance accuracy. Since the errors due to non-linearity could be predicted, corrections to final data could be made (Attachment 2).

Minimizing self-heating errors required knowing the dissipation constant of the thermistor (0.045 mw/°C for the bead used) and keeping the voltage across the thermistor (E_{RT}) sufficiently low. Attachment 3 describes the equations used and resultant errors.

Lead resistance from the bridge to the thermistor as mounted in the breathing apparatus in the chamber amounted to approximately four ohms in series with the thermistor, a factor which could be designed for. Components included resistance of the copper conductors into the chamber, the connectors inside the chamber and resistance of the copper leads inside the chamber. The temperature coefficient of copper is approximately 0.04%/°C, resulting in a net change of 12% or 0.48 ohms over the 30°C temperature range. The effect of this variance is less than 0.03°C in the worst case.

Thermistors which are used at temperatures below 150°C have shown aging characteristics of better than 0.2% per year (typically 0.1% or less for ambient temperatures less than 50°C) which characteristic is nearly constant and unidirectional. Extrapolation for the month period of the experiment yields an expected variation of 0.02% or 0.007°C (coeff of Res $\simeq$ 3.1%/°C), a negligible amount.

Resistors and potentiometers used in the bridge drifted between 0.2 and 0.3% over a month's period when not subjected to severe physical shock, thermal shock or moisture. The conditions of measurement of drift were similar to the conditions of the experiment except that some vibrations of the bridge box was deliberately done during drift measurements. A better choice of components for the bridge would have been exclusive use of stabilized metal film resistors padded to obtain desired values, eliminating the adjustment pots. The elements of the adjustment pots were very stable, however they were subject to mechanical dislocation of the wiper.

A stabilized mercury cell (Mallory RM 12-R) was used as a power source. Measurements under load at the beginning, and after the experiment indicated a variation in voltage of less than 0.1% (1.355-1.354). The life expectancy of the cell exceeded six months, continuously powering the bridge.

A predicted error curve was generated from combined calculated values for non-linearity and self-heating errors. This error curve was based on preliminary data, being produced rapidly to facilitate early correction of data. Later calculations of effects of saliva shunting, lead resistance and approximations of the time response error allowed production of a curve of expected net error in corrected reduced data. The net expected error in reduced data for both static and dynamic conditions at depth is shown in the following table. (If the error is minus the data is below true value and conversely) (See Fig. 2.):

°C	0	4	8	12	16	20	24	28	32	36	40
Static Error °C	-.068	-.013	+.014	+.062	+.084	-.037	-.144	-.184	-.175	-.193	-.157
Dynamic Error °C	-.058	-.003	X	X	X	-.117	-.244	-.284	-.275	X	X

The components making up the net error are believed to represent a realistic approximation of worst case. The dynamic net error figures are for maxima only at the higher temperatures and minima at the lower temperatures and are based upon oscillations between the two ranges of temperature. (See Attachment 4)

Attachment 1 (to Appendix 2)

EFFECT OF SALIVA SHUNTING THERMISTOR THB1

see Fig. Book 142704, p. 23 for SHUNT DATA
see Fig. Book 142704, p. 14 for R_T VALUES

$$\epsilon\ (°C) \simeq \frac{R_T\ (100)}{\text{SHUNT RES}} \left(\frac{°C}{\%\ \Delta R_T} \right)$$

SHUNT RES = 9.1 MEGOHMS

T (°C)	R_T	ΔR_T (To Higher Temp.)	$\%\Delta R/°C$	ϵ (°C)
0	2425	89.79	3.7	+0.007
2	2249.36			
4	2088.71	75.17	3.6	+ .006
6	1941.59			
8	1806.71	63.22	3.5	+ .006
10	1682.91			
12	1569.16	53.41	3.4	+ .005
14	1464.52			
16	1368.16	45.30	3.3	+ .005
18	1279.34			
20	1197.39	38.60	3.22	+ .004
22	1121.68			
24	1051.69	33.01	3.14	+ .004
26	986.92			
28	926.92	28.34	3.06	+ .003
30	871.28			
32	819.66	24.42	2.98	+ .003
34	771.70			
36	727.12	21.12	2.90	+ .003
38	685.63	19.66		
40	647.00	18.3	2.83	+ .003

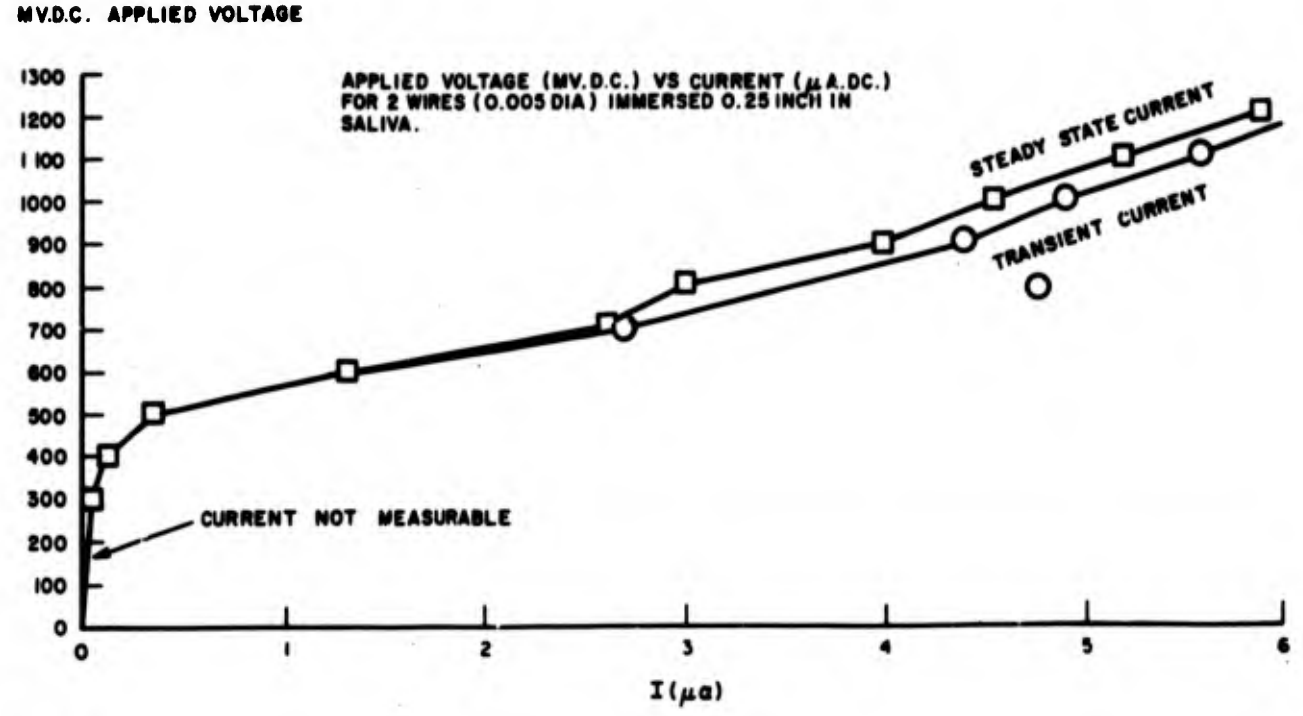
MV.D.C. APPLIED VOLTAGE
APPLIED VOLTAGE (MV.D.C.) VS CURRENT (μA.DC.) FOR 2 WIRES (0.005 DIA) IMMERSED 0.25 INCH IN SALIVA.
STEADY STATE CURRENT
TRANSIENT CURRENT
CURRENT NOT MEASURABLE
1300
1200
1100
1000
900
800
700
600
500
400
300
200
100
0
0
1
2
3
4
5
6
I(μa)

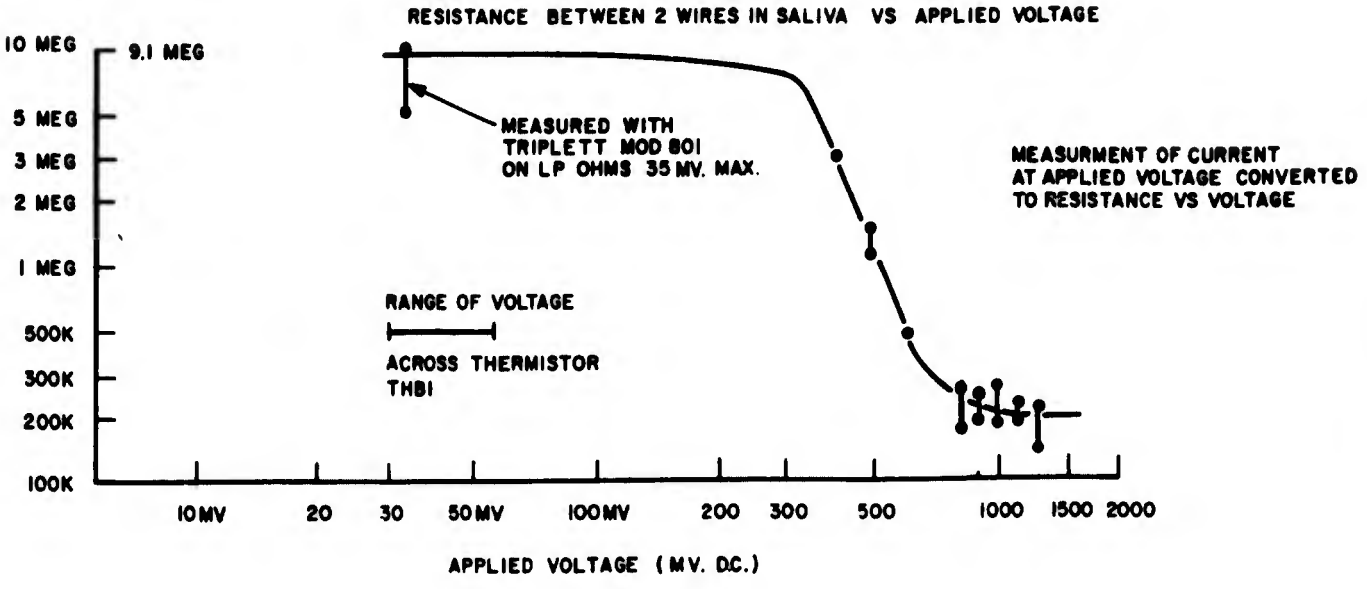
RESISTANCE BETWEEN 2 WIRES IN SALIVA VS APPLIED VOLTAGE
10 MEG
9.1 MEG
5 MEG
3 MEG
2 MEG
1 MEG
500K
300K
200K
100K
MEASURED WITH TRIPLETT MOD 801 ON LP OHMS 35 MV. MAX.
MEASURMENT OF CURRENT AT APPLIED VOLTAGE CONVERTED TO RESISTANCE VS VOLTAGE
RANGE OF VOLTAGE
ACROSS THERMISTOR THBI
10MV
20
30
50MV
100MV
200
300
500
1000
1500
2000
APPLIED VOLTAGE (MV. DC.)

Attachment 2 (to Appendix 2)

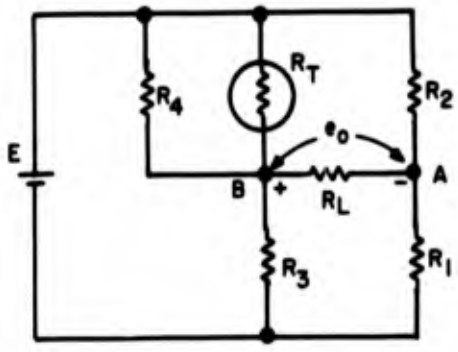

Thermistor is R_T
Output (e_o) measured at B with respect to A

Expression for Output

$$e_o = \frac{E \cdot R_L \left[(R_3 R_4 + R_3 R_T) / (R_3 R_4 + (R_3 + R_4) R_T)\right] - E \cdot R_L \left[R_1/(R_1 + R_2)\right]}{R_L + (R_{P3} R_T/(R_{P3} + R_T)) + (R_1 R_2/(R_1 + R_2))}$$

$$R_{P3} = \frac{R_3 R_4}{R_3 + R_4}$$

Expression for Optimum Linearity

$$R_S = \frac{R_1 R_2 (R_3 R_4/(R_3 + R_4)) + R_L (R_3 R_4/(R_3 + R_4)) (R_1 + R_2)}{(R_1 + R_2) ((R_3 R_4/R_3 + R_4) + R_L + R_1 R_2}$$

$$R_S = \frac{R_T \text{ at } 25°C}{S}$$, S being determined from the equal slope criterion below.

$$S = \frac{T_2 \left[r(T_1)\right]^{1/2} - T_1 \left[r(T_2)\right]^{1/2}}{T_1 r(T_1) \left[r(T_2)\right]^{1/2} - T_2 r(T_2) \left[r(T_1)\right]^{1/2}}$$

where

T_1 and T_2 are end points of the range in degrees Kelvin; r (T_1) and r (T_2) are the corresponding ratios of resistance at T_1 or T_2 to the resistance at 25°C.

CIRCUIT OF THE THERMISTOR THERMOMETER AND EXPRESSIONS FOR OUTPUT AND LINEARITY OPTIMIZATION

Attachment 3 (To Appendix 2)

SELF HEATING ERROR THB1 (VECO E31A401C)

E_{RT} = VDC across thermistor,

$$P = \frac{(E_{RT})^2}{R_T} ,$$

R_T from fig book 139410 pp. 39-41.

$$1 \underline{\text{ATA AIR}} \; \epsilon\,(°C) = \frac{PWR}{4.5 \cdot 10^{-5} \text{ watt/°C}}$$

$$26 \underline{\text{ATA HE}} \; \epsilon\,(°C) = \frac{PWR}{1.35 \cdot 10^{-4} \text{ watt/°C}}$$

T (°C)	E_{RT} (mv)	P x 10^{-6} watt	ϵ (°C) 1 ATA AIR	ϵ (°C) 26 ATA HE
0	57.2	1.35	0.03	0.01
2	56.2	1.40	0.0312	0.0104
4	55.1	1.44	0.032	0.0107
6	54.1	1.48	0.033	0.011
8	52.9	1.53	0.034	0.0113
10	51.7	1.57	0.035	0.0116
12	50.5	1.61	0.036	0.0119
14	49.3	1.65	0.037	0.0122
16	48.1	1.67	0.037	0.0124
18	46.9	1.71	0.038	0.0126
20	45.7	1.73	0.0385	0.0128
22	44.4	1.76	0.039	0.0130
24	43.1	1.78	0.040	0.0132
26	41.9	1.79	0.040	0.0132
28	40.1	1.81	0.040	0.0134
30	39.5	1.80	0.040	0.0133
32	38.4	1.81	0.040	0.0134
34	37.3	1.82	0.0405	0.0135
36	36.2	1.80	0.040	0.0133
38	35.0	1.79	0.040	0.0132
40	33.9	1.77	0.039	0.0131

Attachment 4 (To Appendix 2)

THERMISTOR (THB1) TIME RESPONSE (LAG) ERROR ANALYSIS FOR SUBJECT BREATHING AT WORK RATE NO. 3

To estimate the time response (lag) error of temperature measurement due to the thermistor an analysis of a chart recording (Run No. 26, 15 May, 850 feet during Work No. 3, Chart Pos 36 ft, 7 in. left). Fig. 1 was used in conjunction with a mathematical analysis of thermistor error due to a step change in temperature (Fig 3).

During the subject recording, the chart speed was increased from 1.5 inches per minute (one and one half) to 12 inches per minute (twelve) for several breathing cycles. The narrower peaks occurred at peak exhalation and had a duration in time of 0.3 to 0.5 seconds within 0.3°C of the recorded peak of 26.3°C and a duration of 0.15 to 0.34 seconds within 0.1°C of the peak. These measurements can be analyzed by making the assumption that the temperature Y degrees from the peak was the final temperature of a step change which remained t seconds, the width of the peak, at the final temperature (T) (see Fig. 2). Actually the temperature continued to rise after the assumed final temperature, T, to a final value T_F which is Y degrees greater than T.

The duration of the peak, t, can be converted to percent error of the size of the step by the following approximation:

$$\% \text{ error} \simeq (10^2)\left(e^{-t/\tau} + \frac{\Delta T}{T_F - T_O}\right)$$

Valid where

$$e^{-t/\tau} \leq \frac{\Delta T}{T_F} - T_O, \text{ most accurate when equal}$$

Where

t is the assumed duration of the step previously described

τ is the time constant for the thermistor under the conditions of concern.

ΔT is the range of temperature during period t.

$T_F - T_O$ is considered to be 24°C (27°C - 4°C).

e is the Napierian base 2.718

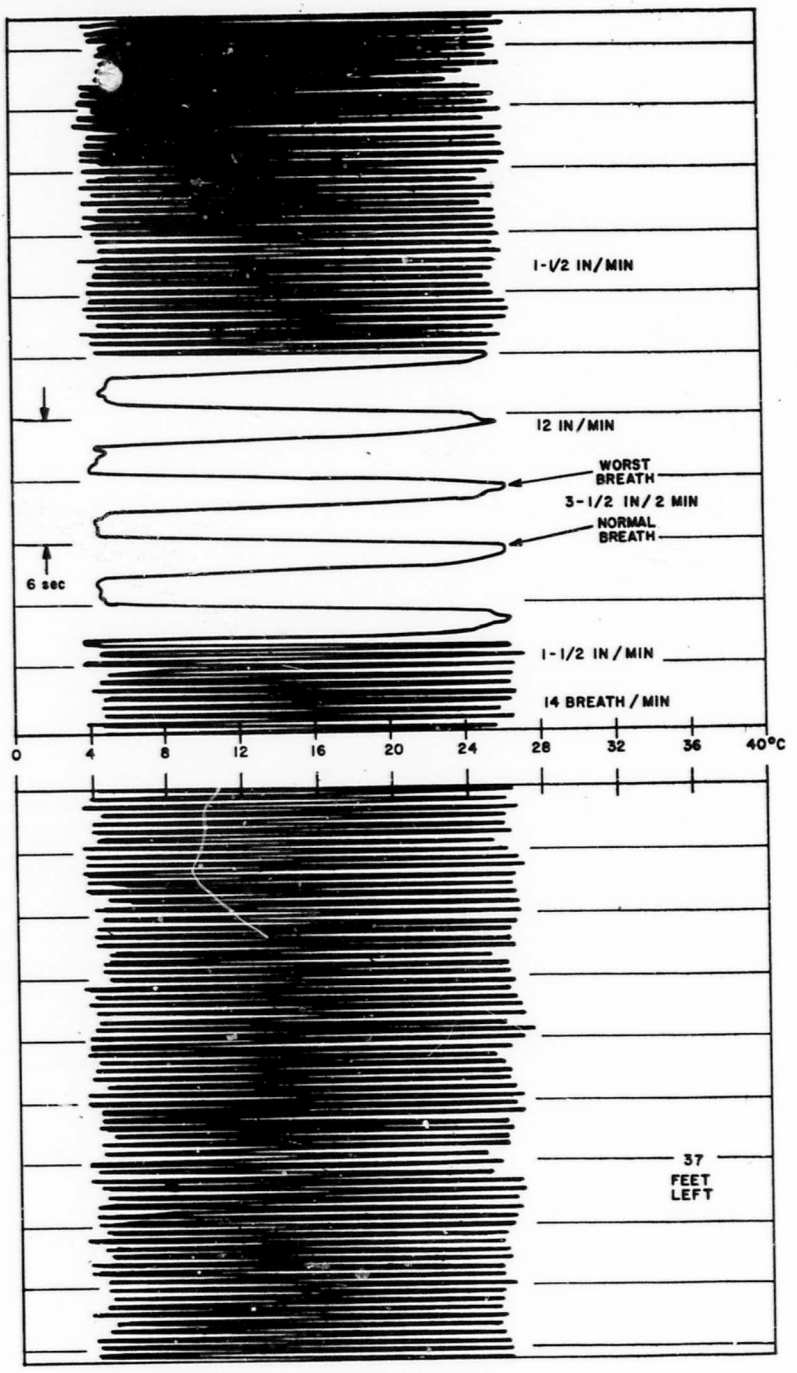

Figure 1. (To Attachment 4)

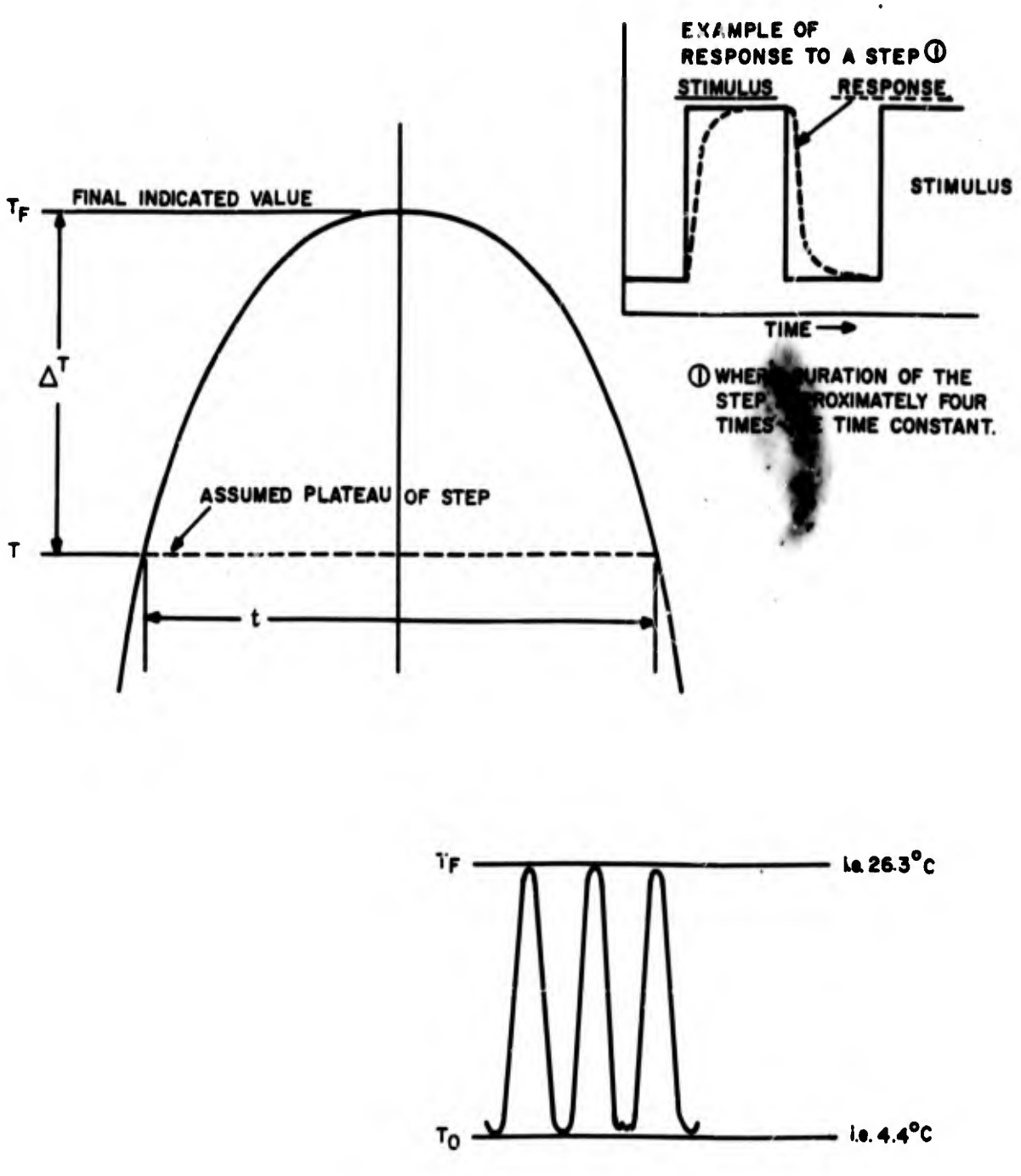

Figure 2. (To Attachment 4)

At 850 ft. in heliox, the % error for the worst conditions of t = 0.15 sec. at $\Delta T = 0.1°C$ and $\tau = 0.01$ yields 0.416% and for t = 0.34 sec. under the same conditions 0.416%, since $e^{-t/\tau}$ is less than $3.06 \cdot 10^{-7}$. Converting this to error in degrees Celsius yields 0.1°C for either value of t. Minute examination of the chart recording shows a probable duration of 0.1 sec within 0.05°C of the peak; although, the accuracy of measurement is questionable since 0.1 sec equals 0.01678 inch on the example used and the width of the pen trace was nearly equal to 0.1°C. Using t = 0.1 sec, $\Delta T = 0.05°C$ and $\tau = 0.01$ yields 0.213% of the step or 0.051°C error. During the measurements at depth, the short time constant ($\tau = 0.01$) placed the time threshold of an error of 0.5% at 0.053 seconds of assumed steady state. At depth the worst error was approximately 0.1°C (lag).

During baseline studies at the surface (1 Ata, Air) errors were larger due to a larger time constant resulting from difference in gas constants. The calculations can be performed using the measurements made from the depth recording, and the time constant for air at 100 ft/min and 1 Ata, $\tau = 0.06$ sec. At $\Delta T = 0.1°C$ and t = 0.15 sec and t = 0.34 sec. the errors are 8.624% and 0.756% respectively. The first value, 8.624% violates the condition for validity where the time constant error is approximately twenty times larger than the error resulting from the ΔT portion of the step. Another value of ΔT must be selected for comparison. At $\Delta T = 0.3°C$ and t = 0.3 sec. and t = 0.5 sec. the errors are 1.924% and 1.274% respectively. In the worst where t = 0.3 sec. the time constant portion of the error is 0.54 times the ΔT portion of the error, or more nearly valid. Translated to degrees Celsius, the error due to the time constant at the worst case in air at 1 Ata and 100 ft/min is 0.46°C (lag).

While worst time response errors have been analyzed, the range of errors at depth was from the maximum to 0.01°C minimum, and at the surface from the maximum to 0.02°C minimum.

In summary the approximate range of lag errors for measurements at depth ranged from 0.1°C to 0.01°C and at the surface from 0.46°C to 0.02°C.

(Figure 3 to Attachment 4)

THERMISTOR TEMPERATURE ERROR (LAG) DUE TO STEP CHANGE IN TEMPERATURE

t = time after step, τ = time constant of thermistor.

$$\% \text{ Error} = e^{-t/\tau} \quad (10^2)$$

t/τ	% Error
1	36.78
1.5	22.31
2	13.5
2.5	8.2
3.0	5.0
4.0	1.83
5.0	0.67
5.3	0.50
6.0	0.25
7.0	0.09
8.0	0.033
9.0	0.012
10.0	0.0045
20.0	$2.0.10^{-9}$

THERMISTOR TEMPERATURE ERROR (LAG) DUE TO STEP CHANGE IN TEMPERATURE

For THB1 (VECO E31A401C) t = time after step (sec), % Error is % of step

Still Air at 1ATA
τ = 0.12 sec

t (sec)	% Error
2.0	<0.0045
1.5	<0.0045
1.0	0.024
0.8	0.125
0.6	0.67
0.5	1.56
0.4	3.58
0.3	8.2
0.2	19.0
0.1	43.5
0.07	56.0
0.05	66.0

Air at 100 ft/min and 1ATA
τ = 0.06 sec

% Error
{Essentially Zero}
$< 2 \cdot 10^{-9}$
<0.0045
0.0045
0.024
0.125
0.67
3.58
19.0
31.2
43.5

Helium at 100 ft/min and 26ATA
τ = 0.01 sec

t (sec)	% Error
1.0	Zero
0.5	$<2 \cdot 10^{-9}$
0.1	0.0045
0.08	0.033
0.07	0.09
0.06	0.25
0.05	0.67
0.04	1.83
0.03	5.0
0.02	13.5
0.01	36.78
0.005	60.65

APPENDIX 3

GAS FLOW SYSTEM RECOMMENDED FOR THE RESPIRATORY HEAT LOSS STUDY

Introduction

A gas flow system for a respiratory heat loss study is desired that results in less than 5 cm. H_2O variation in pressure at a diver's mouth and requires minimum development time and cost.

Maximum variations in pressure at a diver's mouth are assumed to occur in the gas flow system at a worst condition of 150 LPM peak volumetric flow, He-O_2 gas mix with .90 atm P_{O_2}, 460 psia ambient pressure, (1000 ft. SW), and gas temperatures between 32°F and 100°F. An intermediate gas temperature of 68°F is used to simplify most of the analysis.

To minimize development time and cost, as many proven components are used as practical and those that must be developed have a high probability of success for the first model.

Gas Flow System

Figure 1 shows the recommended gas flow system. Chamber gas is pumped into the system by a positive displacement pump with a pressure relief valve and filters. Gas is cooled in heat exchanger tubing upstream and downstream of the pump. Gas from the downstream heat exchanger tube enters the breathing gas loop. The volume of gas that travels through the mouth piece inhalation check valve is equal to the volume of gas that is inhaled. Exhaled gas travels through the mouth piece exhalation check valve, through the pneumotach and to the top of the breathing gas loop. When desired, manually operated valving switches the flow to an upper loop containing a gas volume meter or a gas collector. Normally the gas is not directed through the upper loop. From the top of the breathing loop the gas flows to the exhaust check valve which is located at a level near the level of the divers' lung centroid.

Gas Pump

The recommended gas pump is a Gast Air Compressor 0740 PI06A. It is a vane type, oil-less pump which may be obtained with or without a base plate, motor coupling, motor and other accessories. The volumetric flow is 5.9 CFM (167 LPM) at the recommended

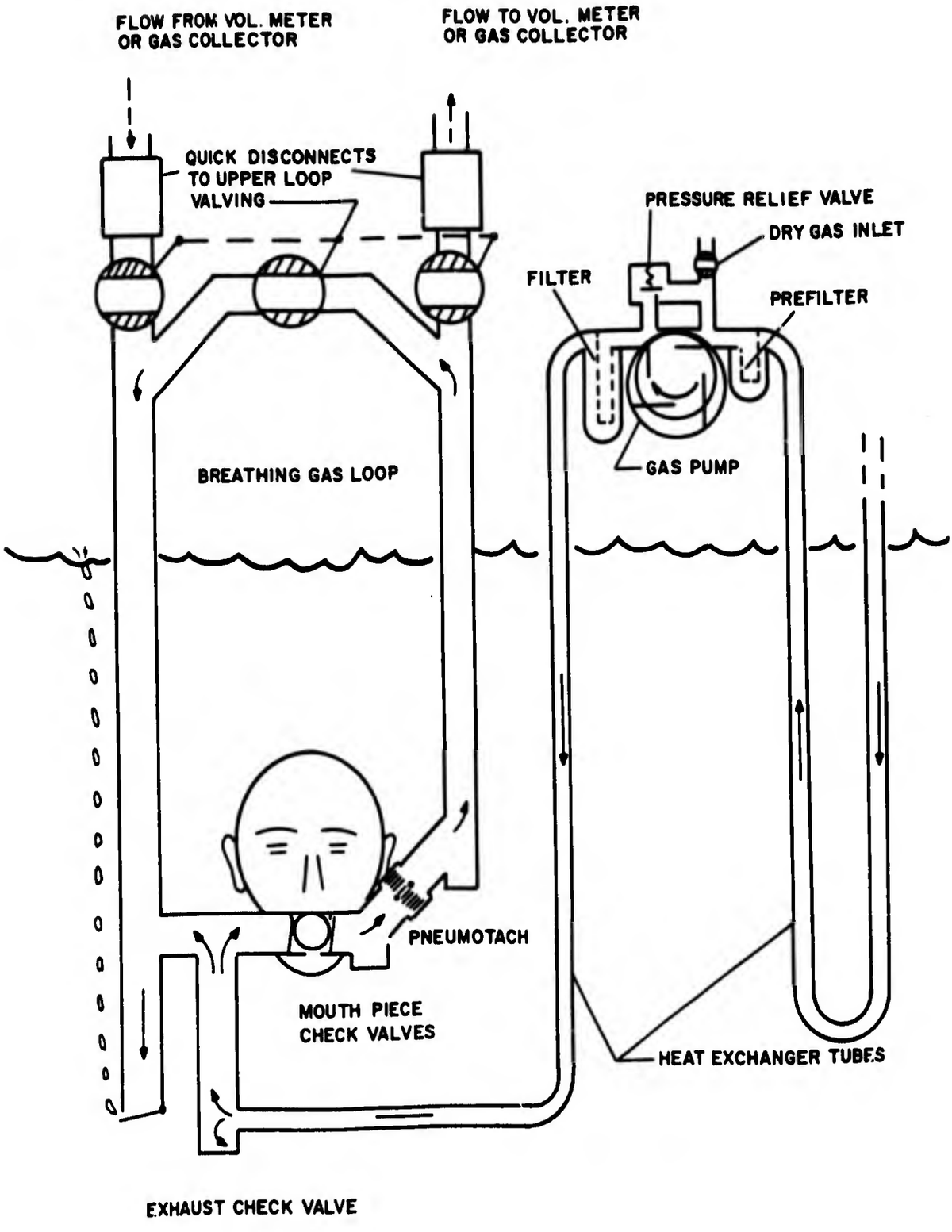

Figure 1. Gas Flow System

pump speed of 1725 RPM, for no gas pressure drop across it. In the recommended gas flow system the pump volumetric flow will be greater than 150 LPM and less than 167 LPM. Pumping power of the pump for the worst condition is about 50 watts. Including pumping losses and chance of pressure overload, a one-third HP motor driving the pump would be sufficient. The drive motor may be a fluid motor using a water based hydraulic fluid. It is recommended that two of the pumps be purchased. One may be used as a spare or used in parallel with the other pump if later it is found that larger flows than 150 LPM are required for shallow depth tests. It is also recommended that one of the pumps be dismantled after it is received to be sure the porting around the motor is large enough to result in negligible gas compression.

If the pump is to be shut down for more than a few hours, the filter and prefilter should be emptied of water, and dry gas from the BIB system should be introduced at the dry gas inlet to purge the pump of moisture. This should be done just as the pump is being turned off.

Filters

A Wilkerson Microalescer filter model 1206-4 is recommended along with a replacement mantle, model 85-141. Mounted downstream of the pump, the filter will effectively remove all of the contamination particles in the breathing gas, including carbon and iron particles generated by pump wear. A Wilkerson Prefilter, model 1137-4 is also recommended. Mounted upstream of the pump, it will protect the pump by filtering out slugs of water that otherwise could enter the pump. Slugs of water will occur from condensation buildup in the upstream heat exchanger tube.

Heat Exchanger Tubing

Heat exchanger tubing upstream and downstream of the pump reduces the breathing gas temperature to about 1°F above water temperature. Each tube is 3/4 inch OD, .049 inch wall, 16 feet long and has as much of its' length submerged in the wet pot water as practical.

The inlet end of the upstream tube has several holes drilled radially into it to lessen the probability of gas stoppage caused by an object accidentally plugging the inlet.

Breathing Gas Loop

The inside diameter of the tubing in the breathing control loop should be about 1.5 inches. For worst case conditions the overall pressure drop caused by the tubing and its' fittings will be about .5 cm. H_2O. To determine the pressure drop in the valves, first the effective area of the valve should be estimated or found by testing. The worst case pressure drop can then be found from Figure 2.

Gas Properties for the Worst Case

For the assumed worst case,

$$\dot{V} = (150 \text{ LPM}) \left(\frac{61 \text{ in}^3/\text{s}}{60 \text{ LPM}}\right) = 152.5 \text{ in}^3/\text{s, vol flow}$$

$$T = 68°F + 460 = 528°R, \text{ gas temp.}$$

$$P = 460 \text{ psia, ambient pressure (1000 ft SW depth)}$$

$$P_{O_2} = .9\ (14.7) = 13.2 \text{ psia, partial pressure } O_2$$

From Arawak IV System Calculations,

$$\%O_2 = 2.87, \text{ percent oxygen in He-}O_2 \text{ mix}$$

$$R_g = 1.490 \times 10^6 \frac{\text{in}}{°R} \frac{\text{in}}{S^2}, \text{ gas constant}$$

$$\rho = \frac{P}{R_g T} = \frac{460}{1.49 \times 10^6\ (528)}$$

$$= .584 \times 10^{-6} \frac{\text{lb}}{\text{in}^3} \frac{S^2}{\text{in}}, \text{ gas mass density}$$

$$\mu = .0029 \times 10^{-6} \frac{\text{lbs}}{\text{in}^2}, \text{ gas viscosity (approx)}$$

$$C_p = 1.04 \text{ Btu/lb F, specific heat}$$

$$Pr = .64 = \frac{C_p \mu}{K} \text{ Prandtl's number}$$

$$K = \frac{C_{p\mu}}{Pr} = \frac{1.04\ (.002 \times 10^{-6})}{.64} (386)(3600)$$

$$= .00655 \frac{\text{Btu}}{\text{hr inF}}, \text{ thermal conductivity (approx.)}$$

Bernoulli Pressure Drop for Worst Case

$$\Delta P_B = \frac{1}{2}\rho\mu^2 = \frac{1}{2}\rho\dot{V}^2/a_e^2$$

$$= \frac{1}{2}\ .584 \times 10^{-6}\ (152.5)^2\ /a_e^2$$

$$= .0068/a^2_e \text{ psi}$$

$$\Delta P^*_B = (.0068/a^2_e \text{ psi})\left(70.4 \frac{\text{cm}H_2O}{\text{psi}}\right)$$

$$= .479/a^2_e \text{ cm } H_2O$$

Figure 2 on the next page is a plot of this function and may be used to size components on the breathing gas loop.

Breathing Gas Loop

Assume the loop has a total effective length of 16 ft. including effective lengths of the tube fittings and valves. Tube length is

$$\ell = 16(12) = 192 \text{ in}$$

Tube inside diameter is assumed to be

$$d = 1.5 \text{ in.}$$

Tube inside area is

$$a = \frac{\pi}{4} d^2 = \frac{\pi}{4} (1.5)^2 = 1.765 \text{ in}^2$$

Worst case volumetric flow

$$V = (150 \text{ LPM})\left(\frac{61 \text{ in}^3/\text{s}}{60 \text{ LPM}}\right) = 152.5 \text{ in}^3/\text{s}$$

Reynolds number is

$$R_e = \frac{\rho V d}{\mu a} = \frac{.584 \times 10^{-6}\ (152.5)\ 1.5}{.0029 \times 10^{-6}\ (1.765)} = 26,100$$

Tube roughness ratio is assumed to be

$$\frac{\epsilon}{d} = .001$$

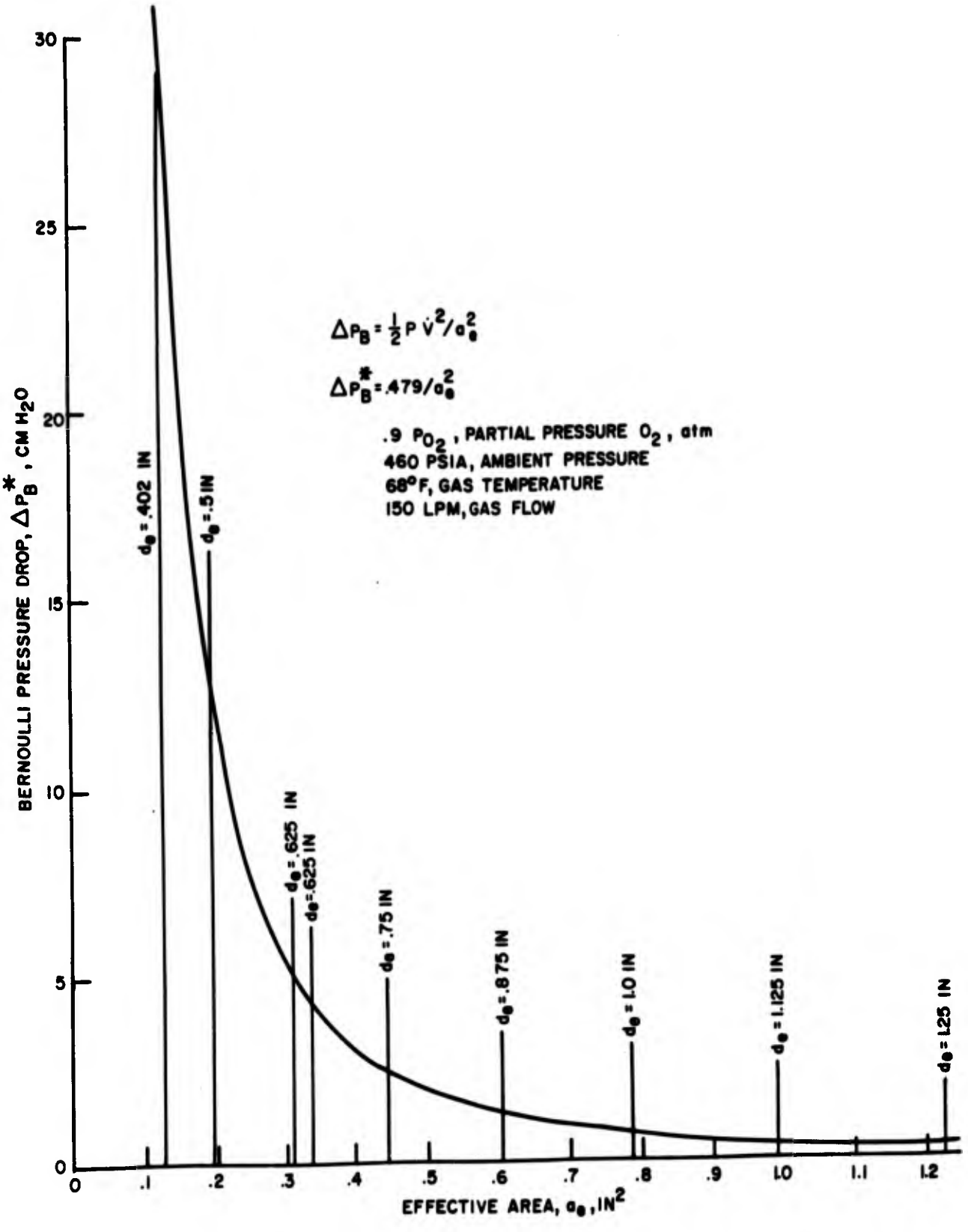

Figure 2. Worst Case Bernoulli Pressure Drop

Friction factor from Moody's diagram is

$$f = .027$$

Pressure drop in the loop is

$$\Delta P = f \frac{\ell}{d} \frac{1}{2} \rho V 2/a2$$

$$= .027 \frac{192}{1.5} \frac{1}{2} .584 \times 10^{-6} \frac{152.5^2}{1.765^2}$$

$$= .00754 \text{ psi}$$

$$\Delta P^* = (.00754 \text{ psi}) \left(70.4 \frac{\text{cm } H_2O}{\text{psi}}\right) = .53 \text{ cm } H_2O$$

Heat Exchanger Tubes

Assume tubes upstream and downstream of the pump are each 16 ft. long, 3/4 in OD with .049 in wall.

Tube length is

$$\ell = 16 \ (12) = 192 \text{ in}$$

Tube inside diameter is

$$d = .750 - 2 \ (.049) = .652 \text{ in.}$$

Tube inside area is

$$a = \frac{\pi}{4} d^2 = \frac{\pi}{4} (.652)^2 = .344 \text{ in}^2$$

Volumetric pump flow is

$$V = (5.9 \text{ ft}^3/\text{min}) \left(28.8 \frac{\text{in}^3/\text{S}}{\text{ft}^3/\text{min}}\right) = 170 \text{ in}^3/\text{S}$$

Reynolds number is

$$R_e = \frac{\rho u d}{\mu} = \frac{\rho V d}{\mu a} = \frac{.584 \times 10^{-6} (170) .652}{.0029 \times 10^{-6} \ (.344)} = 64,900$$

Tube roughness is assumed to be

$$\frac{\epsilon}{d} = .001$$

Friction factor from Moody's diagram is

$$f = .023$$

Pressure drop in each tube is

$$\Delta P = f\frac{\ell}{d}\frac{1}{2}\rho V^2/a^2 = .023\ \frac{192}{.652}\frac{1}{2}\ .584 \times 10^{-6}\ \frac{170^2}{.344^2}$$

$$= .482 \text{ psi}$$

Prandtl number is

$$Pr = .64$$

Nusselt number from McAdams equation is

$$Nu = .023\ (R_e)^{.8}\ (Pr)^{.4} = .023\ (64.900)^{.8}\ (.64)^{.4}$$

$$= 136$$

Heat transfer coefficient is

$$h = \frac{NuK}{d} = \frac{136\ (.00655)}{.652} = 1.37\ \frac{\text{Btu}}{\text{hr in}^2\ \text{F}}$$

Heat flow loss in an incremental length of gas is

$$d\dot{Q} = C_p \dot{V} \rho_g\ 3600\ dt\ \frac{\text{Btu}}{\text{hr}}$$

Heat flow out ot an incremental length of tube is

$$d\dot{Q} = h\ \pi d\ (T-T_w)\ d\ell\ \frac{\text{Btu}}{\text{hr}}$$

Equating heat flow out to heat flow loss

$$\frac{d\ell}{dT} = \frac{C_p \dot{V} \rho_g\ 3600}{h\ \pi d\ (T-T_w)}$$

At the entrance of the tube

$$\frac{d\ell}{dT} = \frac{\ell_i}{T_i - T_w} = \frac{C_p \dot{V} \rho g\, 3600}{h \pi d\, (T_i - T_w)}$$

where a length constant is

$$\ell_i = \frac{C_p \dot{V} \rho g\, 3600}{h \pi d} = \frac{1.04(170)\ .584 \times 10^{-6}\ (386)3600}{1.37 \pi .652}$$

$$= 51.2 \text{ in}$$

Temperature change at the exit, assuming inlet gas temperature is 62°F and water temp. is 32°F, is

$$T_o - T_w = (T_i - T_w) e^{-\frac{\ell}{\ell i}}$$

$$= (62 - 32) e^{\frac{-192}{51.2}} = .706\ F°$$

The heat flow out is

$$Q = C_p \dot{V} \rho_g\, 3600\ (T_i - T_o)$$

$$= 1.04\ (170)\ .584 \times 10^{-6}\ (386)\ 3600\ (62\text{-}32)$$

$$= 4,300 \frac{\text{Btu}}{\text{hr}}$$

Power out is

$$P = \left(4300 \frac{\text{Btu}}{\text{hr}}\right)\left(\frac{1054}{3600}\ \frac{\text{w-hr}}{\text{Btu}}\right) = 1260 \text{ watts}$$

This is high compared to the pumping power of 50 watts indicating there is little increase in gas temp. at the pump.

Fleisch Pneumotach Linear Flow Range

Assume:

850 ft SW, depth

.3 atm PO_2, partial pressure oxygen in $He\text{-}O_2$ mix

98.6 °F, exhalation gas temperature

Ambient pressure is

$$P = \left(\frac{850}{33} + 1\right)\ 14.7 = (26.8)\ 14.7 = 393 \text{ psia}$$

Partial pressure of oxygen

$$P_{O_2} = (.3)\ 14.7 = 4.41 \text{ psia}$$

Decimal percent oxygen by volume

$$\text{dec}\%O_2 = \frac{P_{O_2}}{P} = \frac{4.41}{393} = .0112 \text{ or } 1.12\%O_2$$

Gas viscosity is found by interpolation of data in the "Navy Gas Manual"

$$\mu = \left(1.465 \times 10^{-5}\ \frac{\text{lb}}{\text{ft s}}\right)\ \left(\frac{1}{6.72 \times 10^{-4}}\ \frac{\text{Cp}}{\text{lb/ft s}}\right)\ \left(.145 \times 10^{-6}\ \frac{\text{lb sec/in}^2}{\text{Cp}}\right)$$

$$= .00316 \times 10^{-6}\ \frac{\text{lb sec}}{\text{in}^2}$$

Gas constant is found by mass ratios

$$R_g = \frac{1}{\frac{\text{dec\% He}}{(R_g)_{He}} + \frac{\text{dec}\%O_2}{(R_g)_{O_2}}} = \frac{1}{\frac{.989}{1.76 \times 10^6} + \frac{.0112}{.224 \times 10^6}}$$

$$= 1.63 \times 10^6\ \frac{\text{in}^2}{{}^\circ\text{R s}^2}$$

Gas density is

$$\rho = \frac{P}{R_g T} = \frac{393}{1.63 \times 10^6\ (98.6 + 460)} = .431 \times 10^{-6}\ \frac{\text{lb s}^2}{\text{in}^4}$$

Maximum linear flow rate for ± 1.5% accuracy, for standard air, from the test data in Figure 3 is

$$\forall_{\ell}{}^{*}_{\text{std air}} = (10 \text{ LPS})\ (60\ \frac{\text{s}}{\text{min}}) = 600 \text{ LPM}$$

Maximum linear flow rate for the mix is found by Reynolds number scaling

$$\dot{V}_{\ell}^{*} = \dot{V}_{\ell}^{*}{}_{\text{std air}} \frac{\rho_{\text{std air}}}{\rho} \frac{\mu}{\mu_{\text{std air}}}$$

$$= 600 \frac{.113 \times 10^{-6}}{.431 \times 10^{-6}} \frac{.00316 \times 10^{-6}}{.00275 \times 10^{-6}}$$

$$= 181 \text{ LPM}$$

Info. From: "Report of Test for Pneumotach and Pressure Transducer"
C.E. Bernhardt, Def. & Space Center, Ⓦ
Test No: 71021103, 2/17/71
Fleisch Pneumotach S/N 3.1005
Statham Diff. Press Transducer, S/N 11890
Bridge Exciting Voltage: 8 VDC
Flow in + Direction

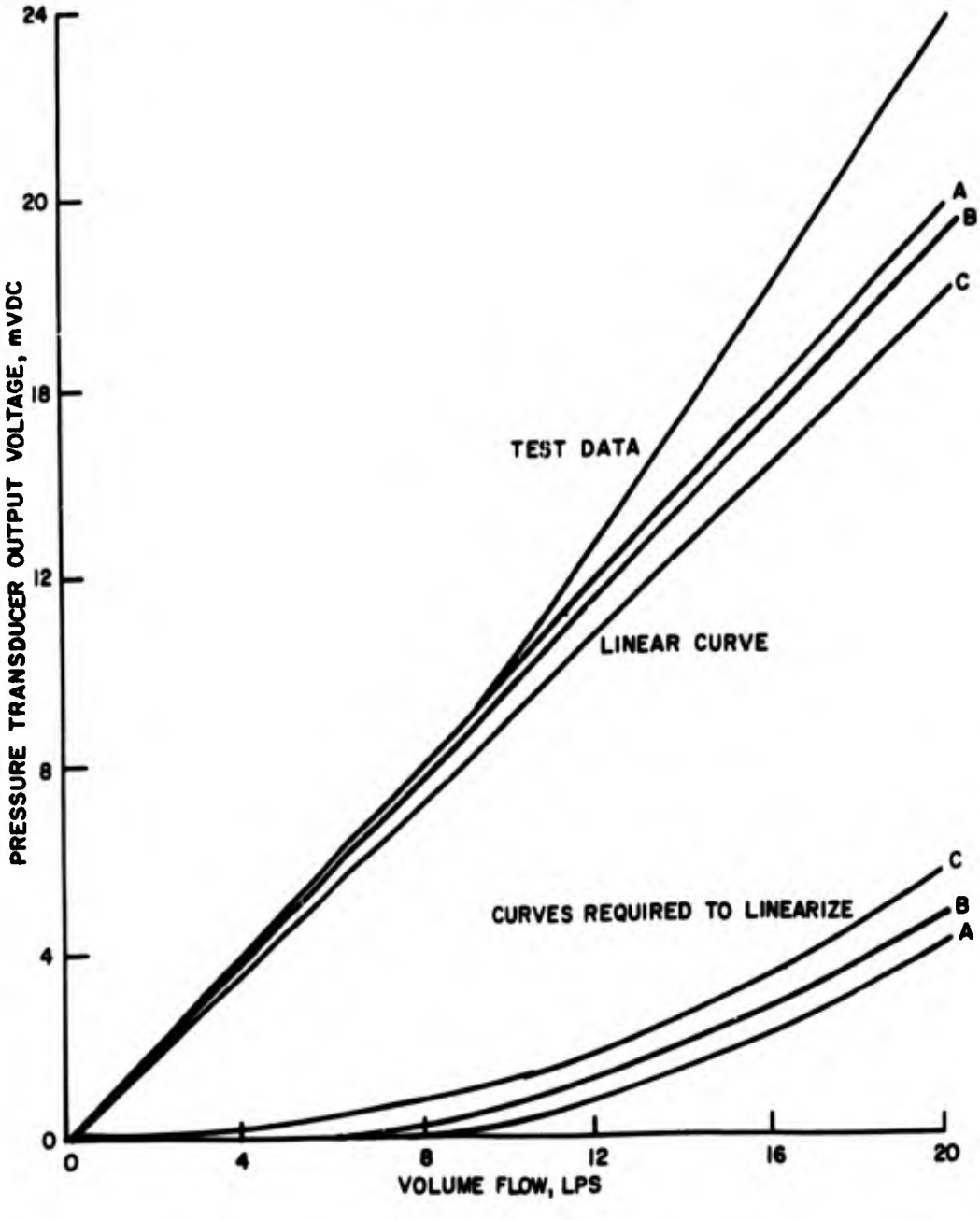

Figure 3. Fleisch Pneumotach - Pressure Transducer Characteristics

APPENDIX 4

THE PNEUMOTACHOGRAPH AND ITS USE IN MEASURING RESPIRATORY GAS FLOW IN UNDERSEA SYSTEMS

INTRODUCTION

The object of this memo is to describe the pneumotach, indicate its principle of operation and discuss its use in undersea life support systems. The description includes a sketch of a pneumotach, a curve showing its general characteristics and typical values of parameters. The principle of operation includes detailed characteristics, causes of some nonlinearities and the expected linear range based on Reynolds number. The discussion presents some recommendations and precautions in using the pneumotach in undersea systems.

The pneumotach has been used for several years for measuring respiratory gas flow. Similar devices with the same principle of operation have been used for measuring volumetric flow of other fluids, both liquids and gases. These devices have a variety of names:

peumotachograph
Vol-O-Flow element
gas flow element
flow element
fluid linear resistor
fluidic resistor
flow to pressure transducer
volumetric flow to differential pressure transducer

DESCRIPTION

The pneumotach is a fluidic device consisting of closely spaced surfaces arranged in an enclosure as shown in Figure 1. Fluid flows into one end of the enclosure, between the closely spaced surfaces and out the other end. Pressure taps are located to measure pressure difference across all or a portion of the length of the surfaces.

Pressure taps in some pneumotachs are located within the length of the closely spaced surfaces. This results in a greater linear flow range compared to the pneumotach with the taps located outside of the length of closely spaced surfaces. Locating the upstream tap within the length is most critical for a greater linear flow range. The primary reason for locating the downstream tap within the length is for greater linear flow range when the flow direction is reversed. It is desirable to locate the pressure taps as far apart as practical so the measured pressure difference is a large portion of the total pressure drop across the pneumotachograph.

Linear range is shown in the general characteristic illustrated in Figure 1. Within this range the ΔP vs $\dot{V}$ curve approximates a linear function $\Delta P = K\dot{V}$ and the accuracy of the pneumotach is greatest. ΔP is measured pressure differential, $\dot{V}$ is volumetric flow and K is the linearized gain of the pneumotachograph.

Maximum volumetric flow of the linear range is maximum linear volumetric flow.

$$\dot{V}_{max.\ lin} = 600 \text{ LPM for std air}$$

Its estimated ideal value is about the same as the peak respiratory flow of a human. The pneumotach pressure difference at maximum linear volumetric flow is maximum linear pressure difference.

$$\Delta P_{max.\ lin} = 1 \text{ cm } H_2O \text{ for std air}$$

Its estimated ideal value is small compared to the pressure drop in a humans airway, but large enough for accurate flow measurement.

Gain of the pneumotach in the linear range is the linear gain.

$$K = \frac{\Delta P}{\dot{V}} = \frac{\Delta P_{max\ lin}}{\dot{V}_{max\ lin}} = .00167 \text{ cm } H_2O/\text{LPM} = .0000233 \text{ psi/in}^3/\text{s}$$

Its ideal value for standard air is calculated from the ideal values estimated for maximum linear volumetric flow and maximum linear pressure difference. All of the ideal values are based on the assumption that the pneumotach is to be used over the maximum range of respiratory flow.

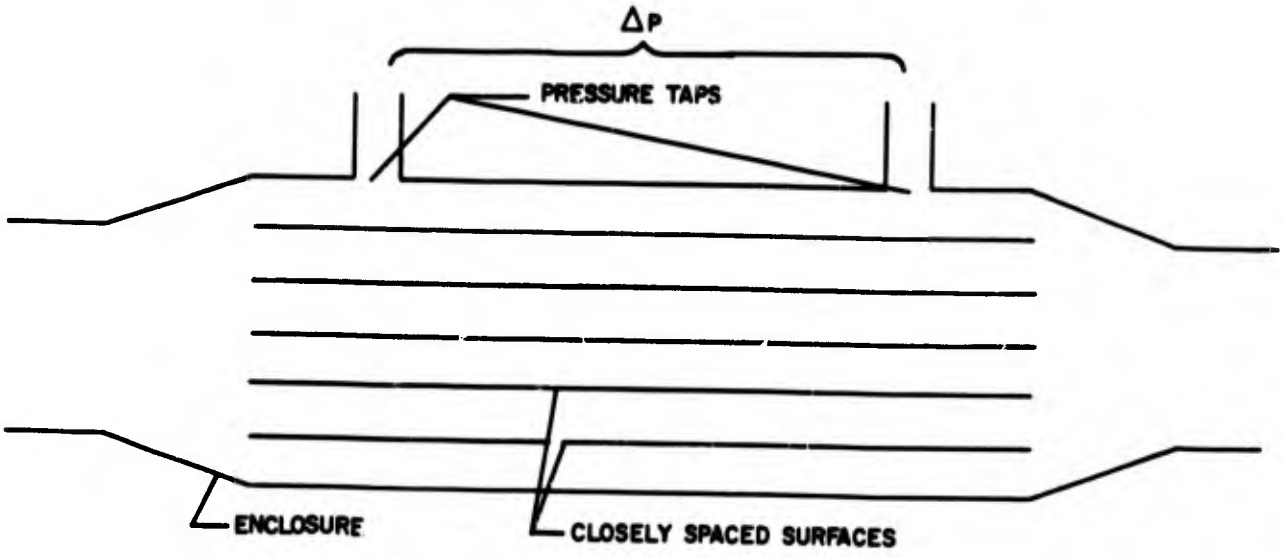

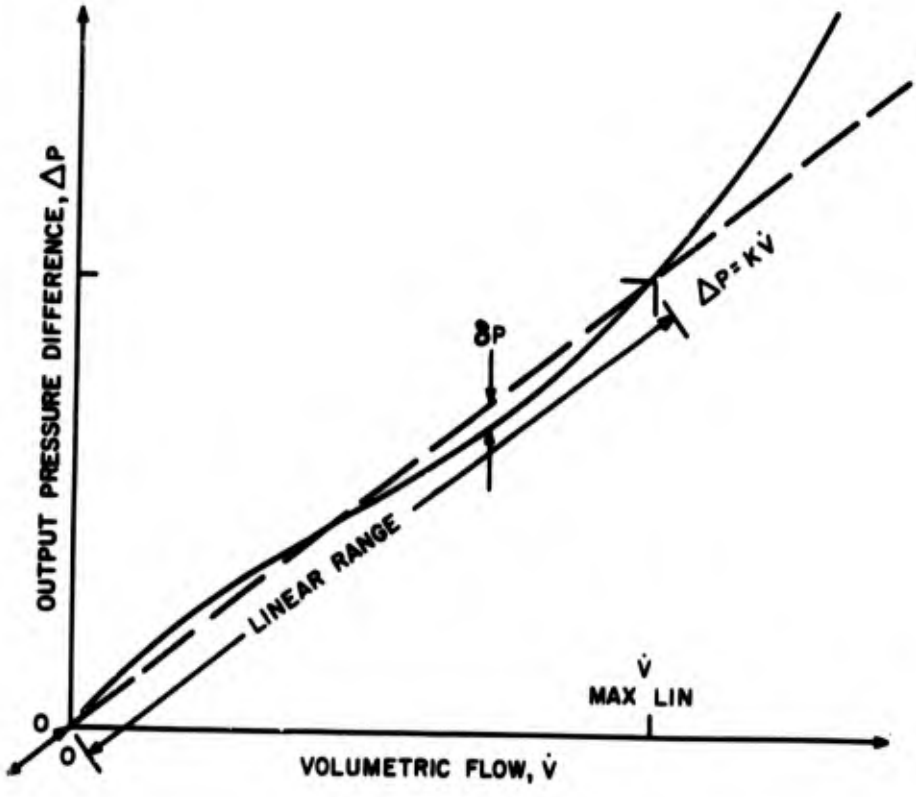

Figure 1. The Pneumotachograph and Its General Characteristics

Accuracy of the pneumotach is described in terms of pressure error relative to the linear function of $\Delta P = K\dot{V}$. The accuracy is:

$$\epsilon = \frac{\delta P}{\Delta P_{max\ lin}} \times 100, \ \%$$

where δP is pressure deviation from the linear function. For standard air, typically good accuracy is $\pm 1\%$. Sometimes accuracy is given in terms of repeatability relative to a calibrated curve. Typically good repeatability is $\pm .15\%$.

PRINCIPLE OF OPERATIONS

The principle of operation is first described for the linear range of operation and then for the nonlinear range. There is sometimes a need for operating beyond the linear range.

In the linear range of operation, the pressure difference is caused by viscous drag of fluid flowing between closely spaced surfaces. The pressure drop, ΔP, is a function of viscosity μ, as well as volumetric flow, $\dot{V}$.

$$\Delta P = C_1 \mu \dot{V}$$

The constant C_1, is a function of the dimensions of the device. As an example for viscous flow through a single capillary tube,

$$\Delta P = \frac{128\ \ell}{\pi d^4} \mu \dot{V}$$

so

$$C_1 = 128\ell/\pi d^4$$

where

P is pressure drop, psi

$\dot{V}$ is volumetric flow, in^3/sec

μ is absolute viscosity, lb s/in^2

ℓ is length of the tube, in

d is inside diameter of the tube, in

These results are obtained from the Hagen-Poiseuille equation for laminar flow in a tube. Assumptions for this simplied analysis are listed below:

(1) Conservation of mass and momentum applies.

(2) Velocity is low enough for negligible inertia effects, so Bernoulli pressure drop is negligible and turbulent flow does not exist.

(3) Velocity is much less than sonic velocity so compressibility effects are negligible.

(4) Fluid is a single phase Newtonian fluid so viscosity is not a function of shear stress and shear stress acts only in the direction of flow.

(5) Steady state flow exists so change with respect to time is negligible.

(6) Fully developed flow exists, so the velocity profile remains unchanged over the whole length of closely spaced surfaces.

(7) Body forces are negligible, so gravity is not acting to accelerate the fluid.

(8) Temperature variations are negligible.

(9) Heat transfer to or from the fluid is negligible.

These assumptions could be applied to flow between closely spaced surfaces found in most pneumotachs. C_1 can also be found as a complicated function of internal dimensions of most pneumotachs, but the most accurate value of C_1 is found by first calibrating the pneumotach and measuring the slope of the linear function that best fits the calibration points. The slope is the linear gain K. Next C_1 is calculated from $C_1 = K/\mu$.

Calibration results are shown in Figure 2 for the Fleisch pneumotach used in the respiratory heat loss study. The linear gain is:

$$K = .0016 \text{ psi/LPS} = .0000271 \text{ psi/in}^3\text{/sec}$$

which is approximately the same as the ideal gain. Since the viscosity of air at 1 atm and 70°F is

$$\mu = .0026\ (10^{-6}) \text{ lb s/in}^2$$

The value of the linear gain constant is

$$C_1 = K/\mu = 1040 \text{ 1/in}^3$$

This value can be used to find the linear gain of the pneumotach for any Newtonian fluid, providing the viscosity of the fluid is known.

The nonlinear range of operation includes the curved portion of the ΔP vs $\dot{V}$ curve at high flows as well as the straight portion of the curve in the linear range. The change from the straight portion to the curved portion is caused mostly by a change to an appreciable Bernoulli pressure drop at the entrance of the closely spaced surfaces and a change to turbulent flow between the surfaces. Since these are changes from a viscous pressure drop to inertia pressure drops the change can be predicted by Reynolds number scaling.

Reynolds number is a ratio of fluid inertia forces to fluid viscous forces.

$$Re = \rho ud/\mu = \rho \dot{V} d_c / \mu a_c$$

where

ρ is fluid mass density

μ is fluid viscosity

u is fluid velocity

$\dot{V}$ is fluid volumetric flow

a_c is a characteristic area

d and d_c and characteristic dimensions.

The maximum linear Reynolds number, $Re_{max\ lin}$ is the Reynolds number at maximum linear flow, $\dot{V}_{max\ lin}$

$$Re_{max\ lin} = \dot{V}_{max\ lin}\ \rho d_c\ \mu a_c,$$

Its value for the pneumotach characteristics given in Figure 2 is

$$Re_{max\ lin} = 26,200\ d_c/a_c$$

where d_c and a_c are in units of inches and square inches respectively. This value may be used to calculate the maximum linear flow of the pneumotach for any Newtonian fluid if fluid viscosity and density are known.

$$\dot{V}_{max\ lin} = 26,200\ \ \mu/\rho$$

The nonlinear range of operation can be expressed as the nonlinear function

$$\Delta P = C_1 \mu \dot{V} + C_2 \rho \dot{V}^2 / 2$$

where C_1 and C_2 are allowed to vary as shown below

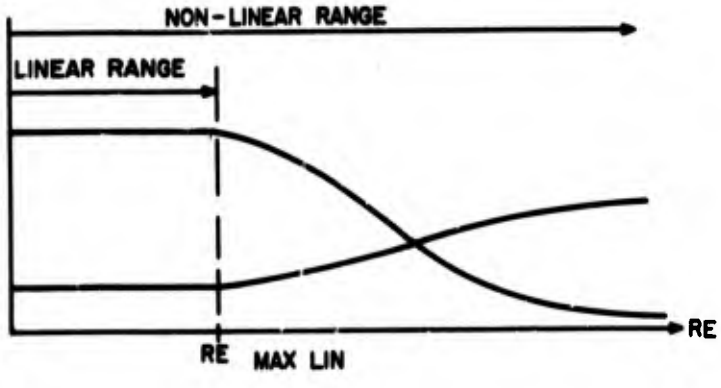

The decrease in C_1 with increased Re indicates the reduction of the viscous flow effect caused by the change to turbulent flow between the closely spaced surface. The flow approaches complete turbulent flow at very high Re, so C_1 approaches zero and C_2 approaches a constant higher value.

USE IN UNDERSEA LIFE SUPPORT SYSTEMS

To obtain accurate volumetric flow measurements with the pneumotach, the apparatus must be properly setup and the fluid viscosity must be accurately known.

An arrangement of pneumotachs for measuring inhalation and exhalation gas flow to and from a subject is shown in Figure 3. The inhalation gas temperature is assumed to be considerably cooler than the exhalation gas temperature. Inhalation and exhalation pneumotachs are recommended, so they operate nearly at the inhalation and exhalation gas temperatures respectively. Little condensation of water vapor will occur in the pneumotachs with this apparatus setup providing the interconnecting tubing is short and adequate thermal insulation is used. Water traps are used to catch condensation and saliva. The pneumotachs shown at a sloping angle are assumed to be the self-draining type. They could also be the type with a heating element.

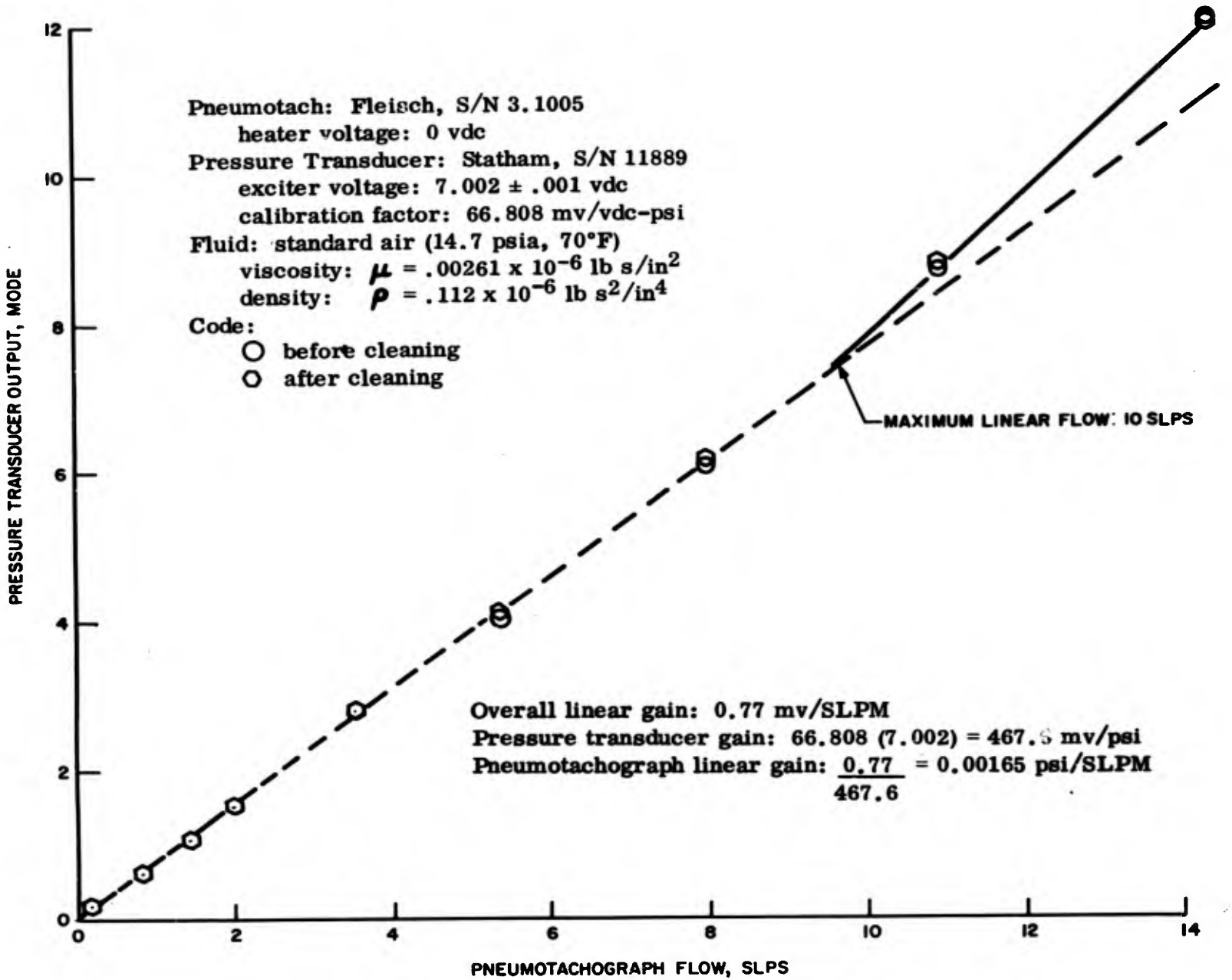

Figure 2. Pneumotachograph Calibration

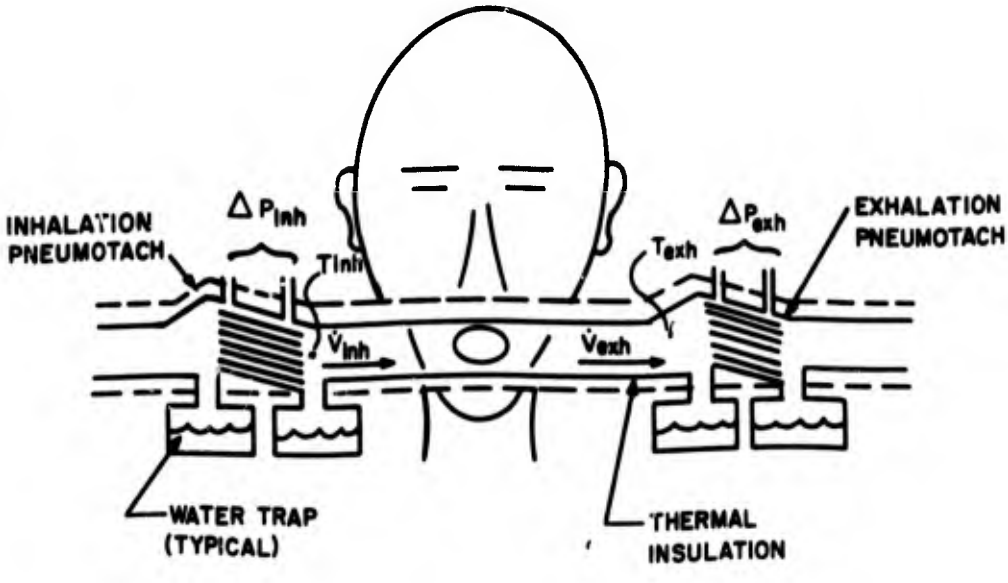

ΔP, PRESSURE DIFFERENCE SIGNAL
T, TEMPERATURE
V̇, VOLUMETRIC FLOW
( )exh, PERTAINING TO EXHALATION
( )inh, PERTAINING TO INHALATION

Figure 3. Pneumotachs Used to Measure Inhalation and Exhalation Gas Flow

Short tubing between the subject and the pneumotachs results in less dynamic flow error as well as less error caused by temperature change in the tubing. The tubing acts as a fluid capacitance between the subject and the pneumotach and can result in considerable dynamic flow error if the fluid capacitance is large and if there is appreciable fluid resistance or inductance in series with the tube.

Apparatus for measuring inhalation and exhalation gas flow could be greatly simplified if the inhalation gas temperature was about the same as exhalation gas temperature and if greater gas dead space in the apparatus could be tolerated. In this case, a single pneumotach could be used close to the subjects mouth to measure both inhalation and exhalation flow without condensation occurring in the pneumotachograph.

Viscosity of respiratory gas used in undersea systems varies with mixture, temperature and absolute pressure. As an example, viscosity of He - 0_2 is shown in Figure 4 to vary as a function of mixture and temperature. This data derived from the "U.S. Navy Diving- Gas

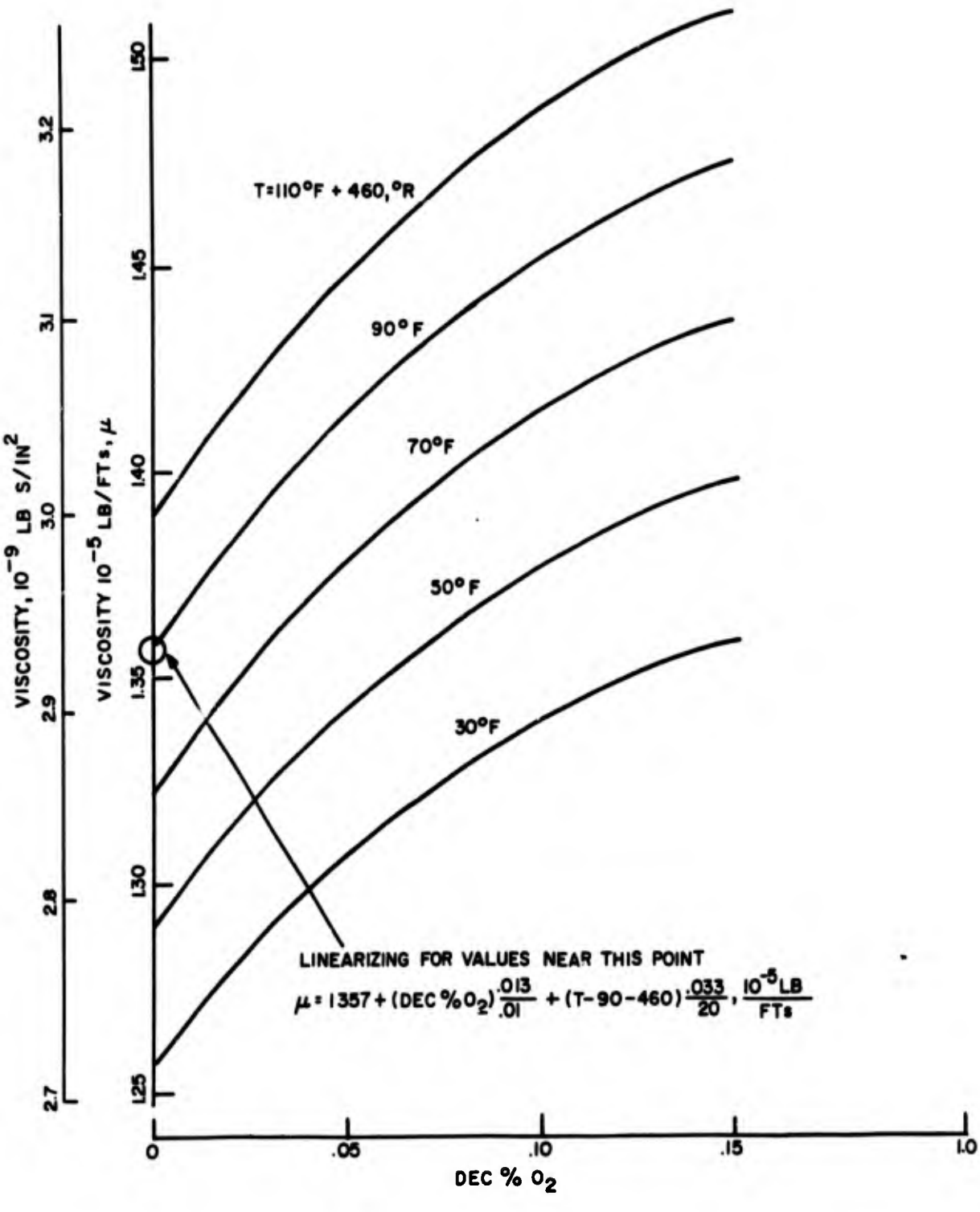

Figure 4. Viscosity of He - 0_2 Gas Mix

Manual " (AD701566) by W. I. Milwee, et al, Battelle Memorial Inst., 1969 shows that viscosity of a mixture can be about 10% greater than the viscosity of pure He or O_2. Viscosity of pure gases and air can be found as a function of temperature and pressure from the method given by E. W. Coming and R. S. Egly in "Viscosity of Gases and Vapors at High Pressures", Industrial Engrg., and Chemistry, Vol. 32 No. 5, 1940 pp 714-718. A pressure increase from 1 atm (0 ft SW) to 46.4 atm (1500 ft SW) was found to cause a negligible increase in viscosity of He at 70°F. Presently there is not enough data available on viscosity of He - N_2 - O_2 gas mix to determine accuracies better than 1% for pneumotachs used in measuring respiratory gas flow in undersea systems. It is assumed that the 1.2 atm partial pressure of N_2 in the He - N_2 - O_2 gas mix used in this study results in 1% greater viscosity than for the He - O_2 gas mix shown in Figure 4. A 1.2 atm partial pressure of N_2 in an He - N_2 gas mix at 15 to 30 atm pressure results in about 1% greater viscosity than for pure He. This was derived from data given in "Viscosity of the Helium - Nitrogen System from 133° to 470°K for Pressures Between 1 and 240 Atmospheres", R. E. Wood and W. J. Boone, Jr., Bureau of Mines Report No. 7405, July 1970. The error resulting from viscosity estimation methods is about ± 1%. The He - N_2 - O_2 gas mix must be tested if greater accuracy is required.

Water vapor condensing in the pneumotach results in two types of flow measurement errors. The errors are caused by less gas flow out of the pneumotach than into it and accumulation of condensate on the closely spaced surfaces.

The error resulting from condensation causing less gas flow out of the penumotach than into it is a small error. The volumetric flow lost as condensate is

$$\Delta \dot{V}_{cond} = \dot{V}_{exh} \frac{\Delta P_{water\ vapor}}{14.7\ (1 + Z/33)}$$

where

$\dot{V}_{exh}$ is exhalation volumetric flow

$\Delta P_{water\ vapor}$ is change in water saturation pressure, psi

Z is depth, ft SW

For the exhalation pneumotach shown in Figure 2, ΔP_{exh} could read about 1% low at Z = 0 ft SW because of this effect alone. At deep diving depths the error caused by the effect is negligible.

Accumulation of condensate on the closely spaced surfaces results in an increased flow resistance of the pneumotach. A manufacturer of a pneumotach with a self draining feature claims the flow resistance is increased less than 2% as the condensate accumulation is increased to maximum. This increase in flow resistance is a function of the pneumotach design and the wettability of the closely spaced surfaces. Self draining pneumotachs should be cleaned, then calibrated in a dry and fully wet condition prior to their use.

To prevent condensation from occurring in some pneumotachs, a heating element is provided that heats the closely spaced surfaces.

A heated pneumotach has errors associated with the rise in gas temperature as the gas flows through it. As the gas is heated, its viscosity and the volumetric flow are increased. As an example, if air is heated from 90°F to 94°F, its viscosity is increased about .5% and its volumetric flow is increased about .5%. Because of gas temperature variations in the pneumotach, the actual increase caused by viscosity increase would be larger than .5% and that caused by volumetric flow increase would be smaller than .5%. Both of these increases cause an appreciable increase in flow resistance of the pneumotach, compared to the unheated pneumotach. The highest gas temperature rise occurs at low gas flows, low absolute pressure, and early in an increasing change of gas flow rate. These variations in gas temperature cause nonlinearities in pressure difference signals with respect to volumetric gas flow, dive depth and time. Because of these effects, only a small amount of heating power should be applied to a heated pneumotach. The heated pneumotach should be cleaned and calibrated at various heating voltages prior to use.

The pneumotach used in the respiratory heat loss study was tested at 100 SLPM flow for the effect of heater voltage. An increase in heater voltage from 0 vdc to 6 vdc resulted in a 3% increase in pneumotach output. Relative to the maximum linear flow of 600 SLPM the pneumotach linear gain increase is only .5%.

Contamination accumulation in the form of dust, grease, saliva, etc., can greatly change the calibration of a pneumotach. With reasonable precautions in setting up apparatus a negligible change in the calibration can be expected.

Dynamic flow errors caused by appreciable fluid capacitances, inductances and resistances are in the form of time lags and resonant oscillations. As an example, the test setup required in the recent respiratory heat loss study had a large fluid capacitance between the subject and the upstream side of a pneumotach and appreciable fluid inductance and resistance on the downstream side of the pneumotach. Lumped parameter, linearized servo analysis can be used in this case to accurately determine the natural frequency and damping of the resonant system.

The capacitance in the example is caused by a long flexible tube and a flexible gas sample bag container. The total capacitance is

$$C = C_f + C_g$$

where C_f is the capacitance caused by the flexible walls of the tube and the container and C_g is the capacitance caused by gas compressibility.

$$C_g = \frac{V}{\gamma P}$$

where

V is gas volume

γ is ratio of specific heats

P is absolute pressure

The value of C_g becomes negligible at deep depths because of the high value of P. The value of overall capacitance can be found by testing for the change in volume, ΔV caused by a change in pressure, ΔP.

$$C = \frac{\Delta V}{\Delta P}$$

The inductance in the example is caused by a gasometer and a long tube downstream of the pneumotach. The total inductance is

$$L = L_s + L_t$$

where

L_s is gasometer inductance

$L_t = \rho \ell / a$ = tube inductance

ρ is fluid mass density

ℓ is tube length

a is tube inside area

The inductance of the gasometer can be found by testing.

$$L_s = \frac{\Delta P_s}{\Delta \ddot{V}}$$

where P_s is pressure change across the gasometer and $\Delta \ddot{V}$ is change of volumetric acceleration through the gasometer. It could also be calculated from the inertia and dimensions of the moving parts in the gasometer. An appreciable fluid resistance is caused by the two check valves downstream of the long tube attached to the gasometer. The resistance is

$$R = R_m + R_f$$

where R_m is the resistance of the mushroom type check valve and R_f is the resistance of the flapper type check valve that exhausts gas into the water. The resistances are best found by testing

$$\text{resistance} = \frac{\Delta P}{\Delta \dot{V}}$$

where ΔP is a change in pressure caused by a change in volumetric flow, $\Delta \dot{V}$.

The change in volumetric flow at the pneumotach relative to the change in exhalation volumetric flow is the transfer function.

$$\frac{\Delta\dot{V}_{pneu}}{\Delta\dot{V}_{exh}} = \frac{1}{LCS^2 + RCS + 1}$$

where S is the Laplacian operator. For sinusoidal variations in flow,

$$S = j\omega$$

$$j = \sqrt{-1}$$

$\omega = 2\pi f$, frequency in rad/sec

The resonating characteristics can be described in terms of damping ratio and natural frequency, which can be obtained from coefficients in the transfer function. The damping ratio is

$$\delta = \frac{R}{2}\sqrt{\frac{C}{L}}$$

and the natural frequency which is very close to the peak resonant frequency is

$$f_n = \frac{\omega_n}{2\pi} \quad \frac{1}{2\pi\sqrt{LC}}$$

The natural frequency of the test setup used in the respiratory heat loss study was found to be considerably higher than the breathing frequency, so it was not necessary to evaluate dynamic characteristics of this specific test setup. The high frequency noise observed on the exhalation flow signal was caused primarily by high frequency flow variations exciting the test setup near its natural frequency. The high frequency flow variations were caused primarily by bubbles forming at the flapper check valve. If time had permitted, the noise on the exhalation flow signal could have been reduced by a low pass filter.

The pressure transducer used in the respiratory heat loss study has a resonant frequency of about 6 cps with a high resonant peak. The resonance was the result of fluid inductance in the long connecting tubes and fluid capacitance in the cavities of the pressure transducer. To add damping to the resonance, fluid resistances were added to the connecting tubes next to the pressure transducer. The resistances are small orifices that act to reduce the unwanted high frequency pressure signals to the pressure transducer. More reduction

in high frequency noise could have resulted from larger fluid resistances (smaller orifices or capillaries). Small orifices or capillaries would have been more susceptible to clogging by condensation droplets. The surface tension of water in a small orifice can cause a large pressure difference error.

$$\Delta P_{capillary} = 4\delta/d_o$$

where

δ is surface tension of water

d_o is diameter of the orifice

REDUCTION OF PNEUMOTACH DATA FOR THE RESPIRATORY HEAT LOSS STUDY

Reduction of the pneumotach data is necessary to obtain peak exhalation volumetric flow, mean exhalation volumetric flow and the maximum linear range volumetric flow of the pneumotach, for each test point. In order to do this, the necessary test constants are given along with forms for a test data list, a calculated data list and a printed calculated data list. All equations necessary for data reduction are included in the two calculated data lists. Constants, data lists, equations and nomenclature are in forms for data reduction by a digital computer.

The printed calculated data list includes specific gas density, specific gas viscosity and overall linear gain of recorded exhalation flow as well as the desired flows. The gas properties and gain can be used as an aid in rationalizing the shape of the volumetric flow curves. High gas density and viscosity values result in high breathing resistance for the diver and may give insight into why a divers breathing varies as it does with depth.

Maximum linear range volumetric flow must be greater than peak volumetric flow. The value of maximum linear range volumetric flow at a depth of 1000 ft SW is about 120 LPM, which is the value on which some of the pneumotach errors are based at this depth.

The total error for the pneumotach could be as high as 5 LPM including all of the previously discussed error possibilities. An additional 3 LPM error is possible as a result of reading the values of volumetric flow from the recorder chart. This 3 LPM flow error is a reading error of .5 divisions (.5 mm) on the recorder chart when the nominal overall recorder gain is 50 div per 300 LPM or .1667 div/LPM. Actual overall recorder gain is given

in the printed calculated data list and can differ from the nominal overall recorder gain by as much as 10%.

Test Constants

recorder gain: K5 = 50 div/4.26 mv = 11.72 div/mv

excitation voltage: E1 = 7 vdc

pressure transducer gain: K4 = 467.6 mv/psi

heater voltage: E2 = 6 vdc

linear gain factor of pneumotach: C1 = 1040 $1/in^3$

maximum linear Reynolds number: RE = 26,200 d_c/a_c

respiratory gas depth minus chamber depth: Z2 = 2 ft H_2O

partial pressure of N_2: PN = 1.2 (14.7) = 17.65 psia

mass density of std air: DA = .112(10^{-6}) lb s^2/in^4

viscosity of std air: MA = .00261 (10^{-6}) lb s/in^2

gas constant of He: RH = 386.3(12)386 = 1.79 (10^6) $in^2/°R\ s^2$

gas constant of N_2: RN = 55.16(12)386 = .256(10^6) $in^2/°R\ s^2$

gas constant of O_2: RO = 48.31(12)386 = .224(10^6) $in^2/°R\ s^2$

Test Data List

test point: I = 1 through 140

chamber depth: Z1, ft SW

dec % volume of O_2: O2

temperature of exhalation gas: T1, °R

temperature of gas into pneumotach: T2, °R

temperature of gas out of pneumotach: T3, °R

peak flow reading: Q9, div

mean flow reading: Q8, div

Calculated Data List

test point: I = 1 through 140

pressure of respiratory gas:

$P = 14.7\ (1 + Z1/33 + Z2/34)$, psia

dec % volume of nitrogen: $N2 = PN/P$

dec % volume of helium: $HE = 1.0 - N2 - O2$

viscosity of gas at the pneumotach outlet:

$M3 = (1.375 + 02\ (1.3) + (T3 - 550)\ .00165)\ 2.18(10^{-9})$, lb s/in^2

linear gain of pneumotach: $K3 = C1\ (M3)$, psi/in^3/s

recorder overall gain: $K1 = K5(K4)\ K3\ (T3/T1)$, div/in^3/s

density of gas at the pneumotach outlet:

$D3 = (HE/RH + N2/RN + 02/RO)\ P/T3$, lb s /in^4

maximum linear volumetric flow:

$V1 = RE(M3)\ T1/(D3(T3))$, in^3/s

Printed Calculated Data List

test point: I = 1 through 140

specific gas density at pneumotach outlet:

$SD = D3/D5$

specific gas viscosity at pneumotach outlet:

$SM = M3/M5$

overall recorder gain of exhalation gas:

$KO = K1\ (61/60)$, div/LPM

maximum linear volumetric flow of exhalation gas:

$VO = V1\ (61/60)$, LPM

peak volumetric flow of exhalation gas:

V9 = Q9/KO, LPM

mean volumetric flow of exhalation gas:

V8 = Q8/KO, LPM